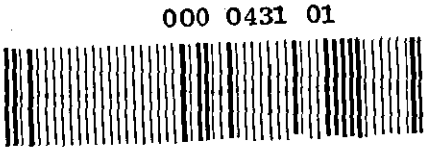

THE NUCLEATION OF CRACKS IN HIGH AND LOW STRAIN METAL FATIGUE.

by

H.McArthur. M.A. (Cantab.). A.Inst.P.

Lecturer, Physics Department of the City of Leicester Polytechnic

Submitted for the degree of Doctor of Philosophy of Loughborough University of Technology.

Supervisors. Dr.J.F.Archard. Leicester University.
Mr.P.J.James. Loughborough University of Technology.
Mr.D.A. Humphreys. Leicester Regional College of Technology.

May.1968

The Nucleation of Cracks in High and Low Strain Metal Fatigue - H. McArthur, M.A.(Cantab.), A.Inst.P.

The thesis reviews the literature concerning the high and low strain fatigue which is pertinent to the nucleation of cracks during cyclic stressing. The methods of investigating the crack nucleation process are discussed with the disadvantages of each method stated. The thesis deals mainly with the examination of the cracks by surface replication and electron microscopy.

A direct carbon replica technique is described which allows the results of macroscopic as well as microscopic deformation to be followed during both low and high strain fatigue. The microscopic deformation (slip) produced an overall macroscopic deformation producing an undulating surface topography with accompanying grain rotations and displacements. The steroscopic electron micrographs prepared from O.F.H.C. Copper subjected to fatigue at room temperature have shown that the grain boundaries slip at their common interface at the surface when subjected to a cyclic shear strain. This grain boundary slip is accompanied by grain rotation as detected by $\frac{1}{4}\ \mu$ scratches, used as surface markers. The degree of grain boundary sliding (at the surface) increased either with number of cycles or with increasing strain amplitude. As grain boundary sliding is detected in both high and low strain fatigue it is suggested that there is only one mechanism by which a material fails under a cyclic stress. A dislocation model is put forward to describe the unidirectional strains built up during fatigue and to describe both the movement of blocks of material within the slip band and the observed grain boundary slip at the slip band/ grain boundary interface. The stereoscopic pairs give a very useful guide as to the high stress concentration which results from the boundary deformation processes, and this can be compared with the comparative large radii of curvature resulting from the transgranular topographical changes associated with the extrusion/intrusion phenomena.

The results of the thesis disagree with recent published theories, and reports upon the effect of surface removal from fatigue specimens prepared from creep tested material which contained intergranular cavities. Fatigue specimens prepared from this material could not give a prolonged life by the removal of surface layers by electropolishing, indicating that subsurface cracks might be capable of crack growth. This agrees well with the results of surface removal from fatigued powder compacts.

The dislocation model developed for the fatigue process can be applied to this later result with success.

Acknowledgements.

I am deeply grateful to the Directors and the Senior Staff of the English Electric Co.Ltd. Whetstone for making available the use of the electron microscope and materials required for this investigation, and to the staff of the Group 5 laboratories who have helped me, and made it possible to undertake this work in the friendliest of atmospheres. I acknowledge the the help of the C.M.L. Research Laboratories and the M.E.L. Group 1 laboratories for their help in allowing time on the high and low strain fatigue machines, and to Loughborough University for the provision of money to erect and undertake the creep programme, and the help given by Mr T Clewly in the erection of the creep frame.

I acknowledge the help from many laboratory assistants who have protected my interests during my absence, and particularly Mr L. Rockley and Mr B. Foster (Loughborough University) for reading the creep apparatus.

It is with pleasure that I acknowledge the help and encouragement which I have received from the Leicester Education Committee, the Principal and my Heads of Department (Mr Langton, Mr Humphreys, and Mr Ingles) which has enabled this work to be undertaken. I am also grateful for the purchase of the following equipment, Reichart interference phase contrast microscope, an E.M.6 electron microscope and ancillary equipment and the provision for laboratory space for electropolishing within the Physics Department during the term of this research and to those members of staff who have given help and assistance where required.

It gives great pleasure to acknowledge the following for their help and stimulating discussions; Mr G.C. Smith,Cambridge University, Mr Roberts,Birmingham University, Mr D.G.Teer, Dr.A.B. Mitchell, Dr.D.Driver, Mr.A.E.King, Mr.R.D.Arnell of the English Electric Co.Ltd. Whetstone Dr.R.Haynes.Loughborough University, and my supervisors Dr.J.F.Archard. Leicester University, 1964-1966 and Mr.P.J.James.Loughborough University.

An acknowledgement would not be complete without mention of the help and assistance which I received from my wife throughout the period of study both at home and at English Electric.

THE NUCLEATION OF CRACKS IN HIGH AND LOW STRAIN FATIGUE.

0.0 Introduction. The reason for research into high strain fatigue.

LITERATURE REVIEW.

1.0 Historical aspects of fatigue.

1.1 Engineering fatigue.

1.2 Relationship between the UTS and the fatigue limit.

1.3 Plasticity.

1.4 Slip.

2.0 Surface removal.

2.1 Persistent slip bands.

2.11 Persistent grain boundaries.

2.2 Slip line characteristics, Stacking Fault Energy.

2.3 Extrusion and Intrusion.

2.4 Internal damage.

2.5 Internal stresses.

2.6 Surface stresses.

2.7 Thin film electron microscopy.

2.8 X-ray asterism

2.81 Subgrain formation.

2.9 Effect of atmosphere

2.91 Effect of frequency.

2.92 Effect of temperature

- 2.921 Annealing during the fatigue test.
- 2.922 Effect of test temperature.
- 2.923. Temperature rise due to lattice friction.
- 2.924 Fatigue at elevated temperatures

3.0 Point Defects

3.01 Hardening.

3.02 Effect on precipitates.

3.03 Effect of fatigue upon a subsequent creep test.

3.1 Measurement of Hardness

3.11 Difference between fatigue hardening and cyclic hardening

3.2 Work softening.

3.3 Summary

- 3.31 Incubation period
- 3.32 The nucleation stage
- 3.33 Crack propagation
- 3.34 Crack propagation in high strain fatigue.

4.0 The fatigue machines used in this investigation.

4.01 High strain

4.02 Low strain Avery machine

4.021 Schenck machine.

4.03 The material

4.04 Electropolishing.

4.05 Orthophosphoric acid - Water 50 $^{v}/_{o}$

4.06 Ethyl alcohol / conc Nitric acid 50 $^{v}/_{o}$

4.07 The variable D.C. supply.

4.11 Methods of investigating crack initiation.

4.12 Engineering approach

4.13 Methods using the electron microscope

4.2 The plastic replica technique.

4.21 Plastic replicas from rough surfaces.

4.22 Plastic replicas for high strain fatigue

4.23 Disadvantage of the plastic carbon method.

4.24 Chemically stripped replicas

4.25 Bromine in methyl alcohol.

4.26 The final replica technique for chemical stripping.

4.3 Scanning electron microscopy.

4.31 Stereo electron microscopy.

4.32 The advantage of stereoscopic pictures with particular reference to fatigue

4.33 Stereoscopic pictures from two stage plastic carbon replicas.

4.4 Taper sectioning methods

4.41 Wood's theory of fatigue.

4.5 Action of metallographic reagents on high concentrations of point defects.

4.6 Taper sections across a crack or intrusion front.

4.7 Summary

4.8 Specimens crept to produce intergranular cavities and subsequently fatigue tested.

4.81. The creep frame.

4.82 The material.

4.83 Metallographic preparation.

4.84 Fatigue of creep tested material.

4.85 Metallography of the fatigued creep material.

5.0. Results and Interpretation.

5.1 Introduction

5.2 High strain fatigue results.

5.21 100% cycles.

5.22 200% cycles.

5.23 250% cycles.

5.24 300 cycles, and greater.

5.25 Displacement of scratches.

5.26 Dwell tests.

5.27 Compression fatigue.

5.3 Low strain fatigue.

DISCUSSION.

6.0 Discussion.

6.1 Critical Resolved Shear Stress.

6.2 The structure of the grain boundary.

6.21 Subgrain boundaries.

6.3 Grain boundary sliding.

6.4 Taylor's theorem.

1 Internal grains.

2. Surface grains.

6.5 Dislocation model.

6.51 The model as applied to static tensile tests.

6.52 Summary of the model.

6.6 Correlation with previous work in low strain fatigue.

6.61 Optical examination of the surface after electropolishing.

6.62 Plastic carbon replicas

6.7 Discussion of the fatigue mechanism.

6.8 Discussion of creep tested material.

6.9 Deformation by creep v. Deformation by fatigue.

CONCLUSIONS.

7.0 Conclusions.

FUTURE WORK.

8.0 Future work.

REFERENCES.

9.0 References.

0.0 Introduction.

With the advance in technological application of materials in the field of high pressure vessels, ballistic missiles and high speed aircraft, the incidence of failure by fatigue has become increasingly apparent. Whilst the crack nucleation stages in low strain fatigue have been extensively examined, the high strain, low cycle region (imposed by mechanical or thermal means e.g. the start up of standby generators) has been given only passing interest.

It was decided initially to make a thorough investigation into the mechanism of crack nucleation in high strain fatigue (mechanically imposed and later as the work on this facet proceeded, with the aid of new techniques of surface examination, the work was extended into the re-examination of the crack nucleation in the low strain region. Previously published work on crack nucleation has been critically examined and reappraised in the light of the results obtained from stereo electron micrographic examination of O.F.H.C. Copper specimens which had been subjected to a programme of high and low strain fatigue cycling.

A specific dislocation model is proposed which is believed to account more satisfactorily for the nucleation of fatigue cracking. The dislocation model can be applied to account for the formation of subgrain boundaries and kink boundaries which may be formed in fatigue.

1.0 Historical Aspects of Fatigue.

Early in the 19th century a form of brittle fracture was observed in good quality high ductile material, at a stress which was well within the U.T.S. and which apparently did not produce any plastic deformation. It was soon observed that this type of failure only resulted if the material was subjected to a cyclic stress and after lengthy periods of service. It therefore became a theory that the material "degenerated", or fatigued under the action of a cyclic stress and its ductile structure became brittle.[1]

Early experiments of Bauschinger[2] showed that there was no difference between the tensile strength and the percentage elongation of the original material and that of a sample taken from the fractured component. Thus his experiments showed that there was no "degeneration" of the crystal lattice upon cyclic stressing, a conclusion which has also been reached by Alden and Backofen using single crystals of aluminium.[3]

The fatigue process can be considered as either a ductile fracture in that the total strain summed irrespective of sign is large, or as a brittle fracture in that failure occurs with little or no elongation.

1.1 Engineering fatigue

In engineering design, the strength of a material is usually defined as the static tensile properties. These properties are determined from a small specimen of material in a static tensile test.

Structural members are traditionally designed so that the maximum stress encountered is no more than $\frac{2}{3}$ of the yield point, the portion A-B fig 1a, represents the safety factor in statically loaded structures. However if the structure is subjected to repeating loads, the possibility of fatigue failure must be considered. The properties of materials under cyclic loading can be determined experimentally, the results are represented on a S/N curve, fig 1b. Each point plotted refers to one test result and represents failure of the specimen at that particular stress. Where no failure results, the point plotted is represented by an arrow. Two types of fatigue curves are obtained, type A typical of metals with a b.c.c.

structure, and/or a metal which exhibits strain ageing and type B, which is typical of metals which have a f.c.c. structure.

One of the pecularities of the determined S/N curve is that all modes of stressing the material (push-pull, torsional, and bending) produce the same type of curve only displaced vertically such that their fatigue limits are different [5]. The fatigue limit in rotating bending is lower than that obtained from push-pull [5]. Furthermore, the slopes of these curves are to a first approximation independant of the prior heat treat--ment. In these cases the fatigue limit is raised as the U.T.S. is raised. For all materials the S/N curve has been divided up into two regions called HIGH STRAIN or LOW STRAIN fatigue. The region of demarcation is considered to be 10^5 cycles. As more work has been performed on low strain fatigue it will be the convention throughout this thesis to refer to low strain fatigue simply as fatigue.

1.2 Relationship between U.T.S. and the fatigue limit

Many attempts have been made to relate the fatigue strength of of steel to either the U.T.S or the yield stress or elasticity in the hope that the expensive fatigue tests may be avoided. This has so far not been achieved, but a very rough correlation has been found in certain cases and is :

$$\frac{\text{Fatigue limit at } 10^6 \text{ cycles}}{\text{U. T. S.}} = 0.5 \quad (6)$$

$$= 0.3 \quad (7) \quad \text{for Aluminium 4 \% Copper precipitation hardening alloys.}$$

A true S/N curve should always be used to confirm any application.

1.3 Plasticity.

Fatigue failure only occurs if the material exhibits plastic deformation[8,9] and hence it may be argued that the phenomena of fatigue cannot take place without slip, which reveals itself as a slip step on the surface, being a surface manifestation that plastic deformation has taken place.

1.4 Slip

The slip step produced by fatigue is 10^{-7} cm.[10] compared with

10^{-5} cm. produced in a static tensile test; and up to 5 % life in the low strain region, the slip lines are straight and evenly distributed in the grain. The slip lines are fairly sharp as they have been formed by an avalanche of dislocations.[11] After 5% life the slip lines cluster into bands, which are characterised by their width and non uniform distribution throughout the grain[12,13, 14] and are seldom observed traversing the whole length of the grain at any stage in the fatigue life.[15] The base to tip height of a slip band is 5 to 7 μ,[16] a factor of 10 greater than the depth of field of the optical microscope (0.2μ) at a magnification of 2,500 x. The stress level of the fatigue test influences the spacing between these bands [16] which are often referred to as fissures[17], These bands are thought to be softer regions[18] in a work hardened matrix, such that the slip formed on subsequent cycling takes place in these bands, giving rise to no displacement of a scratch which is at right angles to the band[15] fig 1c. In a static tensile test a scratch is displaced across the slip trace fig 1d, which suggests that slip is initiated in new planes as a result of the unidirectional macroscopic deformation [15].

The dislocation sources giving rise to these slip bands are thought to be deep seated[17] but this fact does not agree with the silver print out experiments of Forsyth[19]

In high strain fatigue the surface becomes very rough $\pm 20\mu$ [20] and the deformation becomes more uniform and evenly distributed in the grains as the strain amplitude is increased[21]. The slip now traverses the length of the grain and there is little fissuring[21].

2.0 Surface removal.

Early experiments[22-24] on the periodic removal of the surface layers resulted in an extended fatigue life of the specimen. Since these experiments were performed in rotating bending, it could be argued that the beneficial results of surface removal would not apply to cases where the specimens were uniformly stressed, e.g push-pull. It has been subsequently shown that the beneficial effects of surface removal are

obtained in push-pull tests in both low[14] and high strain[25,26] fatigue and Summers work[25] indicates that the crack nuclei are about 0.0001 in. (2.5μ) deep after 100 cycles (20% life).

As the fatigue life is increased by surface removal, it suggests that the Manson[27]- Coffin[28] relationship $\{\epsilon_p N^{1/2} = \text{constant}\}$ applies to surfaces rather than the bulk material.

2.1 Persistent slip bands.

If the fatigue crack is initiated in the surface layer (< 10μ) it would be very quick and easy to detect a crack with the optical microscope if the surface irregularities were within the depth of field of the microscope *1.4. Thompson et.al[14] were the first to distinguish between the slip features leading to crack nucleation in the striations and the more general slip markings which take little part in the nucleation of the crack. By the electrolytic removal of 2μ from the surface , the surface roughness was removed which made some slip bands invisible whilst others became accentuated and these were called "persistent" slip bands. These persistent slip bands were found to be the origin of the fatigue crack as they penetrated deeper into the material with increasing number of cycles. This accentuation of the slip bands by electropolishing methods could be due to a complex electro-chemical reaction with the regions of distortion at the band front[29]. The term persistent is a misnomer [30] and has no bearing on the fact that the dislocation sources are thought to be deep seated[17] * 1.4

In the region between the persistent slip bands , termed slip-less [11,16], the surface exhibits corrugations[16,31], which are accompanied by high lattice curvature[16,31]. This is absent in single crystals.[32]

During the later half of the fatigue life, it is possible to detect a crack[14,33] in the persistent slip band by the application of a tensile stress. In these cases the degree to which the crack opens up will depend upon a) the crack or persistent slip band depth

b) the crack or persistent slip band length.

Forsyth & Stubbington [33] concluded that this method does not show that

cohesion is lost across the intrusion in the persistent slip band, as slip lines are often observed at the intrusion edges.

2.11. Persistent grain boundaries.

Little mention has been made of grain boundary damage in fatigue.[34-37] Wadsworth et.al.[14] showed that the grain boundaries in copper played an important role in the early stages of fatigue, as they prevented the slip bands from invading the adjacent grain boundary. Smith[35] showed with the repeated electropolishing of Aluminium, that the grain boundaries could be brought into relief in the same way as persistent slip bands. He was able to show that the grain boundary was often as deep as , and in some cases, deeper than the transgranular damage.

Persistent grain boundaries and persistent slip have not been reported in high strain fatigue.

2.2. Slip line characteristics, stacking fault energy.

Slip lines are often spoken of as being planar (i.e. two dimensional and characteristic of a low stacking fault alloy,) and wavy (three dimensional and characteristic of a high stacking fault alloy). The transition from planar to wavy slip is temperature dependant. *3.1

A factor influencing the nature of the surface topography which developes during fatigue is the degree of wavy slip. The detrimental surface topography is more easily formed in high stacking fault alloys, and thus the fatigue resistance increases with decrease in stacking fault energy.[38-41]

The crack initiation theories of Mott[42] have assumed the importance of cross slip. Later experimental work on materials which do not show cross slip have been impossible to fracture by cyclic stressing.[43,44]

2.3 Extrusion and Intrusions.

In the study of partially aged Al-4Cu, Forsyth[45] observed the extrusion of a thin ribbon of material from the slip band, and when Forsyth and Stubbington[46] found that an increase in the temperature of testing produced thicker ribbons, the over-ageing mechanism for their formation seemed substatiated. However since then, extrusions and intrusions have been found in pure metals[47-49], iron[50]

stable alloys[21] and at 4°K [48]. Calnan et.al[51] have observed them in static tensile tests.

Since activated diffusion cannot take place at 4°K, several mechanisms have been postulated for the extrusion formation, the more notable being Mott's cross slip mechanism[47] and Cottrell and Hull's method of intersecting slip planes[48]. Neither mechanism explain the formation of the extrusion/intrusion phenomena in materials[44] which exhibit only basal slip,[43] or where cross slip is difficult[44].

2.4 Internal damage.

By using crystals of AgCl which are transparent to light Forsyth[19,52], was able to show that internal voids were not formed at the base of the intrusion, which confirmed earlier observations[14] of the total absence of subsurface damage. These results are in complete contrast to those of Wood and Bendler[15] who claimed that cracks or 'pores'[31] could exist which were wholly internal. There is some evidence[53,54] that internal damage can be nucleated at second phases which are present in the sub-surface layer (about 0.025 in. 600 μ).

Although the study of the damage ahead of an intrusion is complicated by the tendancy for the juxtaposed surfaces to undergo cold reweldment[55] with the possibility of the entrapment of air[19], it is a widely held view that there is no internal damage .

It will be shown later that internal damage *4,42 can also arise from the preferential chemical attack[56] at regions of high dislocation density when taper-sectioning methods (*4.4) are employed for the examination of subsurface damage.

2.5 Internal stresses.

The stability of the internal stresses produced by the various modes of testing can be investigated by step-wise annealing experiments[57]. The stored energy released can be correlated with other physical properties. Considerable differences between the specimens tested in fatigue (High and low) and static unidirectional tests were found. In the high strain range , the majority of the energy was released by a recovery process and little by recrystalisation, whilst the reverse was found for material deformed by the static tensile tests.

even though the Xray asterisms *2.8 produced by these two modes of testing were identical[32]. *2.8 . In the case of low strain fatigue the energy is released by a recovery process which continues up to 900°C (for O.F.H.C. Copper), indicating the high stability of the dislocation structure formed. This internal dislocation structure can be examined by thin film electron microscopy (T.F.E.M. *2.7.)

2.6. Surface stresses.

The fatigue strength of a component depends a great deal upon its surface condition. The fatigue life is increased by smooth stress free surfaces[58], and by residual compressive surface strains, and reduced by rough surfaces (stress free) or residual tensile surface strains[50,59].

Thus the following processes increase the fatigue life because they introduce a compressive surface stress : Nitriding, Carburizing, Light grinding, Surface rolling, Flame and induction hardening.

The following processes lead to a reduction in the fatigue life Decarburization Heavy surface grinding.

Similarly a static tensile stress superimposed upon a cyclic stress reduces the fatigue life, whilst a static compressive stress superimposed upon a cyclic stress increases the fatigue life.

In high strain fatigue the above parameters are not so important because in this case, the plastic strain is larger than the elastic component and this results in a high strain fatigue cycle about a new mean strain; i.e. If the cyclic strain is $+e_1$ to $-e_2$, the cyclic strain range is $\frac{1}{2}\{|e_1| + |e_2|\}$ about a new mean as an arbitary zero. (e_1 is the tensile strain and e_2 the compressive strain.)

2.7. Thin film electron microscopy. (T.F.E.M.).

Some of the earlier work[60,61] found no correlation between the internal dislocation structures and the persistent slip bands because these observations were not near enough to the specimen surface.

Later experimental techniques[62-67] showed that the persistent slip bands were regions of very high dislocation densities[62,63] forming a ladder like structure[64,65,69.] giving rise to subgrains.[67] This dislocation structure was only related to the persistent slip bands in the surface layers , estimated at 10 μ [63;66] which is in agreement to the slip band penetration determined by electropolishing methods[14].

The fracture surface has been investigated[67,68,] and in the later work[67] single crystals have been used. Precautions were taken to prevent the fracture surfaces from coming into contact with each other on the compressive cycle.[67] The examination of the fracture surface by T.F.E.M. has substantiated earlier work that the fracture surfaces are composed of many subgrains[68] of $\frac{1}{2}\mu$ diameter[67] increasing to 1 μ at 4 μ from the fracture surface .

In high strain fatigue the whole of the specimen is composed of a cell structure[70], whose dimensions depend upon the strain amplitude[71].

2.80. X-ray investigations.

X-rays are diffracted from fine grained randomly orientated polycrystalline material to give rings of uniform intensity. Coarse grained material gives rise to spotty rings (discrete spots on a faint ring) whilst a material with preferred orientation will give rise to arced spots, elongated in the circumference of the rings in which they are placed. The spots constituting the rings may be broadened in a radial direction if the grain size is less than $1000^{0}A$[72,78]. Any deformation in a fine grained material leading to misorientation within the grains will produce line broadening or x-ray asterisms. *6.21.[73,74]

In static tensile and high strain fatigue tests there is considerable misorientation, which is found to depend upon the strain amplitude. Little or no misorientaton is detected in low strain fatigue.[75] Moller and Hempel[23] report that after fatigue testing the removal of ~3mm. of the surface restored the blurred X-ray reflections to their original sharpness, which is in agreement with Fourie[74], who found that the surface layers of a statically deformed crystal produces a greater degree of asterism than is obtained from the centre of a crystal. This asterism is not necessarily the indication of "turbulent "[75] plastic flow on the micro scale.

Taira and Honda[76-77] are attempting to use the degree of line broadening as a non destructive method of estimating the fatigue life left in a cyclicly stressed specimen.[78]

2.81 Subgrain formation

The X-ray asterism *2.8 within the surface of a grain is explained by the formation of subgrains[75] which are a pre-requisite for ductile fracture. Holden[68] claims that a crack is non-propagating if the plastic volume at the crack tip is contained in one subgrain and the tendancy to form subgrains increases with the stacking fault energy.[79] *2.2. The mechanism of crack formation therefore appears to be the opening up of the subgrain boundaries[67] (*6.21 *2.7) rather than the renucleation of a crack[80] (termed "pore"[31]) within the matrix.

2.9. Effect of atmosphere.

Any agent which affects the surface of the material will to to some extent influence the nucleation stage of the fatigue crack, and also the propagation rate of the crack by preventing the cold reweldment of the crack interfaces in the compression cycle[55].

The early experiments[81-83] showed that the fatigue life of most metals could be increased by the exclusion of air. Later tests have indicated that the shorter fatigue lives in an atmosphere are a result of

the increase in rate of crack propagation or growth[82-85] as opposed to crack nucleation[86]. Some work has been performed in a vacuum[83-88] and with traces of inert gases in order to distinguish between several proposed models and theories. In order to differentiate between the proposed mechanisms, lower pressures, different strain amplitudes and higher frequencies are required. If chemical attack of the highly stressed regions is the underlying mechanism, then there should be a pressure low enough at which the damaging atmosphere or ion[89] cannot "diffuse" down the crack to the crack front in the time taken for the specimen to undergo the next half cycle. Such pressure / amplitude and frequency effects have been obtained for lead [86-88].

The effect of atmosphere on high strain fatigue is small[85] and many materials obey Coffins law[27,28] better in a vacuum than in air.[55]

2.91 Effect of frequency.

Due to the time consuming nature of obtaining a complete S/N curve, it is often necessary to obtain results quickly by increasing the speed of cyclic stressing. In general high strain fatigue tests are undertaken with a cyclic frequency between 1 and 10 cycles per sec. Low strain fatigue tests are subjected to frequencies between 100 and 10,000 cycles per sec.

In 1950 the A.S.T.M. Committee formally stated that there was no frequency affect up to 1 kc/s on pure metals[58]. (neglecting strain ageing alloys). Since 1950 several investigations [91-93] have been undertaken which indicate that the fatigue life is enhanced at higher frequencies and this is more marked in the adsorption sensitive range [89].

In tests at elevated temperatures the higher frequencies lead to longer fatigue lives [94-96].

The affect of frequency is more marked in high strain fatigue. Increasing the frequency tends to give better performance, but this is more marked on some materials than others[91].

2.92. Effect of temperature.

2.921. Annealing during the fatigue test.

The early experiments[97-99] on removing the latent damage due to fatigue cycling by annealing were carried out at 10 % life and after the onset of the severe surface topography *3.1 and did not result in the expected increase in the fatigue life unless very high temperatures were used[99]. The later experiments of Alden and Backofen [3] have shown that an increase in life is achieved if annealing is carried out at 0.01 % life. Annealing tests have not been performed in high strain fatigue.

2.922. Effect of test Temperature.

In general the fatigue strength of a material increases with decrease in temperature[58]. This increase is no more or no less than the increase in the static strength of the material with decrease of temperature.

In view of the evidence pointing to the early stage of crack nucleation *2.921, it is surprising that the fatigue specimens do not show a brittleness due to the severe notch produced during the cyclic life at low temperatures. McCammon and Rosenberg[103] have shown that the family of S/N curves at different temperatures have , to a first approximation, identical slopes. This suggests that the fatigue mechanism operates efficiently at all temperatures from 4°K to 300°K. This fact alone is thought to rule out the suggestion that the fatigue crack may be vacancy initiated[58]. However Dieter[104] suggests that fatigue failure at room temperature is aided by the generation and condensation of vacancies, because the fatigue strength decreases with increase in temperature at a greater rate than does the tensile strength. This vacancy theory must be rejected on the following grounds:

1). The fatigue life is increased indefinitely by the periodic removal of the surface layers *2.0. This assumes that plastic deformation takes place uniformly across the cross section of the specimen[74]* 2.80.

2). The slip band appearance in copper at 4°K is much the same as the slip band appearance at room temperature[49] suggesting that the fatigue damage results from the passage of dislocations rather than the accumulation of point defects.

3). Nucleation of the fatigue crack is very early in the fatigue life of a specimen as shown by fracture experiments in liquid air [105].

4). Theorectical considerations on the vacancy diffusion in a tensile test indicates that any voids formed will be situated in the grips of the specimen rather than at the surface .[94,106-109].

2.923. Temperature rise due to lattice friction.

Calculations have been made on the instantaneous heat flashes in a slip band at room temperature[100-102] in order to account for the phenomena of over ageing in some alloy systems. * 3.02. The calculated rise in temperature (for 300°K tests) is about 2°C [102], 10°C[100], 100°C[101], which last for about 1 micro second at the speeds considered. At 4°K , assuming the same derivation, and substituting the specific heat at 4°K, (a factor of 10^3 lower than that at room temperature) and thermal conductivity (a factor of 10 higher at 3°K but reduces as the temperature rises above 4°K) the temperature flashes are $\pm 2 \times 10^2$ to $\pm 100 \times 10^2$ i.e. ±200°C and ±10,000°C lasting for 1 microsecond. Even with these high temperature flashes the vacancies would not undergo many jumps before the thermal spike was over.

16

2.924. Fatigue at elevated temperatures.

Fatigue tests at high temperatures have been for design information and only recently [94.110-113] have observations been made as to the basic mechanism which has features in common with creep. * 4.8.

3.0. Point Defects.

Early work [57.114.] in fatigue could be explained on the assumption that point defects were produced in fatigue. Seitz[115] had suggested that jogs on a moving screw dislocation could generate point defects, and later it was shown [116] that there was a greater density change for a specimen subjected to a cyclic stress than for a static tensile test.[116]

The theories [58,117.106.] postulated that point defects concentrate in the slip band and cause "degeneration of the crystalline order" and hence cracking. *1.0 *2.922.

3.01 Hardening.

The point defects[118] formed in fatigue harden the matrix[18,119] between the slip bands rather than 'soften' the slip band[118]. Single vacancies are reported to cause little or no hardening[121.120.] whilst clusters of 10 to 100 cause an increase in the yield stress[121,122,] and clusters of 100 to 1,000 may be just resolvable in the electron microscope.[123] . *2.7.

The mechanism of hardening by vacancies has been the subject of much discussion[120,121,124,125].

3.02. Effect on precipitates

The effect of plastic deformation[126-129.] and fatigue[131-132] upon the diffusion rates at various temperatures[129,132] has been widely reported.

Alloys strengthened by precipitation are mechanically unstable under a cyclicly applied stress.[133] The reason for this is under review,[136] and it would appear that the most likely explanation lies in the dislocations cutting the precipitates to below their critical size for stability.[134] Therefore the precipitates would dissolve, called "reversion", at room temperatures. At high temperatures however, where the rate of diffusion is higher, the precipitates would grow (because the rate of growth would be greater than the rate of solution or reversion) and " overageing " takes place.

3 .03. Effect of fatigue on a subsequent creep test.

A fatigue hardened material has a superior creep resistance than a non hardened specimen.[135] This statement only holds if the creep strain is large. If the creep strain is small, the creep resistance of the fatigue hardened specimen is low as might be expected on fundamental grounds of cyclic stressing producing vacancies.[136] *3.0

3.1 Measurement of Hardness.

It is not correct to measure the micro-hardness of a metal, which has undergone mechanical deformation, by means of indenters, since the hardness of steel is greater when strained in compression than when strained in tension.[137] In fatigue the hardness of the specimen is determined by the stress required to impose the next fatigue cycle in a constant strain cycling test,[138] and therefore the hardness is independent of the residual surface stress.

It is found that fatigue cycling after a certain fraction of the life (represented by the point X in fig.1e) ceases to cause strain hardening and is referred to as "non hardening slip."[138] This point X on the hardening curve is accompanied by the clustering of the slip lines into bands *1.4 [3,138]. The depth of these bands are no greater than 10 μ[140.14 *2.7] and the ratio:

$$\frac{\text{Volume occupied by the slip band}}{\text{The volume of the specimen}}$$

indicates that the hardening cannot be due to the processes leading to the formation of persistent slip bands. * 2.1. The rate of hardening and the occurrence of slip bands depends upon the stacking fault energy (* 2.2) and the point X represents the onset of cross slip[3,40]. Several other interpretations[99,141] have been put forward but the most important point is that the fatigue damage can only be removed by annealing[3] before the onset of the non hardening strain (point X) and as such may be considered as the beginning of "crack nucleation."

3.11. Difference between fatigue hardening and cyclic hardening.

Fatigue hardening is produced when a fatigue test is conducted under constant strain amplitude cycles, whilst cyclic hardening is produced when a fatigue test is conducted at constant stress cycling. This is significant as under constant stress cycling few additional slip planes are activated on the termination of hardening. With constant strain amplitude however, new slip systems must be activated because as the specimen hardens, so the stress increases as a result of the imposed strain amplitude.[139]

3.2 Work Softening.

Cyclic stressing affects previously work hardened metals[138] in different ways, depending upon the amount of prior work hardening and the cyclic strain amplitude[71]. Cyclic stressing of annealed and cold worked metals to failure results in a characteristic cell size[71], hardness[142] and sometimes hysterisis loop[144], which are dependant upon the strain amplitude.[71] Thus a metal strain softens if its prior history leaves it with a smaller cell structure than the characteristic cell structure to which it would transform upon fatiguing.

3.3 Summary.

Cyclic stressing is equivalent to a greater state of thermal activation. Diffusion rates are increased and complex metallurgical changes take place within the slip bands. For metastable solid solutions precipitation takes place, whereas for dispersed phases, re-solution occurs within the slip band.

For pure metals, the point defects diffuse from the slip band, thereby increasing the mechanical properties of the material as shown by the application of a tensile stress. The fatigue process may be divided into three sections :

3.31). Incubation period. Concerned with the change in the mechanical properties which result from changes in the bulk of the material. These changes are independant of the orientation of single crystals,[145] and the grain size in polycrystals,when subjected to low strain fatigue.[39] These variables are important if the material is subjected to high strain fatigue.

3.32). The nucleation stage. The nucleation of the crack is concerned with the surface 10 μ[63-65]. This thin surface layer has a large influence over the mechanical properties [146-150]. Crack initiation may develop at regions where the applied strain is concentrated, the most likely being at:- intrusions, surface inclusions, non deformable second phases, twin boundaries and subgrain boundaries or wherever a discontinuity of slip or slip direction occurs.

3.33. Crack propagation.

Once the crack is initiated, the initial propagation of the crack is parallel to a slip plane in which the critical resolved shear stress is exceeded. As the crack moves to the adjacent grain, it follows the slip band of that grain[151]. Metallographically the slip lines are shown as fine lines which do not open out with the application of a tensile stress,whereas a crack does open[14]. This slip plane dependance is characteristic of the earliest stages of cracking, as subsequent crack growth is transgranular, without any dependance upon the slip plane . The former mode of cracking has been designated STAGE 1 by Forsyth[151], and the latter stage is the onset of STAGE 2.[151]

The growth of the crack in stage 1 is very slow and when it reaches a grain boundary , its growth may be arrested if the orientation of the slip bands in the neighbouring grains are not favourable for propagation. These cracks are called non propagating cracks, and a crack is estimated to spend 50 % of its life in this state.[151]

Once the crack reaches the Stage 2 mode, in which the crack is progressively opened by the application of the tensile half cycle,it may steadily move across grain boundaries and therefore assumes a characteristic transgranular nature, which is typical of the fatigue failure.

The crack grows giving rise to " ripples "[102] on the fracture surface. The factors which control the crack growth per cycle are complicated and so far unresolved.

3.34. Crack propagation in high strain fatigue.

Crack propagation (and nucleation) is mostly intergranular in high strain fatigue.[85]

4.0. The fatigue machines used in this investigation.

4.01. High Strain.

The high strain fatigue tests were carried out in a Forrest bending fatigue machine [179], and is described below.

The method of operation is illustrated in fig 2 a which is a line diagram of the main features of the machine. The specimen (a bar 7 " x $\frac{3}{4}$" x $\frac{1}{4}$") is clamped between two shafts B and D which are rotated through a known angle θ in opposite senses, but in phase with each other. i.e. the neutral line of the specimen BYD is caused to oscillate through an angle θ to BCD and BGD. The shafts are driven as follows. A motor drives through a worm gear box which has two output shafts which rotate in opposite directions. Long adjustable connecting rods HX and ZI transmit the drive from the eccentrics to lever arms rigidly fixed to the shafts B and D by a large section bar fig 2b , The eccentrics have an adjustment which allows θ to be varied from 0 to 32° about the position BYD. As the specimen bends to BCD the chord length BCD' decreases, and to accommodate this the shaft B is fixed and the shaft D is mounted in a linear ball race to allow free horizontal movement. The test may be stopped in any position in the fatigue cycle by tripping the microswitch near the shaft D.

To measure the surface strain of the specimen a spherometer is used. The bending moment at any time in the test may be determined by the load measuring device incorporated in the connecting rods. This consists of a compound strut composed of two members held in a pre-bowed state such that a compressive load tends to increase the bow and a tensile load to decrease the bow. The deflections were measured by means of a dial gauge reading to 0.0001in. This fatigue machine is a constant strain machine .*3.11.

4.02. Low strain. Avery machine.

The low strain fatigue tests were performed in an Avery bending machine (fig 3 a) which is produced commercially. This produces a bending moment on a specimen AB (machining details fig 3 b) by means of an eccentric cam C fig 3 a. The specimen is held at the other end by means of a callibrated spring D which is made to extend and compress as the eccentric cam rotates. The bending moment is obtained from dial gauges incorporated on the machine. This machine, although it imparts a constant deflection through the eccentric cam, is not a constant strain machine, because this constant deflection is cushioned by the spring D. It is therefore neither a constant strain nor constant stress machine. *3.11.

4.021 Schenck Machine.

The fatigue programme on material, later creep tested *4.8, was conducted on a Schenck pulsating machine fig 3 c. This machine imparts a push - pull stress cycle to the specimen (machining details fig 3 d)

The eccentric cam imparts the push pull cycle to the specimen grip X which is kept horizontal by the parallel guides k. The other end of the specimen is fixed to a dynamometer to which is attached a small graticule . The optical microscope is fixed to the rigid end of the dynanometer and is focussed on the graticule. The eyepiece of the microscope contains a graduated scale, and by the means of callibrated charts, the applied load is measured. The machine, although it imparts a constant deflection to the specimen through the cam , is not a constant stress or constant strain machine because the dynanometer acts as a spring obeying Hookes law.

4.03. The material

The material used in this investigation was O.F.H.C. Copper containing : Oxygen 3.0 p.p.m. by wt.

Hydrogen 1 p.p.m. by wt.

Nitrogen trace.

The material was in the form of 1½" diameter soft tempered rod. The specimens for the high strain fatigue programme were bars of size 1" x ¾" x ¼" and for the low strain fatigue programme the material was machined to the dimensional details as shown in fig 3 . b. The specimens were electropolished in orthophosphoric acid *4.04 to remove the surface deformed layers, and then annealed at 500°C for 1 hour in vacuum. The surface was given a final electropolish.

4.04 Electropolishing.

Over the period of this investigation, electropolishing techniques have been used to prepare stress free flat surfaces. The electrolytes and compositions available are well documented.[155,168] In this investigation improvements were made and are described below.

4.05. Orthophosphoric acid- water 50 v/o. This electrolyte was used at a potential of 1.8 v D.C. from a supply described in *4.07. This electrolyte did not give good results if the anode was vertical. If the anode was horizontal it gave good results which could be further improved upon by surrounding the cathode with filter paper. This prevented agitation of of the electrolyte by the gases evolved at the cathode. The cathode area was larger than the anode area. Poor results could be obtained from insufficient washing, which allowed a phosphate film to remain on the surface. This was best removed by washing in a very dilute nitric acid followed by a wash in running water and rinsing in alcohol before drying in a current of warm air.

If this electrolyte is used on vertical anodes, slight etching or pitting is obtained. In either case the electrolyte gives better results

if the polishing times are kept short and the specimen washed periodically.

4.06 Ethyl alcohol / conc Nitric acid 50 $^{v}/_{o}$ at 0°C

This electrolyte was found to be the best for vertical anodes when surrounded by a cathode of fine stainless steel gauze. The operating voltage was found to be 6 volts. The solution was liable to decomposition (violent in some cases) if industrial alcohol was used. This decomposition could take place even if the electrolyte was standing in a mixture of ice and common salt. Absolute alcohol is therefore recommended and the periodic replacement of the electrolyte is necessary.

Foreign ions, especially Fe^{2+} cause irregular pitting on the surface. This is manifested as etching "rosettes" on the surface of the anode. This could be detected during the polishing operation as the anolyte layer became granulated and pale blue in colour. The correct appearance of the electrolyte at the anode should be dark grey or black. This anolyte region is a very viscous liquid which falls from the anode forming a black deposite at the bottom of the bath. To prevent the contamination of the electrolyte, the crocodile clips were protected with lacomite and dried thoroughly before use.

4.07. The variable D.C. Supply. The circuit diagram for this supply, and the component parts are listed in fig.4.

4.11. Methods of investigating crack initiation.

A single phase high purity metal fails by fatigue as a result of the propagation of one crack out of many hundreds which are formed on the surface.[20] Therefore early observation of the fatigue damage does not necessarily mean that this region will constitute any part of the final crack.[14]

An initial appraisal is therefore directed at reviewing the methods which are available in the study of crack nucleation.

4.12. The engineering approach[14] is to start with a stress raiser at the surface and observe the nucleation of the crack at the stress raiser. This method has obvious limitations. Thompson et.al.[14] started using this method but found that it could be improved by blunting the stress raiser by electropolishing. This technique was again improved by dispensing with the scratch and observing the surface after fatiguing by the removal of 2 μ from the surface. Hence it was possible to :-

1). See any surface damage which extended to a depth greater than "2 μ . Backofen [140] used a similar technique and removed 5 μ

2). Use the optical microcope in the higher magnification ranges as the surface of the specimen was flatter.

3). Remove the slip traces which tended to mask the transgranular cracks.

However this technique has the disadvantage that free crack initiation is not being observed at the surface, and there is a possible adverse reaction of the electrolyte upon the regions of high dislocation density *2.1.

4.13. Methods using the electron microscope.

The electron microscope has a very high depth of field approximately 1,000 x the resolving power[158,159]. Hence the surface roughening associated with fatigue is well within the depth of field *1.4.

With a two stage replica (plastic-carbon)[49] the problem of post fatigue metallographic preparation is overcome, with the added advantage that the technique permits the continued observation of a definite area.

4.2. The plastic replica technique.

The replica is prepared as follows:[160]

1) a suitable plastic material is dissolved in an organic solvent which is poured onto the surface to be replicated and allowed to dry.

2). a backing application is applied to increase its mechanical strength.

3). when thoroughly dry the plastic is backed with a pressure sensitive tape (selotape) and the whole composite is stripped from the surface.

4). The replica is transfered to a carbon evaporator and carbon is deposited under a vaccuum of 10^{-4}mm.Hg. To increase the contrast, the carbon film is high-lighted with a heavy metal (gold-palladium alloy) which is deposited at a shallow angle (45°).

5. The supporting grid is stuck onto the composite replica and the plastics removed in their respective solvents.

6). A positive of the surface is prepared by shadowing on the plastic/carbon interface whilst a negative is prepared by shadowing on the prior plastic/metal interface.[160]

4.21. Plastic replicas from rough surfaces.

Examination of the fatigue process with the use of plastic carbon replicas[82,49] to give a negative of the surface ensures that the crack is easily recognisable. With rough undulating surfaces, the selotape does not make good adhesion with the plastic in the troughs of the undulations, and so this plastic is not always removed from the specimen. This destroys the plastic replica. One way of overcoming this is to swamp the surface with the backing plastic to fill in the crevices in the specimen, thus making the plastic thicker at these points. This however makes the cleaning of the carbon film a long and costly process. This was attempted and a redistillation system was built for the specimen cleaning and is shown in fig 5.

Wadsworth[30,82] found that the replicas were easier to remove if the tests were carried out at very low strains, thus preventing the formation of a rough surface and also of deep cracks which " Keyed " the plastic onto the specimen 'surface. Thus Wadsworth could only examine the surface in low strain fatigue.

4.22. Plastic replicas for high strain fatigue.

The plastic replica technique *4.2 formed the basis for the high strain replication. The keying of the plastic film by the cracks was reduced by replicating the surface at maximum tensile strain and the backing solutions of 2 and 5 % formvar in chloroform and collodion in acetone were used (fig 6.)

4.23. Disadvantage of the plastic-carbon method.

The disadvantages of all the plastic-carbon methods is as follows:

1). It is difficult to ensure that the replica is a faithful reproduction of the surface. In order to help with the removal of the plastic, it is often beneficial to breathe heavily onto the replica which turns opaque when the adhesion between replica and metal is reduced by water vapour. The microdroplets left on the surface often interfere with subsequent replication e.g. fig 11 b. γ'.

2). The resolution of the plastic-carbon replica is limited to the resolution of the primary plastic replica which is approximately 150°A maximum.

3). The plastics are often difficult to remove, and the electron beam is inelastically scattered by unremoved plastic.e.g. fig 11 b. γ.

4). The carbon films tend to break due to the swelling of the plastics when the composite is first put into the organic solvents for the removal of the plastic film.

5). The penetration of the plastic primary replica into the cracks and narrow fissures is very poor.

4.24. Chemically stripped plastic replicas.

A programme of work was started to replicate the same area at a different stage of life and to compare these mechanically stripped replicas with plastic replicas removed by etching away the subsurface layers. It was found that formvar was superior to fax-film, nitrocellulose in ethyl acetate or collodion in acetone as it was the only plastic which still dissolved in its solvent after long immersion times in dilute Nitric acid. The clarity of these replicas was poor due to the undissolved plastic. It was decided to compare the plastic replicas with replicas of carbon prepared by the single stage technique [160,209] and by correctly choosing the prior carbon/metal interface, to prepare a negative replica. First attempts to achieve this were not successful, because of the small pieces of carbon film obtained due to the gases evolved in many of the electrolytic or chemical reactions.

4.25. Bromine in methyl alcohol.

A 10 % solution of bromine in methanol reacts with most metals without the evolution of a gas, [161] and thus the resulting carbon films from fractographic studies [161] are extremely good. For the replication of the fatigued surfaces of copper the disadvantage arises from the thick viscous products formed which may give rise to contamination or to the fragmentation of the carbon film during the washing process.

This technique was improved by allowing the chemical reaction to take place over 24 hours with a much weaker solution (2 % Br_2 in methanol) which ensured that the carbon film was removed from the deepest cracks. Also it was found that it was easier to find the correct side of the carbon film and the orientation of the carbon film to the stress system , if the surface of the fatigue specimen was scratched with $\frac{1}{4}\mu$ diamond paste before the specimen was tested. This also had a beneficial effect as the result of the plastic deformation could be detected even though resolvable slip steps were not produced. e.g. Fig 41 c-h. and micrographs fig. 30a and 32b. Several methods of applying the $\frac{1}{4}\mu$ scratches were tried (selvyt + $\frac{1}{4}\mu$ paste:"Kleenex tissue"+ $\frac{1}{4}\mu$ paste) but these were inferior to the method finally used, of a well washed finger impregnated with $\frac{1}{4}\mu$ diamond paste and lubricated with "Hyprez" fluid.

4.26 The final replica technique for CHEMICAL stripping.

After electropolishing the surface of the fatigue specimen prior to fatigue , the surface was scratched with $\frac{1}{4}\mu$ diamond paste such that the scratches were perpendicular to the zones of maximum critical shear stress. The specimen was then fatigued. Carbon was evaporated onto the surface which was then scored into small squares ($\approx$ diameter of a grid) and subsequently removed in 2 % bromine in methanol. (Reaction time 24 hours) The solution was then poured into water which diluted the dark brown colour, permitting the carbon films to be removed on a copper grid and transferred to a bath of methanol/ dilute hydrochloric acid. These carbon films tended to curl up such that the prior carbon metal interface was on the outside. In order to straighten the films out and to eliminate folds, they were transferred to a water bath containing a small amount of methyl alcohol, which was added to lower the surface tension. The films were collected and shadowed at 45 $^{\circ}$ to the surface on the prior carbon/metal interface. i.e. a negative carbon film was made.

The scratches were applied in such a manner that they were continuous over the grain surface and at grain boundaries. In order to achieve this, particular attention was paid to the electropolishing conditions *4.05.

4.3 Scanning electron microscopy. Courtesy Dr. Sumner U.K.A.E.A. Springfield.

Whilst this programme of work was in hand, a parallel investigation was performed on the scanning electron microscope. A section of a fatigue specimen * 5.26, which showed a large number of tubular holes[52] or spikes[49] when examined by the two stage plastic - carbon technique, was examined in the scanning electron microscope. The three dimensional effect produced in these micrographs was most striking fig 7 , but the resolution (300°A) claimed by the manufacturer was not obtained due to 'noise', and the tubular holes [52] or "tapered spikes"[49] were not seen.

The electron microscope has a much better resolution (10-20 Å) than the scanning electron microscope, but the shadowed replicas require more specific interpretation. In this interpretation, the eye cannot differentiate easily between the surface phenomena shown in fig 8.

4.31 Stereo electron microscopy.[159]

Replicas may be made to have a three dimensional aspect by using the principles evolved from stereo aerial photography. Basically this involves the photography of an object from two positions subtending an angle of θ° fig 9a. These photographs are then viewed by means of mirrors or lenses such that the images are superimposed by the brain from which the 3 D perspective is obtained fig 9 b.

In the electron microscope the camera cannot be moved, but the same effect may be produced by tilting the object normal through 3 to 5 degrees of either side of the electron optic axis fig 9 c. If these two micrographs are arranged so that they correspond to the field of view as seen by the right and left eye respectively and viewed with the aid of a stereo viewer, a 3 D effect can be readily seen. Several stereo-viewers are produced ranging from £ 10 to £40 but they basically employ the same principles as are described below using two convex lenses of focal length 10 cms. The micrographs in this thesis are set out so that they may be viewed using the two lenses which must be held near to the eyes (in the position where spectacle lenses would be placed, but not instead of spectacles if they are worn.) The eye-photograph distance should not be greater than 10 cms.fig 9 d and both photographs should be in focus if the distance is between 6¾ and 10 cm. If one lens is moved in a NORTH-SOUTH direction the image corresponding to this lens moves in the opposite direction (south-north) fig 9d. . Once the brain distinguishes between the two separate images and recognises that they correspond to the left and right eye-lens respectively, it is a simple matter to move one or other of the lenses in the opposite direction to which the image must be moved to make the respective images superimpose i.e. condition of no parallax. Once this is done the stereo-scopic relief is evident and this aids in the interpretation of the negative carbon replicas. Using this method it readily becomes apparent that the two lenses act as a simple magnifying glass and the visual magnification is raised by a factor of 2.5 to 3.5x that that of the micrograph fig 9 d-f.

4.32. The advantage of stereoscopic pictures with particular reference to fatigue.

The replicas were prepared by the method outlined in *4.26 The micrographs are set out so that the interpretation and three dimensional effects are similar to those which would be obtained if the observer were situated within the metal surface.

Fig.10 consists of two stereo pairs, and is an attempt to compare and contrast the additional information gained from a 3 D picture. In fig.10 a, which is a negative carbon film, the carbon Q gives rise to shadows which in mono view would be interpreted as a micro crack. When viewed in stereo, it becomes readily discernable that these shadowed points Q', Q", Q"' are merely steep ridges formed by the action of slip adjacent to the grain boundary. Consider Q'"; this appears to have a small carbon interface which in mono view could be interpreted as the carbon replica of the crack, because the contrast conditions are all satisfied. However when looked at in stereo it becomes obvious that this carbon film is on the side of the carbon film away from the plane of the paper, .i.e. it cannot be a crack, but it is part of the extruded ridge formed by slip at the boundary, which is at an angle to the carbon film. The boundary is 1,2,3,4, points 2,3, being the points below the plane of the micrograph and in air (because this is a negative carbon film) i.e. these small ridges are carbon replicas of a slip step formed by transgranular slip and grain boundary slip as shown diagrammatically in fig.10 b. Q" is the only point which appears to have a small crack associated with the re-entrant step, as formed by grain boundary slip which may be detected from the stereo effect. The boundary is also shown to have slipped at U and this slip is associated with little slip in the adjacent grain boundary. Also shown in fig. 10 a, is the slip band intrusion G which in stereo does not appear to form a very narrow crevice as the taper sectioning techniques *4.41 have portrayed. Monovision would indicate that the shadowing G is a result of transgranular crack nucleation. In fig.10 c the transgranular phenomena are shown which in stereo show that the intrusion may form a narrow fissure G, but the orientation of these to the surface is not identical. The fatigue topography can be detected by using stereo, and the small dark lines which appear e.g. G' are due to further intrusions in the shadow of the major intrusion. This fact has been shown before in taper sections *4.41[15].

In fig.11 a the intergranular phenomenon is shown which has occurred in a migrating grain boundary S'", because there appears to be two positions of the boundary. These two positions have been detected as a result of grain boundary slip and the boundary has cracked at A whilst in the second position of slip S"'. The overall macroscopic deformation involving the surface undulations or rumples and grain boundary relief S"" can be readily seen with greater ease than could be detected by the graduation in intensity due to the high-light shadowing.

4.33. Stereoscopic pictures from two stage plastic carbon replicas.

A large volume of work was carried out on comparing the results of carbon films obtained from the primary plastic replica * 4.2 with those obtained direct from the metal surface * 4.26. Similar results were obtained from both methods but they differed in the depth and acuity which was given to the crack.

Plastic carbon replicas.

The examination of the final carbon replica *4.2 by stereo electron microscopy (fig 11 b,c,) showed that the primary plastic film distorts upon stripping fig 11c. The origin of this distortion is more clearly outlined in fig 12 a-h.

The residual elastic strain from the stretching of the plastic finger causes it to distort still further. These effects are demonstrated visually in the stereo pictures of fig 11 b,c,. Fig 11 b shows a grain boundary with many small cracks (tubular holes[19]) situated in the grain at points A and F . The stereo effect using the plastic-carbon technique is less striking than the 3 D effect obtained from the direct carbon replicas floated off in 2 % bromine in alcohol and is most likely due to the elasticity of the primary plastic film. This effect can be easily demonstrated by stretching a thin plastic sheet to fracture (eg. a small piece of polythene). The fracture ends tend to curl and shrink to give rise to a large amount of distortion. If this happens on stripping, and the evidence is that it does fig 11 c , an artefact is produced, as the replica fails to be a faithful reproduction of the surface. These artefacts can be recognised and interpreted very easily by stereo vision.

Consider first the monovision interpretation of fig 11 c and in particular the crack A'.A".A"'. In mono vision the crack appears to be in the surface and of length A"A"'. In stereo vision A'A".is the stretched piece of plastic which was inside the crack.i.e. the replica of the crack walls, but upon stripping the plastic has stretched and on release from the surface crack, it has twisted and curled to lie in a north-south orientation, parallel to the surface plastic (see fig 12 g (1). Thus the crack front A" is lying parallel to the object surface and appears to be the base of the crack A"'A". The shadow of this crack A' gives the clue to the collapse of the plastic film upon stripping prior to shadowing. The crack A"" however does not give any indication that the plastic was stretched upon stripping, but the tongue of plastic replicating the crack at A"" was perpendicular to the object surface plastic during carbon and metal evaporation, but subsequently fell onto the surface when the plastic was being dissolved from the carbon film.

Conclusions.

1) Primary plastic replicas from rough surfaces tend to exaggerate the depths of the intrusions and cracks, and may be used on this basis as a detector of crack nucleation.

2). The crack depth of any shadowed negative replica depends upon the length of the shadow, which in turn depends upon the inclination of the crack replica to the direction of shadowing, at the time of shadowing .

3). The results from the entire fatigue programme are wholly interpretated using the direct carbon replica which gives a faithful replica of the surface.

4.4 Taper sectioning methods.

A useful technique for the observation of the accumulated fatigue damage in the rough surface has been that of taper sectioning developed by Wood and Bendler [15] and modified by Wood et.al.[153]. The surface topography is protected by an electrodeposited layer of metal and the taper section is obtained by grinding a flat 100 μ beneath the surface of the cylindrical specimen fig 13 a. The surface may then be examined by optical and electron microscopy[153].

4.41. Woods theory of fatigue.

Using taper sections and two stage plastic replicas from the metallographically prepared surface, Wood[17, 31] divided the process of fatigue into two distinct mechanisms ; an intergranular phenomenon (high strain fatigue) and a transgranular phenomenon (low strain fatigue). This division is supported by others.[162,163]

Later papers by Wood[153] postulated the presence of pores, or internal microcracks ahead of the primary transgranular crack originating from the surface. As the crack advances it ' sweeps' up these 'pores ' which give rise to irregular cracks on the fracture surface as the crack propagates through the metal.

The disadvantage of this theory is as follows:

1) The 'pores' which have clean surfaces could reweld on the compression cycle *2.4

2). As the 'pores' are formed ahead of the crack and are not connected to the atmosphere, one could argue that successive removal of the surface by electropolishing should not increase the fatigue life *2.0. *4.8

3). Theories required to postulate the formation of 'pores' are thermodynamically unfavourable unless these voids are formed on second phase particles.[164.165.]

The following sections discuss alternative possibilities which were not considered by Wood[153].

4.5 Action of metallographic reagents on high concentrations of point defects.

In order to produce a large concentration of point defects, a piece of O.F.H.C. Copper was thermally cycled by quenching into water from 1,000°C. This was repeated 10 times and after each quench a section was cut out of the specimen. The final piece was annealed at 300°C for 10 hours to relieve the quenched in stresses. The sections were examined metallographically.[155,160,167,168] It was found that there was a definite region adjacent to the surface which was oxidised as a result of the cycling. At greater distances from the surface all the reagents [154,155] alcoholic ferric chloride, 10% ammonium persulphate and ammonium hydroxide gave a higher rate of attack at the grain boundaries as shown in fig. 14.

Conclusion. The results indicate that the metallographic sectioning technique [15,153] described in *4.4 could lead to misinterpretation due to preferential attack at the regions of high concentrations of point defects, a conclusion subsequently supported by Grosskreutz et al.[156]

4.6 Taper sections across a crack or intrusion front.

Fig 13 shows diagramatically another interpretation of the results of Wood[153]. A crack front (or intrusion front) is irregular *5.3 fig 37. and any section across the metal surface as indicated in fig 13 a,b will cut regions of metal in which the crack has not passed as well as regions regions through which the crack has passed. Fig 13 c represents a plan view of the crack (or intrusion) front as will be seen optically. The crack will appear to be that region contiguous with the surface and the 'pores' will appear to be regions of the matrix decohesion ahead of the crack whilst in reality they are segments of the irregular crack(intrusion) front fig 13 b,c. A similar argument has been put forward by Laufer and Roberts[157a] and Teer and Wesson[157b].

Another effect of taper sections is to decrease the angle subtended at the vertex of the intrusion fig 13 e,f, as well as producing a vertical magnification which tends to deepen the intrusion with respect to its surface base. fig 13 f.

A programme of work to test Wood's hypothesis *4.41 is given in * 4.8

4.7 Summary.

The direct carbon replicas prepared as outlined in *4.26 are considered far superior to the other methods described for the purpose of investigating how the crack nucleates on the surface. This is based upon the fact that the crack nucleation can be detected at the free surface without any metallographic preparation after the fatigue cycling. The only artefact which can be produced is due to the folding of the carbon film. This however can be readily detected in the electron microscope and these regions may be easily discounted. The method described is also superior because about 80 to 90 % of the grid is covered with carbon film, although with higher strains and longer lives, the carbon replicating the crack tends to fold and lie parallel to the object surface. e.g fig 30b

The scratches on the surface of the specimen are deformed as a result of slip and hence the macroscopic displacements parallel as well as perpendicular to the surface can be seen using stereo vision.

4.8 Specimens crept to produce intergranular cavities and subsequently fatigue tested.

The object of the experiment is to test the hypothesis put forward. *4.41 (2), namely that if 'pores' were formed internally, then the periodic removal of the surface during the fatigue test should not increase the fatigue life indefinitely.

It is well known that many metals fail under prolonged stresses at elevated temperatures by the occurrence of intercrystalline cavities[169]. In general the cavities are more abundant at a given temperature if the strain rate is low, and for a given strain rate the cavitation is more marked, the higher the temperature. The cavities are associated with those grain boundaries which are perpendicular to the stress axis, and are dependant upon the orientation difference between the grains. Cavities are not associated with a twin boundary. The cavities are regularly spaced in the early stages of development and the intercavity distance increases as the test temperature increases e.g. 10^{-4}cm at 120°C; 10^{-3}cm. at 400°C.[169] The smallest cavities observed (by optical microscopy) were no greater than 0.5×10^{-4}cm. [169].

There is considerable controversy as to the nucleation and growth

of these cavities[169-175]. Ishida et.al.[174] have shown that the lower creep rates result in a high ratio of $\frac{e_{g.b}}{e_t}$ where e_t is the total strain and $e_{g.b.}$ is the strain due to grain boundary sliding. Cavitation has been observed in the three stages of creep ; primary, secondary, and tertiary[166] Hence internal cavities could be introduced into a fatigue specimen if the material from which they were made had been previously creep tested at a very low creep rate.

If this material is tested in fatigue in the push-pull mode so that the cross section is uniformly stressed, then cracks which nucleate at the surface could propagate by joining those cavities at the grain boundary formed during the prior creep history. However if the surface of the fatigue specimen is removed after cyclic stressing for 25 % of the fatigue life *2.0, the life could be prolonged indefinitely[14] if the internal cavities formed during creep do not act as crack nuclei. If the internal cavities do act as crack nuclei, then the electrolytic removal of the surface layers will have little or no effect on the fatigue life.

Similar tests have been performed on powder compacts[178] where the total internal surface area of the pores is much greater than the free surface of the specimen. These tests showed a tendancy towards longer lives with the periodic surface removal, but the lives thus obtained were within the scatter obtained for the straight forward fatigue tests of powdered compacts.

4.81 Creep frame.

Eight points of a B.N.F. creep frame were wired up as shown in fig 15 and 16. Each furnace was a three zone furnace with upper, middle and lower windings. The power to these windings could be varied by the two variable resistors M and N in the following manner. Resistor N was permanently connected to the middle winding and the resistor M could be either placed in series with the upper or lower furnace windings by means of the double pole switch K. By this means an even temperature could be obtained over a 7 inch region of the furnace. The furnace could be moved vertically so that this region spanned the gauge length of the specimen.

The furnace control worked on the expansion of the central tube to the furnace relative to the rod J which seated on a diaphragm fig 16 . A contraction of the furnace tube(equivalent to a temperature drop) forced mercury into the narrow bore glass tube d where it made contact with a platinium electrode at a . This completed the 8 volt circuit which activated the relay b which in turn operated a mercury switch e to restore the full power to the furnace. As the furnace tube expands, the level of mercury falls in the narrow glass tube to break the 8 volt circuit which in turn interupts the power to the furnace through the mercury switch e . C is a small resistor to limit the current drawn

when contact is made at a . The increment resistor 1, fig 15, was in parallel with the mercury relay b, its function being to allow a certain percentage of the power to go through to the furnace when the relay was open circuit. This decreased the frequency of the power cycle and led to a more even temperature over the gauge length.

The current through the furnace was read from a millivoltmeter A which recorded the potential difference across the resistor P . This was callibrated to record the current flowing in P . The over temperatu cicuit was controlled by the Ether controller t which was set 15°C higher than the creep test temperature and if activated, power was cut from the furnace through the relay S. This relay could only be reset manually by the double pole switch U.

The time of the creep test was measured by the time clocks q and the bulb r indicated that power was on to the furnace.

The test specimen S (dimensional details fig 18) was clamped in the collars A (fig 17) of the extensometer which were of the dial gauge type if the gas boxes were used. These consisted of a metal rod B fixed to the top of the specimen. A tube C fixed to the bottom of the specimen surrounded the rod B , and was fixed to the micrometer D which then measured the relative difference between the points B and C as the specimen was creep tested.

Axiality of the specimen was obtained by the universal joint E and loading was by means of a 5:1 lever ratio .

4.82. The material used initially in this investigation was 70/30 single phase ∝ Brass. This material gave negligible ductility at 200°C and subsequent metallographic examination showed the presence of a second phase at the grain boundary fig 19 . Chemical analysis showed that the material was of low impurity level and well within the British Standard Specifications.

O.F.H.C. Copper was then obtained which was tested at the following temperatures : 149°C, 204°C, 249°C, at stresses between 11,820 and 5,190 p.s.i. The results are shown in fig 20.

At the completion of the test the load was removed and the complete section as shown in fig 17. was removed from the furnace and the grips E quenched in cold water to cool the specimen S. The time taken for this operation was 2 minutes (5 minutes for the gas boxes).

4.83 Metallographic examination.

Metallographic examination was carried out with a modified Cocks and Taplin[167] method which showed that intergranular cavities were present at all the test temperatures fig 20 . If the longtitudinal sections were electropolished in the ethanol- nitric electrolyte * 4.06. many more cavities could be detected. It was found by interferometry that the

cavity profile altered with increase of the electropolishing time. Therefore to keep the electropolishing time to a minimum, the specimens were metallurgically prepared on 'brasso' or γ Alumina with a small amount of 10% ammonium persulphate and ammonia to remove the flowed layers. The specimens were then electropolished for 30-45 seconds. The results are shown in fig 21 a,b,c.

4.84 Fatigue of Creep tested material.

Four fatigue specimens fig 3 d were machined from the gauge length of the creep specimen fig 18. These were electropolished in an ethanol- nitric acid bath * 4.06. at 0°C until all the machining marks had been removed. Two of these specimens were then fatigued in a Schenck push-pull machine at a stress of $\pm$ 11,600 p.s.i. to life *4.021. The other two specimens were fatigued for 1.8×10^5 cycles (25% life). After the removal of a known depth from the surface, the specimens were retested at the same stress for a further 1.8×10^5 cycles and this proceedure repeated until failure.

During electropolishing many of the intergranular cavities became visible and in an attempt to prolong the fatigue life by surface removal [14] several microns were removed from the specimen. The results are presented in Table 1.

The creep tested material was observed to contract when subjected to the initial thousand cycles, which resulted in the stress cycle being performed about a mean positive stress of $\sim$ 600 p.s.i. This was not corrected on the specimens fatigued to life, but it was corrected on those specimens whose surface was removed after 25 % life.

The same polishing conditions were used to prolong the life of a specimen machined from the as received material. One specimen was satisfactorily tested for 8 surface removals giving a life of 250 % of the normal life and broke due to clamping failure. The second specimen was repolished 14 times in all giving a life of 370 % of the normal life indicating that the polishing medium does not produce stress concentrations at the base of the surface intrusions, and as such the electrolyte was not responsible for the inability to prolong the fatigue life of the previously creep tested material.

4.85 Metallography of the 'fatigued' creep material

A longtitudinal section of a fatigue tested sample manufactured from the creep tested material revealed a possible explanation as to why the fatigue lives were not increased by the periodic removal of the surface layers. The grain boundary cavities were found to have linked together to form a crack 400 microns beneath the surface, fig 21f. (note this is not a taper section * 4.4.).

5.0 Results and Interpretation.

5.1 Introduction. The fatigue machines used in this investigation are described in * 4.01 *4.02 *4.021. The material and dimensional details are discussed in *4.03 and after the second electropolish the surface was scratched with $\frac{1}{4}\mu$ diamond paste as described in * 4.25. Other deformation modes were also investigated i.e High strain dwell tests *5.26 and compression fatigue tests *5.27. Each micrograph is interpreted in terms of the dislocation theory and the model which is discussed in *6.0 to *6.5. Whilst this practice may overlap the discussion, it is considered preferable.

5.2 High strain fatigue results.

Specimens of O.F.H.C. Copper were tested for $100\frac{1}{4}$, $200\frac{1}{4}$, $250\frac{1}{4}$, $300\frac{1}{4}$ $350\frac{1}{4}$ $400\frac{1}{4}$, 450 $\frac{1}{4}$ $500\frac{1}{4}$ cycles at a strain range of $\epsilon_p \pm 1.0\%$ to $\epsilon_p \pm 1.16\%$ at room temperature giving a life of 1,600 to 1,000 cycles. The average fatigue life was 1,200 cycles. fig 22 a.

The specimens were cycled such that the scratched surface always went into tension first followed by the compression cycle. The test was stopped such that the the scratched surface was undergoing the tensile cycle. This ensured that the cracks were opened up for the subsequent replication * 4.26.

During these high strain fatigue cycles the specimens increased in length by 3 %. If the specimen were allowed to dwell for 10 minutes every 10 cycles with the same surface in tension, then the elongation could be as much as 6% at 25% life. This could arise from the small tensile force which arises from friction in the floating shaft *5.1. and the Ronay effect.[131.]

In all cases given below there has not been any post fatigue preparation apart from replica preparation, and so any surface relief produced at grain boundaries etc. is due solely to the result of dislocation interaction during fatigue. The surface was also very carefully prepared to ensure that that it was flat over the boundaries; the latter could not be detected by stereo electron microscopy or optical microscopy prior to fatigue.

5.21. $100\frac{1}{4}$ cycles.

In the first 1% life little evidence of crack nucleation was detected. Deformation was found to proceed by slip and the surface topography produced must be a combination of the slip systems operating and the orientation of the operative slip system to the surface. Fig 23 a shows the slip traces a, b, and c produced in the two grains 1 and 2. The scratches W are not displaced within the matrix except adjacent to the grain boundary (ABC) at U. In this region there has been considerable slip activity in which the grain boundary has acted as a source of

dislocations, as shown by the displacement of the $\frac{1}{4}\mu$ scratch . Examination in stereo shows that the deformation in this region has resulted in the relative movement of grains 1 and 2 at their common interface both parallel and perpendicular to the surface.

This deformation at the grain boundary is usually seen where the slip planes are nearly parallel to that part of the grain boundary which slides.

An alternative method of grain boundary slip is shown in fig 23 b which shows the well reported phenomena of grain boundary intrusion and extrusion. The grain boundary extrusions C are separated from the grain boundary intrusion B by 'islands' of grain boundary which are at the same level as the two adjacent grains. The intrusion extrusion phenomena has led to the relative movement of the two grains at their common interface as shown by the displacement of the scratch M at the boundary.

Where slip is nearly parallel to the grain boundary interface, a third phenomena can be detected. This is the migration of the intersection of the grain boundary with the surface interface, (as opposed to the subsurface boundary itself). Fig 24 a. shows two such examples S and S', the former resulting in a pronounced widening of the boundary between the grains 1 and 2. This boundary deformation often leads to crack nucleation fig 25 a. Fig 24 b is a low magnification picture to link the surface topography of fig 24 a to 24c.

Fig 24 c shows a mixture of transgranular and intergranular deformation. The lower grain 1 shows a transgranular extrusion H and an intrusion G which have not caused the displacement of the $\frac{1}{4}\mu$ scratch c.f. fig 1c . However stereo vision also shows that these intrusions are not as sharp as would be seen on taper sectioning, although they are sharp enough to cause stretching of the primary plastic replica as experienced in the work outlined earlier. *4.33. In the adjacent grain 3 the trans—granular phenomena appears to give rise, in mono view, to crack initiation at Q. This region Q is a transgranular intrusion at the base of an extrusion. The surface profile at this point is indicated in fig 24d and as can be seen the carbon marked X is giving rise to the long shadow and is the small intrusion occurring adjacent to the extruded material. This profile could not have been detected in monovision from the graduation in intensity from the shadowing deposit.[159] Section 4 of the upper grain has suffered very little plastic deformation and therefore has not brought the grain boundary between 2 and 4 into relief, even though the boundary between grains 3 and 2 has suffered relative movement at u, which from stereo vision can be seen as a grain boundary slip step, the step riser being the grain boundary. The boundary between grains 1 and 4 shows that grain boundary slip has occurred across the slip bands M and N perpendicular to the surface (*6.5).

The boundary between 5 and 1 shows the first signs of crack nucleation at N N' and N" due to a process leading to grain boundary slip and microcracking. This can be seen more easily in a larger magnification of these plates.

The grain boundary widening between grains 1 and 2 fig 24 a is possibly due to reorientation of the grain boundary region as reported by Snowdon[180] and is shown in fig 25 a and b . This reorientation leading to serration of the grain boundary, occurs with the relative movement of the grains with respect to each other (U) and this may lead to cracking K when grain rotations also occur fig 25 b.

These features become accentuated with increase of the number stress reversals.

5.22 200¼ cycles

At 200 cycles all grain boundaries are delineated as a result of the dislocations contained in them or as a result of the passage of dislocations through them. The grains at the surface are extruded to to allow grain boundary slip and rotation (Fig 26). The scratches on the surface (fig 26a) show that the boundary has slipped at U as a result of the slip band causing the extrusion H which runs to join the triple point. The intrusion or fold G has caused the grain boundary ridge at U' as indicated by the displacement of the scratch U".

Fig 26 b is a low magnification picture which links figs 26 a and c. In fig 26b the scratch W' shows that the grains 1 and 2 have suffered a rotation of 10 degrees. The scratch is continuous across the surface grain boundary at W' but the two parallel scratches, indicated by W" shows that the grain boundary has slipped at U. Note the scratches W" cannot be resolved without the use of a magnifying glass.

The scratch W"' in fig 26 b is the scratch W"' in fig 26c and shows that the grain 2 has altered its orientation with respect to the grain 1 and 3 due to the deformation which has taken place during fatigue cycling, and is probably a direct result of the dislocation motion which has taken place in grain 4 in the slip band S . The evidence for this, is derived from the displacement of the ¼μ scratches W' and W" which indicates the macroscopic deformation. When these grain rotations and translations are taking place, it is quite possible for the grain boundaries to slide over small distances.e.g. over the boundary between grains 3 and 4 in fig 26 c the scratch W' is displaced at U"" but not at U'".

The scratches running across the slip planes δ show that the reverse slip does not take place in the adjacent slip plane as shown by Wood and Bendler for low strain fatigue [15]. In this case the slip δ has been initiated to allow for the orientation of the grains in these regions and the reorientation has probably caused crystallite formation Z .

(The clarity of the scratch across this region of the surface indicates tha the surface was macroscopically flat in the pre-fatigued state.)

The formation of a grain boundary intrusion along the length of a boundary fig 27 a B allows transgranular dislocations to escape from the crystal onto two free surfaces. A higher magnification of this micrograph shows more clearly that the region at the base of B has suffered little heterogenous deformation, whilst the intrusion sides B show clearly the consequence of complex slip processes arising from dislocation movements c.f. Fig 41 c,d,e,f,g,h,

Some of the grains become the sites for large folds, corrugatio or intrusions, see fig 27 a at X and fig 27 b at G . These folds allow grain boundary sliding U to occur with the formation of microcracks O within the the boundary fig 27 a or at triple points U' fig 27b . Fig 27 c shows the transgranular deformation resulting in the formation of intrusions and extrusions H which invade the neighbouring grain. Stereo vision gives an overall picture of the macroscopic deformation, viz the extrusion of one grain with respect to its neighbour and the general undulating surface topography. The intrusions G, when viewed in stereo can be seen to be devoid of crack nuclei at their tips, whilst in mono vision it could be interpreted that these shadows are the result of the carbon within the intrusion crack front.

With increasing life the surface becomes progressively rougher and the crack nuclei become deeper and longer by microcrack nucleation and linkage at the surface.

5.23. 250¼ cycles.

The surface rapidly becomes rougher and grain boundary intrusions G begin to form cracks J at their bases fig 28 a . The slip line 7 fig 28 a and 7' fig 28 b,c, have a curved appearance due to the small scale surface roughening. c.f. fig 43 d . This has been referred to as lattice bending [181], and is very common in high strain fatigue particularly near to grain boundaries. In fig 28 c η", stereo vision shows that in this case the "lattice bending" is a result of the superposition of an intrusion type slip band adjacent to an extrusion type grain boundary and vice versa. Thus an inclined plane (the slip plane) appears bent. (fig 43 e.)

The transgranular slip steps Q'and Q" fig 28 b between the undulations are sharp reentrant semicircular slip steps. Monovision gives the false impression that these regions Q' and Q" are transgranular cracks. This transgranular phenomenon Q, Q' and Q" is shown in fig 28 b and and shows the small regions of heterogenous deformation which occurs in

high strain fatigue. In fig 28 b the high contrast at Q is due to the carbon film on the slip step being perpendicular to the plane of the object and not due to the carbon film lying in the crack.

Grain boundary sliding results in the formation of microcracks (or 'pores' connected to the surface) which link up in the plane of the boundary to form a crack which then propagates by the linkage to other microcracks formed by the stress concentrations. In fig 29 a, the micro crack A' has grown by the linkage of smaller micro cracks A"' which are nucleated in the same grain boundary. (note the shadow A"" is not due to a grain boundary crack, but is due to the slip band intrusions G and G', which have very . sharp crevices at their bases.) Stereo vision shows that there are small cracks associated with these intrusions. The carbon film lying in the boundary crack interface does not cast a shadow as it is overshadowed by an intrusion G'. At this stage of life ,there are several other examples of crevice formation at the root of the slip band intrusions near to grain boundaries. However these are not as deep as the grain boundary crack A' or the microcracks A"'

The grain boundary crack A" has taken place in a migrating grain boundary S as can be readily observed using stereovision. However at the point S' the migrating grain boundary has withstood the crack nucleating mechanism as can be seen from the shadowing. A similar result could have been obtained had the carbon film moved into the shadowing direction at this point, and stereo vision suggests that this has not happened in this case. The other transgranular phenomena G° fig 29 a is due to the re-entrant slip steps and not due to transgranular cracking. The re-entrant slip step G_t^2 does however contain a microcrack at its base, where the transgranular slip is parallel to the grain boundary. At this stage of life, cracking was observed in those boundaries associated with separate grains, which had undergone different amounts of plastic deformation. c.f. fig 29 a and b.

5.2.4 300 cycles and greater.

Once the crack nuclei are produced on the surface, they must grow laterally along the surface before they can increase in depth. The replication of the surface then becomes difficult as the carbon film tends to be keyed on to the surface by the deeper cracks. However even when the carbon film is removed from the surface, there is the problem of the replica folding, to lie parallel to the surface of the object plane. This effect is complicated also by the folding of the carbon film during preparation, although this can be reduced by successive transfers between (water + alcohol) and (absolute alcohol) baths paying particular care to the surface tension of the liquids. However not all grain boundaries show microcracking and in fig 30 a, the grains are coplanar at D but from D to E the grains are displaced across their common interface and the scratch

W' is displaced at E. The dislocation loops producing the deformation in the slip plane XD can also be responsible for the deformation along DE assuming that they may cross slip in the plane of the boundary, or a parallel plane. But these dislocation loops are not directly responsible for the deformation in the neighbouring grain, i.e. that deformation giving rise to the displacement of the scratch at E. Therefore whilst a dislocation can cross slip along the boundary between two grains, it does not allow the dislocation to pass into the neighbouring grain. For the stress to be transferred from grain to grain, other slip systems have to suitably operate in the adjacent grain . The serrated grain boundary ABCDEFGHIJ fig 30 a , is shown in a line diagram in fig 43 b, and acts as a stress concentration upon dislocation sources in the neighbouring grain in such a manner that the slip produced relieves the stress concentrations at the boundary.

In some regions where the deformation mechanism has progressed more favourably fig 30 b, the grain boundary slip can be fairly large $\simeq 0.65\mu$ at U and this accompanied by large grain reorientations. In this micrograph A is the grain boundary crack where the carbon replicating the crack interface is lying parallel to the object plane and B is a grain boundary intrusion.

As the fatigue process continues the deformation becomes more characteristically unidirectional. Fig 30 c shows the junction of three grains 1, 2 and 3 which are crossed by two scratches W and W'. The transgranular slip in grain 2 has caused a unidirectional displacement of 0.5μ in the scratch W' at each slip band. This results in the displacement of 2μ along a distance of 8μ in grain 2. This unidirectional displacement is accompanied by the sympathetic movement of material in grain 1 as indicated by the scratch W . Slip has taken place in the grain boundary interface between the grain pairs 1 and 3, and 1 and 2 to give rise to grain boundary cracks A' and A.

Fig 31 shows how the cracks grow laterally in the surface layers. Fig 31 a shows an intruded grain boundary A which has opened up to a width α (fig31 b) by slip at the boundary interface between grains 1 and 2 as shown by the displacement of the scratch W in fig 31 c . This relative movement within the boundary interface ($\simeq 0.35\mu$), which lies at 45° to the maximum surface tensile stress , has produced microcracks at the slip band / grain boundary intersections denoted by N in both fig 31 a and b.c . Further along the boundary, between grains 1 and 2 fig31 c the slip in the grain boundary has not given rise to the formation of microcracks. The boundary at X' has given rise to slip perpendicular to the micrograph in such a manner that the step does not cast a shadow. At X the slip is not confined to the boundary and probably results from a grain boundary ledge * 6.2 as the boundaries at X' and X" are not coplanar.

The crack A' has occurred at the intersection of four grain boumdaries of which the only boundary to remain coherent is that between grains 1 and 4. fig 31 a . The transgranular slip occurring in grains 1,3 and 4 has not given rise to intrusion cracking.

With increasing fatigue cycling , more grain boundary micro-cracks are nucleated in the surface layers allowing them to grow laterally. Transgranular slip may take place more easily as the surface grains are surrounded by unconstrained surfaces perpendicular to the surface of the specimen and the intergranular cracks grow deeper until the bulk of the crack is propagating by the stage 2 mode *3.33 .

5.25 Displacement of scratches.

Wood and Bendler have shown that there is no displacement of a scratch as a result of fatigue cycling. *1.4 In this investigation scratches were found to have been displaced and rotated across the slip bands (e.g. fig 32 a W"' and W"") and at grain boundaries, and these displacements increased with either strain amplitude or number of cycles. These displacements at the grain boundaries are summarised in Table 2.

Fig 32 a shows this effect when a replica is viewed in stereo. It can be seen that the scratches in the active slip region are displaced to one side of the main scratch W' and W" whilst the overall displacement across the slip band is zero. This suggests that the slip causing the intrusions are formed by dislocations of similar burgers vector and not from dislocations of opposite sign. *6.5 In the same grain the scratches are displaced across the slip bands by 0.1 μ at W"' and W"". This displacement was similar to the displacement reported for unidirectional tests[15] * 1.4.

Fig 32 b shows the displacement and rotation of the scratch across the slip bands and at regions between the slip bands (termed slipless [11,16]). The displacement of the scratch at W' and W"' without the formation of slip steps is consistent with the passage of a screw dislocation parallel to the surface c.f. fig 41 e . Another factor of significance is the difference in the displacement of the two parallel scratches within the same slip band/ plane . For example the displacements of the scratch at W' is not identical to that at W" and that at W"' is is not identical to that at W"". This is over a distance of 2 μ and may well arise from cell formation within the grains. * 2.7.

5.26 Dwell tests.

High strain fatigue tests were interupted every 10 cycles after the first $\frac{1}{4}$ cycle and the cycling stopped for 10 minutes. In this mode of fatigue testing the appearrace of the slip lines became similar to a static unidirectional test or creep test [182]. The specimen elongated 6% at 25 % life.

Fig 33a indicates an additional deformation mechanism to those already described. Slip systems were found to nucleate cracks at their mutual intersection with the surface, e.g. L" and L"'. The remaining shadows arise from the slip steps resulting from their intersection e.g L' . As the fatigue process progressed these microcracks became deeper without spreading along the slip planes and could be better described as 'pores'[153].

5.27 Compression fatigue.

High strain fatigue tests were performed in push-pull with a compressive preload in a Schenck fatigue machine *4.021. Due to the test being performed in the plastic strain region, the mean of the cyclic plastic strain range (*2.6) moves towards the zero mean with increasing life. The latter part of the fatigue life is therefore spent cycling about a mean zero. Theoretically the diameter of the specimen increases and its length decreases. This has been observed on the macro-atomic scale.

Fig 33b. shows that certain sections of the grain boundary may slip at the physical boundary interface at the surface, to give rise a flat slip surface. This is shown on the photographs as S The other regions of the boundary show that 'co-operative' slip has taken place, i.e. where an intrusion is formed on one side of the boundary, an intrusion must form on the other side. The former may be said to apply to regions of a grain boundary which are coherent across the interface whilst the latter applies to regions where the boundary is incoherent across the interface. * 6.2 This co-operative slip gives the impression that the dislocations have crossed the grain boundary. *5.20.

At the base of the intrusion J a small microcrack has nucleated which extends 3 μ from the grain boundary into the grain. The other intrusions have large radii of curvature at their extremities. The deformation around the triple points is shown in fig 33 c. The grain boundary triple point A has intruded beneath the surface due to its line tension preventing it from extruding with the rest of the surface. Once again the intrusion G is shown to have a large radius of curvature at its front, whilst the slip steps G' shows the irregularity of the surface within the slip band. Where the slip bands intersect the twin boundary V,V',V",V"',V"", the boundary has slipped with the production of cracks. There is also an absence of slip within the twin boundaries.

Some twin boundaries do not arrest the slip process and allow some of the dislocations to pass through the boundary. These boundaries are still hosts for crack nuclei as shown in fig 34 d A,A', but in general the surface topography is very rough in the regions adjacent to the boundary e.g. H.

In many micrographs there has been insufficient evidence to prove

that grain boundary migration takes place, in order to allow the grain boundaries to slide at the interface. Fig. 34 a,b, shows this migration. The grains are outlined in fig 34 b and the grain boundary AB rotates and migrates to CD to allow the dislocations to cross slip in the new grain boundary . These dislocations slip over a distance of approximately 10 μ in this boundary. The scratch W indicates how the material is displaced at this interface and the scratches W' and W" indicate that the slip . .in the slip bands N and O is not a to and fro movement as has been postulated.[15] The dislocations passing in the slip band N, return along both slip bands O and P.

5.3 Low strain fatigue.

The O.F.H.C. copper specimens (dimensional details fig.3.b) were prepared by electropolishing and scratched with ¼ μ diamond paste and tested in an Avery bending fatigue machine *4.02. The tests were stopped and examined destructively after 10 %, 25%,50%, and 100% life.

The examination of the numerous micrographs obtained from the low strain fatigue tests gave initial indications that the processes involved,prior to any evidence of fatigue damage during the incubation period *3.31,were basically similar to those occurring in high strain fatigue. Although the cyclic strain imposed on the specimen in low strain fatigue is nominally elastic, the anisotropic nature of the individual grains will set up small plastic strain components in some grains [183]. It is this small plastic component of strain which leads to a smaller percentage of true damage per cycle.

The plastic deformation taking place is concentrated into slip bands which may be arrested by shallow ¼ μ scratches, fig 35 a. Most of these bands are arrested at grain boundaries where grain boundary relief can be detected fig 35 This slip within these bands is not fully reversible as may be shown by the displacement of a square network of ¼ μ scratches fig 35c. This results in a misorientation within the surface material,and over many thousands cycles a unidirectional displacement is produced.e.g. fig 36 a W',W", when viewed along the the plane of the micrograph. This deformation mode produces a strain concentration at the boundary which slips to form an intrusion from which intergranular cracks nucleate A fig36 a. Triple points also suffer deformation by sliding on one or

more of the grain boundaries, as shown in fig.36 b at U, U' and U''. The transgranular phenomenon that occurs in the early stages of fatigue is on the whole non damaging, although there are some regions where cracks nucleate at the tip of the intrusions e.g. fig 35 b, R. Stereo electron microscopy shows that the majority of the transgranular phenomena taking place is non damaging, although replicas (either direct carbon or plastic carbon replicas) suggest severe transgranular crack nucleation when examined in monovision. Fig 37 a indicates slip (U) in the grain boundary having a small grain adjoining it which has suffered severe deformation showing both extrusions H and intrusions G. The long shadows are due to the steep steps and re-entrant angles Q produced at the intrusion / extrusion / surface boundaries and not due to the carbon film penetrating a crack,as could be the interpretation if monographs were used. The stereo and mono vision interpretations are shown in fig 37 b and c respectively.

Fig 38 a shows the boundary conditions as a result of the transgranular deformation. Consider the grain boundary extrusion C . This micrograph is best interpreted in conjunction with fig 38 b, where 5,8, represents the boundary at the plane of the surface of the specimen and the plane 5,8,9,10, is the slip plane of grain A , which allows slip to take place to give the extrusion 5,8,7,6,1,2,3,4, on the plane 5,8,9,10, and parallel planes by slip through the regions which are considered of 'good' fit * 6.2. in the boundary 5,6,7,8, this accounts for the width of the slip band in grain A and the short slip band plane 1,2,3,4, fig 38 a in grain B. This interpretation is a direct result of the replica being a negative of the surface. It is worthy to mention that had the replica been a positive replica then the slip band 1,2,3,4, would be a result of deformation initiated and executed solely in the grain B. Being a negative of the surface means that this deformation contained in the box 1.2.3.4 in grain B is an external manifestation of the slip taking place within the bulk of grain A. Fig 38 c shows conventional grain boundary extrusions C and C' which have taken place in, but not through the islands of "good" fit. The region of misfit between the two good fit regions has restricted the extrusion process α and this is shown by the surface contour of the extrusion. Monovision would suggest that E and E' were grain boundary microcracks, but stereo vision shows these to be re-entrant slip steps at the grain boundary.

Low strain fatigue is traditionally associated with transgranular damage. Fig 39 a is an attempt to compare the damage caused by cyclic stresses in the grain boundary and within the grains. Fig 39 a shows a general low magnification picture of the surface topography formed during low strain fatigue. It shows grain boundary delineation as follows: the boundary 1-2 is delineated by two grain boundary microcracks A' and A" and an intruded boundary B. The boundary 2-3 is delineated by the serration phenomena * 5.21 at B" which changes into grain boundary intrusion at B' and B"' leaving

a portion of the material specimen between B' and B"' as the grain boundary extrusion at C This boundary has probably migrated in the region C and B'

The boundary 2-4 is faintly seen when viewed in stereo and the boundary 4-5 shows some relief due to slip in the neighbouring grain which has given rise to the crack nucleation at the base of the intrusion J.

The boundary 4-6 contains a sharp re-entrant slip step which appears to be associated with the triple point of the boundaries 4-6 and the continuation of 8-7.

The above transgranular phenomena are not considered damaging except for the cracks at the base of the intrusion J. The other highly shadowed areas e.g. Q and Q' are steep re--entrant slip steps c.f. fig 37.

In fig 39 d, the boundaries are delineated as follows Boundaries 1-2,3-4, 3-5, 3-6, 7-8 9-10,2-3 are delineated and the results can be observed by stereovision. There is one grain boundary crack A in the boundary 7-8. The transgranular phenomena in the grain bounded by boundaries 5-3-,3-4, are as follows; The shadows Q are a direct result of a sharp slip step on the surface and not due to a microcrack, The microcrack nucleation at the bottom of the intrusion is shown in stereo to be J J' and J"of which J' is the deepest . Whilst several micrographs show this crack nucleation at the base of the intrusion, the frequency of occurrence is far less than was expected from the published results of Wood.[31]

As the number of fatigue cycles increases the unidirectional displacements within a slip band increases, with an accompaning strain con- - centrations at the slip band/grain (or twin) boundaries, which causes either a crack in the boundary A (fig 40 b) or very large extrusions C or slip within the boundary interface region U . These phenomena are also accompanied by transgranular cracks as shown by J,J',J". as shown in fig 40 b. In these cases the slip across the twin boundary is not continuous, i.e. the slip lines are not formed by the same dislocation changing planes over the boundary, because at the end of each of the glide planes a step is formed.

6.0 Discussion.

The stereo electron micrographs have shown that the grain boundaries at the surface undergo plastic deformation when subjected to cyclic stressing . In the early stages of the fatigue process, this deformation is shown by the grain boundary relief which occurs prior to the grain boundary slip over small regions of the boundary.

The degree of grain boundary sliding (at the surface) increases with increase of strain, or for a particular strain amplitude as the number of cycles increased, which agrees with Smith[35] and suggests that the small number of stress reversals required to fracture specimens in the high strain region, where the S/N curve is steep is not a fundamental change of mechansim from the mechanism operating in the low strain region, as suggested by Wood.[17] The high strain fatigue mechanism is the hastening of the accumulative damage which preceeds the decohesion of the matrix.

Initially models are proposed to account for the grain boundary relief obtained during fatigue. This model is developed to explain the clustering of slip into slip bands and the unidirectional displacement of blocks of material within the grain leading to stress concentrations at the grain boundary/ slip plane junctions, which leads to intergranular crack nucleation.

6.1. In a stressed single crystal, slip takes place upon a plane when:

$$S_s = S_n \cos\theta \cos\lambda$$ [183, 184.]

where S_s is the shear stress component responsible for deformation.

S_n is the normal tensile stress.

$\cos\theta \cos\lambda$, Schmid factor where θ is the angle between the tensile stress and the normal to the slip plane and λ is the angle between the slip direction and the principal axis of the specimen. As the deformation proceeds, the normal to the slip plane tends to rotate into the direction of the stress axis. The magnitude of S_s increases with plastic deformation, and depends upon the orientation of the single crystal with the stress axis. This governs how many of the 12 (for f.c.c. metals) slip systems will operate.

In polycrystalline material the grain boundary separates crystallites of different spatial orientations and differing slip characteristics. Material in the polycrystalline state is highly anisotropic, which leads to some grains yielding before their neighbours. This necessitates that this deformation must be accommodated at the boundaries.

The highest stresses exist at the end of the glide plane bands and the accommodation of the stress or strain at the boundaries can be by grain boundary slip or by the operation of any 5 of the 12 slip systems[200] in order to retain coherency across the boundary.

6.2. The structure of the grain boundary.

The mechanism of grain boundary sliding will be determined by the interface structure and the orientation difference between the two grains. The interface structure will depend upon;

1. The concentration of point defects[185,187] at the boundary which permits the orientation transition from one grain to the adjacent neighbour, becoming very complex at the triple point.
2. The atomic planarity or smoothness of the interface[185,186].

A dislocation model can be ascribed to grain boundaries of low angle, i.e. if the misorientation θ is less than 15^{o} [188]. In this model, the boundary is described as a combination of tilt (rotation about an axis in the boundary) and twist boundaries (rotation about an axis normal to the boundary Fig 41 a and b. The former is described as a special orientations of edge dislocations and the later of screw dislocations.

For high angle boundaries the dislocation array becomes complicated as the individual dislocations loose their individual identity, and a specific dislocation model cannot be given.[176,177]. The macro atomic nature of the large angle grain boundary is thought to embody the following points:—

a. the boundary is not atomically smooth, but contains jogs at the interfaces these jogs are often called protrusions and have been observed by field-ion microscopy.[189-191].

b. The arrangement of the atoms are such that the boundary atoms do not have 12 nearest neighbours

c. There are regions of good fit and bad fit [186,192]. The regions of bad fit being of an amorphous nature due to the high disorder contained therein. The regions of bad fit should allow the grain boundary to slide in a visco-elastic nature if it were not for the protrusions in the boundary which are obstacles to the processes of grain boundary sliding.

The regions of good fit are regions of low coherency strains resulting from the absence of dislocations in the grain boundary interface.

This elementary picture of the nature of the grain boundary is confirmed by some of the recent work using the field-ion microscope.[190-193].

6.21. Subgrain boundaries[194,177b,* 2.8, *2.81].

It is convenient to describe crystal boundaries corresponding to a misorientation of 1^{o} as sub-boundaries. These boundaries are made up of an array of edge dislocations. (A single array of screw dislocations is unstable.)

6.3. Grain boundary sliding.

Previous investigations into fatigue deformation have not given any indication that grain boundaries might slip during continuous cycling at room temperature.

Definition of grain boundary sliding. "Grain boundary sliding is the relative translation of a pair of grains by a shear movement at their common interface. This definition is meant to include cases where shear takes place in a zone of finite width around the boundary, and cases in which sliding is a shear confined completely to the interface, if indeed this latter ever actually occurs in practice."[196].

Smith[35] found with Aluminium (at 20°C) that the grain boundaries were persistent to a greater depth than the transgranular phenomena, and if tested at a lower temperature, the intergranular damage was reduced. Broom[198] in a recent review paper, suggests the question which needs resolving in the fatigue of Aluminium at room temperature , is how much grain boundary sliding arises from

1. a creep like process.
2. a ratchetting process,
3. alternating grain boundary sliding.

Several papers have been published recently on the fatigue of metals at high temperature(* 2.924) where grain boundary sliding has been shown to take place using internal markers. It seems possible that grain boundary sliding could be responsible for the intergranular cavitation which accompanies high frequency, high temperature fatigue.

The results of the present investigation is that grain boundaries at 45° to the maximum tensile stress may slide over certain regions of the grain boundary.c.f. ref. 199 The sliding in this investigation was detected at room temperature by the displacement of ¼ μ. scratches and stereo electron microscopy. The sliding of grain boundaries has been observed in both low and high strain fatigue.

6.4 Relief of stress concentrations at grain boundaries by Taylors theorem.[200].

This may be divided into two separate sections depending upon position of the grain in the polycrystal.

1. A grain at the centre of the polycrystal.

This would cause the initial slip system to require a higher operating stress, because the grain is totally surrounded on all sides. Therefore the operating stress σ_o required to produce transgranular slip in a polycrystal may be written.

$$\sigma_o = \sigma_{c.r.ss.} + \sigma_{g.b.}$$

where σ_{crss} is the critical resolved shear stress

$\sigma_{g.b.}$ is the restraint exhibited by the grain boundary due to Taylor's theorem.

In this case before there could be any appreciable (unidirectional) deformation in the grain under consideration, the critical resolved shear stress must be reached on 5 slip systems in the adjacent grains. Thus for deformation to take place within the bulk material, the operating stress will be very high.

2. A grain situated at the surface.

In this case the surface acts as a sink for the egress of dislocations from the grain. The grain boundary component $\sigma_g.b.$ is now reduced and in some directions $\neq 0$; the presence of the surface will make slip easier to take place. Therefore slip systems giving egress of dislocations at the surface are thermodynamically more favourable than those which constrain the dislocations to the adjacent grain.

6.5. Dislocation Model .

If the dislocation originates from a Frank-Read source in the grain interior, the dislocation loop will be arrested at the free surface / grain boundary interface due to the lack of compatibility in the slip systems in the neighbouring grains fig 42 a and b. This remains as a stress concentration and will produce some local surface reorientation by its presence. fig 42 c. On the reverse cycle this stress concentration should be annihilated by reverse slip. However slip appears to be a quasi-ratchet mechanism[198] in that the full slip displacement does not take place in the same slip plane in the reverse cycle. Slip takes place on a new slip plane and is concentrated into bands. On the present model this would require a new dislocation source to operate in a parallel plane.

It has not been satisfactorily explained why slip is concentrated into bands in cyclic stressing. One possible explanation could be that these slip bands appear only at the regions of good fit in the grain boundary. This proposal affects the traditional model above in the following manner :

When a dislocation reaches the boundary the stress builds up to some value where the next favourable slip system is the one in which a screw component can cross slip in the good fit region of the boundary fig 42 d. Thus the dislocation is already on a new slip plane when the stress is reversed. This proceedure, if followed would result in a unidirectional displacement of a block of material within the slip band, or within the volume contained by the slip and cross slip planes. fig 42 e and f. This displacement is detected as a result of the displacement of a scratch by a dislocation, fig 41 c and d. A screw dislocation emerging parallel to the surface fig 41.c. displaces a scratch without forming a slip step whilst a screw dislocation perpendicular to the free surfaces does not

displace a scratch, but causes a slip step. fig 41.d. The opposite is true of an edge dislocation fig 41. f,g,h, Hence direct evidence for such a mechanism can be obtained, and is contained in fig 33 b,34 a,b, 35,b, 36,a, for example. However fig 32 a shows clearly the unidirectional displacement within a slip band at W' and W" and also the grain boundary relief which results if cross slip takes place within, or adjacent to the boundary.

Any residual dislocations left must slip on the plane containing the dislocation line and the Burgers Vector. For the residual edges fig 42 a the only planes available are the slip planes ABCD, and ADGF for the edges E and H respectively. (i.e. the planes upon which the screw dislocation cross slipped. The edge will only move if the stress exceeds the value

$\frac{ub}{\ell}$ on this plane where u is the shear modulus
b is the Burgers Vector
ℓ is the length of the dislocation line

The slab of material is displaced according to the inclination of the operative slip system to the surface. As each slip line observed on the surface can be the result of the operation of three slip systems, and each slip system is on a(111) type plane in a [110] direction, the actual result of slip can be more complicated than is suggested by fig 42 e and f.

Therefore the slip displacement within a grain boundary is confined to the region of good fit and the transgranular slip is confined in width and subsurface depth (fig 43 f) by the extent of the cross slip in the boundary and this may account for many of the observations which have given the surface such prominence in fatigue damage.

The extent of the region of good fit will depend upon θ, the relative orientation of the adjacent grains, but at the free surface this could extend over a larger area by reorientation of the dislocations in the bad fit region of the grain boundary. Furthermore if these processes are contained within a small region of the boundary, a series of intrusions and extrusions are formed fig 23 b. These processes do not assume that the mirror image of the surface topography is produced within the bulk material because the residual dislocations in the bulk may not be free to move far from the regions of good fit, i.e. out of the volumes contained by the slip systems. Dislocation interactions then take place to form dislocation subboundaries and the substructure which has been so widely reported * 2.81. As the number of cycles increases, the unidirectional strain becomes larger, and the dislocations produced will move from the pile-ups adjacent to the boundary of mis-fit into the subgrain boundaries, giving rise to the small scale surface roughening called rumples,[202] due to the orientation difference which must imposed by the high concentration of dislocations fig 42 d. These reorientations of the subgrains alter both θ and λ. * 6.1

and thus other sources, now located within the subgrains, act in a similar manner subdividing the subgrain into smaller subgrains. This is a process which proceeds until the stable subgrain size, characteristic of the strain amplitude, is achieved. If however local stress concentrations exist, the subgrain size will be smaller than the average and this is in agreement with the observations that the subgrain size decreases as the crack front is approached * 2.7.

The effect of this subgrain formation is to concentrate the plastic deformation or slip in the subgrains thereby giving rise to the small regions of intense slip within a slip band.

6.51. In a static tensile tests, where the strain is nominally unidirectional, the same cross slip mechanism can take place within the grain boundary, but the dislocation still requires the initiation of the five slip systems[200] to relieve the stress concentration which exists due to its presence. Hence the increase in the strain in a static unidirectional test activates new dislocation sources in new planes when the back stress prevents the source from operating. In this case the grain boundary offers considerable interference to the transgranular slip processes. The hardness of the grain boundaries will increase due to the increase in dislocations and as a result of the stress concentration, additional slip systems will be forced into operation to satisfy coherency across the boundary.

6.52 Summary of the model.

Fatigue is a progressive deterioration of the continuity of the medium by subgrain formation through which the crack propagates, * 2.7. The formation of the subgrains is related to the total region of slip which is that volume bounded by the slip sytem and the boundary of good fit. This subgrain formation is a result of the accumulation of unidirectional strains at the ends of the slip bands or slip planes. The model quoted is a particular case for one slip system. If a screw dislocation emerged an edge dislocation would be left at the grain boundary which cannot cross slip thereby causing a stress concentrations.

The general case will be a dislocation loop with its Burgers vector at some arbitary, but fixed angle to the surface and in this case only the screw components can cross slip at the boundary or in the region adjacent to the boundary. * 6.3.

6.6 Correlation with previous work in low strain fatigue.

The nucleation of the fatigue crack has been shown to be at or near the grain boundary, in both high and low strain fatigue, and with some crack formation at the base of the transgranular intrusions.

This latter form of crack nucleation does not occur so frequently as the work of Wood[21,31], and others[19,22,50,203] have indicated. This probably arises from the effect of a taper section across an intrusion which decreases the vertex angle of the intrusion as well as deepening the damage Fig 10, * 4.6 .

Stereo electron microscopy has shown that intrusions can vary between semi-ellipsoidal scallops out of the surface, previously described as tubular holes[19] to deep valleys several microns long with rounded fronts or semi cylindrical slip steps, depending upon the orientation of the slip direction to the surface. (i.e. the slipped region in a fatigue specimen, after the initial work hardening, may be represented by a prolate spheroid (ellipsoid) whose major and minor axes may be inclined at any angle to the surface.) This restricted ellipsoid of slip comes about as a result of the model postulated *6.5. See * 6.7.

Crack nucleation within the grain in low strain fatigue is confined to the regions of the matrix adjacent to the boundary c.f.fig 39 a. or at the grain boundary itself c.f. fig 36 a, and this is more marked in the case twin boundaries c.f. fig 40.

This is a result of the unidirectional stresses being built up at the ends of the glide planes, together with the imposed rotations and displacements of the grain as shown by the reference scratches. On this basis therefore crack nucleation is not considered to be initiated from within the grain. This immediately opens up the question of the mechanism of fatigue of single cystals. The fatigue of single cystals has been undertaken for the examination of the internal dislocation arrangements by thin film electron microscopy[205-206]. as opposed to surface investigations. These crystals form subgrains and the final crack propagation is between these subgrains *2.7. but this gives little evidence of the nucleation method.

Kink boundaries have been reported to be the sites of crack nucleation in bicystals of Aluminium[207] and in copper whiskers[9] (the boundary of the bicrystal was not orientated in the maximum shear zone.) These results confirm the importance that the boundaries play in the crack nucleation mechanism. If a single crystal of aluminium is anodised, the subgrains are still formed beneath the surface of the oxide film, but the cracking associated with them is absent[3], which suggests that there is a definite link between the specimen surface and boundaries which separate regions of crystallites of differing orientation. Thus the important factor lies not in the physical grain boundary, but in the subgrain / grain boundary / specimen surface interfaces.

6.61 Optical examination of the surface after electropolishing.

The reaction of an electrolyte upon the surface of a metal is "chemical" in nature and therefore it would be expected that the reaction depends upon the nature and profile of the surface. During this investigation

it was found that 50/50^{V}/o Phosphoric acid- water was a poor electrolyte if the anode was vertical, in that it produced severe pitting.*4.05

Thompson and Wadsworth[14] used this electrolyte in their sub-surface examination *2.1 *4.12 and found that as well as showing up the persistent slip markings, it also brought into contrast some features which had remained unnoticed. Kemsley[208] found that this electrolyte only showed up persistent slip bands if the surface was electropolished between 10 and 25 % life, but were absent if the specimen was cycled to failure. This suggests that the electrolyte was attacking the region of high dislocation density, which are being formed in localised regions during the incubation period of crack nucleation. * 3.31. Hence if the profile of the slip band consists of a series of extrusions and intrusions of a similar profile to fig 37 , with each change of surface curvature associated with a high dislocation concentration[73], then the simple theory of electropolishing, viz. removal of metal at asperities through a viscous anolyte layer is not basically sound. With the three dimensional surface topography shown in fig 37, the amount of the surface which has to be removed in order to leave little or no contrast at the slip band, depends primarily upon the differential polishing rates at the extrusion and intrusion fronts. Thus surface removal by electropolishing is not considered to be a satisfactory way of ;

1. investigating crack nucleation in fatigue.
2. determing an accurate estimate of the number of cycles required to nucleate a microcrack.

6.62 Plastic- Carbon replicas.

Other evidence for the transgranular initiation of the fatigue crack in low strain fatigue has come from electron microscope studies using two stage plastic carbon replicas. Stereo pairs from replicas prepared by this technique have shown that the primary plastic film exaggerates the depth of the intrusion or crack front by stretching * 4.33 4.31 This has led to the negative replica of the intrusion being referred to as tapered spikes[49].

Direct carbon replicas[209] are difficult to interpret fully and do not reveal all the information when viewed in monovision as it is impossible to obtain the third dimension from shadowing alone. If however the direct carbon replica is floated off the metal, and viewed to give the third dimension * 4.26, * 4.31 , further information can be obtained. Furthermore there is no metallurgical preparation required nor do the replicas suffer from any residual elastic/ plastic deformation due to stripping and therefore the introduction of known artefacts are considerably reduced.

6.7 Discussion of the fatigue mechanism.

The application of a cyclic stress to a polycrystalline metal produces a ratchet type slip process within the grains resulting in a high stress concentration at the end of the glide planes. This requires a small reorientation between the adjacent grains. This ratchet type slip mechanism, and its accompanying grain reorientation has been detected by the displacement of surface markers after 10 % life in high strain fatigue. Whilst the displacement of a scratch is just detectable in low strain fatigue, the same mechanism is considered to take place on a smaller scale and requires many cycles to become detectable as a surface topographical manifestation, i.e. surface roughness or as a resolvable displacement of a $\frac{1}{4}\mu$ scratch. Thus the application of a cyclic stress about a mean zero results in a self-imposed unidirectional strain e.g. figures 26a,30c,32a, *5.22,*5.24, *5.25. Many of the micrographs given in the results and interpretation section (5.0) have been interpreted using the dislocation model elaborated in *6.5 which may successfully be used to describe the unidirectional displacement together with the observed grain boundary delineation early on in the fatigue life. This dislocation model is also capable of describing a possible mechanism for the banding of slip lines into discrete bands e.g. figures 30a and c, 32a, by cross sliping in certain regions, termed "good fit" of the grain boundary as given in *6.5.

The model postulates that a complex dislocation arrangement is left bounding the volume contained by the slip planes and the region of good fit, which may act as a stress concentrator for dislocation sources in the adjacent grain. The model does not postulate the continuous slipping of dislocations through the grain boundaries, or the presence of the mirror image of the surface topography within the bulk of the specimen.

A possible reason for the formation of subgrains and the migrating grain boundary is seen as a stress relieving mechanism in a polycystalline metal. Considering first the subgrain formation as a result of the proposed dislocation model *6.5 and *6.52, with the particular case of an edge dislocation emerging from the grain surface (fig 42 a-e) The continuous operation of this source under cyclic stressing would produce several edge dislocations DC and DG (fig 42 e) and whilst edge dislocations of a like sense and similar Burgers vector cannot directly combine, it is highly probable that under the pile-up stress, which would tend to stop the dislocation source from operating, these dislocations e.g DC (fig 42 e) would combine and interact in a complex manner with those dislocations in the bad fit regions of the grain boundary. The dislocations e.g DG (fig 42 e) could not react in this manner, and so would occupy a distribution within the grain and in a plane containing the Burgers vector and the dislocation line.

A simple tilt boundary fig 41 a in the plane DCG fig 42 e can be made by the screw dislocation ab only cross sliping, say $\frac{3}{4}$ of the distance CD before cross slipping in the plane parallel to ADFG Fig 42 e. The edge E is again absorbed in the bad fit region of the grain boundary by dislocation interaction and the process repeated again except that the screw dislocation ab only slips say $\frac{1}{2}$ the length of the distance CD etc. If this process is followed by many dislocations, the characteristic surface contour of the slip band is formed, as has been observed by stereo electron microscopy and surface markers, together with a subsurface tilt boundary.

Thus this subgrain formation is seen as a stress relieving mechanism which cut the crystallites into smaller fragments, and their formation, if on the proposed model outlined above, will account for the small scale surface roughening e.g. figures 26c.*5.22; fig 37 a *5.3 fig 39 *5.3. The average subgrain size decreases with cyclic stressing until a stable subgrain size is reached which bears some relationship to the cyclic strain amplitude[71] *3.2, *2.81 whereupon crack nucleation proceeds e.g fig 31. due to grain/ subgrain boundary slip because further subgrain formation is thermodynamically unfavourable at the particular cyclic strain and stress concentration, i.e. its ductility is exhausted.

The continued operation of the Frank Read source ab fig 42 a in the manner described above will lead to extrusions of blocks of material as shown by Q Q' in fig 39 a , 39 d * 5.3.

For this stress relieving mechanism of subgrain boundary formation to be a possible explanation of the fatigue process, the transgranular dislocations must be capable of cross slip at the subgrain / grain boundaries. If the grain boundary is not favourably orientated for such a process, it may be possible for the dislocations to pass through the regions of good fit trailing their edge components in the adjacent grain, and to rejoin their parent grain further along the grain boundary. Hence when the edge components reorientate themselves with the dislocations of the bad fit region, the grain boundary moves into the adjacent host grain e.g fig 34 a *5.27. Another possibility is that the boundary moves due to the excess of dislocations on one side of the interface e.g fig 29b as a result of cross slip being difficult, i.e. those boundaries which do not slip, migrate under a suitable driving force[210] to new positions to relieve the build up of stress c.f. fig 43 b fig 30 a and either slip is initiated in the adjacent grain, or if rotation of the adjacent grain occurs, this migration can lead to crack nucleation at the boundary c.f. fig 25 *5.21.

In most boundaries, migration can only be detected by grain boundary slip as observed by Ritter and Grant[181] with aluminium at high temperatures. This migration usually results from a difference in the

concentration of slip lines on either side of the boundary. If however the slip plane is inclined to the surface, this boundary slip can result in the appearance of bent slip planes fig 43 e and fig 28 c.

Slip lines could also be given a curved appearance if the slip plane is inclined to a rough undulating surface c.f. fig 43 d *5.23.

The unidirectional displacements within the grain increases with increase of cyclic strain amplitude. This results in macroscopic reorientation of the surface grains by a mechanism involving grain boundary slip over regions of the boundary which are at 45° to the maximum tensile stress. This in turn requires the folding of the adjacent grain to accommodate the strains c.f. fig 27a fig 43 a . As this self imposed unidirectional strain is greater with higher strain, these surface manifestations are readily detected in high strain fatigue than in low strain fatigue.

The transgranular intrusion is not a crack, which is defined as the dechesion of the matrix at the surface. This follows from the observation that the scratch is continuous across the intrusion, whereas a crack would show a sharp arrest of the scratch at the crack walls. Some grain boundaries show slip activity in forming extrusions and intrusions in regions of the interface e.g. fig 23 b *5.21 fig 30c * 5.24. This slip activity within the boundary could accommodate the grain displacements and reorientations required between the adjacent grains.It cannot be fully established that the grain boundary intrusion is not a crack with a rounded crack front as it has not been possible to observe a $\frac{1}{4}\mu$ scratch running directly across the grain boundary intrusion front (c.f transgranular intrusion sited earlier) The failure to observe a $\frac{1}{4}\mu$ scratch across the grain boundary intrusion is due to the combination of low frequency of occurrence and the regionalised nature of the phenomenon.

6.8 Discussion of Creep tested material.

The fatigue life of previously creep tested material (to produce intergranular cavities) *4.8 might not be increased by the periodic removal of the surface by electropolishing, indicating that the subsurface cavities are capable of crack growth to produce failure, by their interaction with dislocations [211].

In the cavitated material there is a greater region of free surface to each grain, and the processes outlined in *6.5,which could only take place at the free surface, now take place within the material at the cavitated boundaries beneath the surface. The cavities in the grain boundary can link up to form a microcrack whose length can be of the order of 1 grain diameter.c.f. fig. 21 e and f, and this would tend to suggest that Wood's postulation *4.41 (No.2) viz. that pores are formed in subgrain boundaries ahead of the surface based crack is not substantiated experimentally.

6.9. Deformation by Creep v Deformation by Fatigue.

Creep is a high temperature deformation process which involves grain boundary sliding producing cavities.[212] This is in agreement with the finding that single crystals do not produce any voids (within the limits of detectability)[166] during creep, and with the selective experiments where cavities have been observed to grow in conditions where grain boundary sliding [214] can take place, whilst vacancy condensation could not [215]. More recent work [217,218], has suggested that the presence of a gaseous environment produces a greater degree of cavitation during creep than is obtained in a vacuum, which would account for the increase in the density of cavities near to the surface of a creep specimen.[166,174]. The ratio $\frac{e_{g.b}}{e_c}$ * 4.8 is given by Ishida [174] to be 15 % at the surface decreasing over the subsurface layers of 10 thou (250 μ) to 12 % which is then constant throughout the specimen.

Scaife and James [217] explain their results upon the reduction of activation energy for grain boundary sliding due to gaseous diffusion at the boundary, thus making it easier for the grain boundaries to slide.

The fatigue tests reported in this thesis were conducted at room temperature and by using surface markers , the grain boundaries at the surface were observed to slide in a region adjacent to their common interface over small sections of the boundary. The deformation processes taking place in high strain fatigue are very similar to those which have been put forward for the mechanism of creep deformation[175].

In fatigue of O.F.H.C. Copper at temperatures between 300°C and 450°C , Gittins [219] found that the internal grain boundaries became cavitated [220]. Gittins concludes from the fractional change in density for materials of different grain sizes, that the cavitation is not produced by grain boundary sliding. However Williams and Corti [199] found a greater incidence of grain boundary cavities on those boundaries which were at 45° to the stress axis in a push pull fatigue test at 400°C which suggests that the cavities are produced by grain boundary sliding, a conclusion which has beem supported by metallographic evidence using a hydrided Mg-Zr alloy [220].

Hence fatigue at room temperature may be considered as a microscopic unidirectional deformation mechanism which proceeds by surface grain boundary slip at low temperatures and by internal grain boundary slip at high temperatures. The overall picture of a fatigue test at room temperature is complicated by the proposition put forward in * 3.3 that cyclic stressing is equivalent to a greater state of thermal activation. This would embody the traditional high temperature deformation modes[175] which would lead to the postulation that a fatigue test at constant stress and elevated temperature should produce more intergranular cavities than a creep test under the stress and temperature conditions, a postulation which has been observed by Gittins [221].

It may be that the effect of atmosphere on the fatigue test is an alteration in the activation energy for grain boundary sliding as well as an adsorption process.*2.9.

7. Conclusions.

1. The application of stereo electron microscopy to primary carbon replicas prepared from a scratched surface of an electropolished specimen has shown that the fatigue process has been accompanied by the sliding of the juxtaposed grains at their common interface with the surface of the specimen. These boundaries which slip were in the maximum critical shear stress and at 45° to the plane of bending, and that sliding preceeded crack nucleation.

2. The degree of grain boundary sliding at the surface increased either with increase of strain amplitude or number of cycles. It is suggested that the large number of stress cycles required to fracture a specimen in the low strain region, where the S/N curve is shallow is not due to a fundamental change in the mechanism of fatigue, but from the accumulative unidirectional damage.

3. The application of stereo electron microscopy also shows that the intrusion phenomena does not give rise to a high stress concentration, as the base radius is many times larger than the radius of curvature produced by the intergranular phenomena.

4. Examination of two stage plastic carbon replicas by stereo electron microscopy showed that rough surfaces stretched and distorted the primary plastic replica to produce artefacts.

5. The transgranular intrusion - extrusion phenomena is a surface manifestation of the dislocations which have left the surface and are formed by slip within smaller crystallites. These regions were not found to be major contributors to crack nucleation.

6. The fatigue life of O.F.H.C. Copper, containing intergranular cavities formed by creep testing was not extended by the removal of the surface layers after 25 % life. These tests were not sufficient in scope to justify a more definite conclusion being reached as to the effectiveness of surface removal on the fatigue life.

8.0 Future work.

1. The application of stereo electron microscopy to direct carbon replicas, which can be prepared from the specimen without intermediate specimen preparation could be applied to tensile and compression test specimens in order to investigate the displacement of scratches at the surface grain boundaries.

2. The fatigue work should be expanded on bicrystals of known orientation which could be prepared as follows. Cold roll to $\frac{1}{8}^{th}$ inch. strip followed by a high temperature anneal in vacuum to obtain a large grain size, and with the grain boundary perpendicular to the strip surface. The orientation of the two grains could be determined from a back reflection Laue photograph. Small tags which must be spark machined out of the strip could then be polished and scratched and stuck onto the surface of a fatigue specimen (polycrystalline) and fatigued in the same manner as described by Mitchell and Teer.[222] Direct carbon replicas could be removed from the surface tag *4.26 and then examined by stereo electron microscopy * 4.31. The tags could then be examined by thin film electron microscopy.

3. A fine grained material should be creep tested to produce the inter-granular cavities, so that when the specimens are fatigue tested, the amount of surface removed could be on the average be greater than one grain diameter.

9.0 References.

1 Rankine. W. 1843, Proc. Inst. Civil. Eng. 2. 105.

2 Bauschinger. J. 1886, J.Inst.Civil.Eng.2.463.

3 Alden T.H. Backofen.W.A. 1961. Acta. Met.9.352.

4 e.g Lipsitt H.A Wang D.Y. 1961. A.I.M.M.E. 221.918.

5 Buch. A. 1967. Int. J. Fract. Mech. 3,(2) 145.

6 Timoshenko.S. Young.D.S.1963. Elements of the Strength of Materials.

7 Kennedy.A.J.1962. Processes of Creep and Fatigue.in Metals. Oliver & Boyd.

8 Mason.W.P. 1960 A.S.T.M. Spec. Pub. No.237

9 Eisner.E. 1960. Nature. 188.1183.

10 Wood. W.A. 1959. Fracture. J.Wiley & Soans N.Y. p.412.

11 Sines.G. Waisman. J.L. 1959.Metal Fatigue. McGraw-Hill.

12 Bullem.P.F. Head.A.K.Wood.W.A. 1953 Proc.Roy.Soc.216. 332

13 Ewing.J.A.Humphrey.J.W.C. 1903.Phil. Trans. Roy. Soc.200.241

14 Thompson.N. Wadsworth.N.J. Louat.N.1956. Phil Mag.1.113.

15 Wood.W.A. Bendler.H.M. 1962.T.A.I.M.M.E. 224 18 &22

16 Forsyth. PJ.E. 1952. R.A.E. Rep.No. Met 70. & 1953/4 Jnl.Inst.Met.82.449.

17 Wood..W.A. 1958. Phil Mag.3. 692.

18 Broom.T. Ham.R.K. Proc.Roy. Soc. 1959. 251. 186

19 Forsyth.P.J.E. 1958. A.S.T.M. Spec. Publn. N.237 p.21.

20 Boettner.R.C. Laird.C. McEvily.A.J. 1965.T.A.I.M.M.E. 194. 379.

21 Wood.W.A. 1959. Fracture.p.412.Wiley and 1962/3.Jnl.Inst.Met.91.225.

22 Lissner .O.E. 1955 Colloquim on fatigue Berlin. Springer- Verlag.

23 Moller H. Hemple.M. 1954. Arch.Eisenhuttenw.25.39

24 Siebel.E. Stahli C. 1942 Arch. Eisenhuttenw. 15 519.

25 1967 Private communication. Dr.G Sumner.

26.Raymond M.H. Coffin. L.R. 1963. Acta. Met. 11.801.

27 Manson S.S. 1965 Exp. Mech. July.p.193.

28.Coffin.L.R. 1959. Internal Stresses and Fatigue in Metals p.363,Elsevier.

29 Maleka A.H. Barr.W. Baker A.A. 1960-1 Jnl. Inst. Met. 89 176. and 205 207

30.Wadsworth N.J. Private communication.

31 Wood.W.A.1962. Jnl.Inst. Met.91. 304. and references 21,and 153.

32 Patterson M.S. 1955 Acta. Met. 3.491.

33 Forsyth P.F.E. Stubbington.C.A.L. 1955 Jnl.Inst.Met.83 pages 175 and395.

34.Kemsley.D.S. 1956/7 Jnl.Inst.Met. 85 pages 420 and 153

35 Smith.G.C. 1957. Proc. Roy Soc. 242 .189.

36 Honeycombe. R.W.K. 1957. Proc Roy. Soc. 242. .213

37 Elwood E.C. Ducket. 1934.Nat.137.497

38 Laird C. Feltner.C.E.1967. Acta Met.15. p 1621,and 1633

39 Avery D.H. Backofen.W.A. Acta Met. 11. 653.

40 McGrath.J.T. Thurston.R.C.A. 1963 T.A.I.M.M.E. 227. 645

41 Forsyth P.J.E. 1963. Acta MEt. 11.703

42. Mott.N.F. 1958.Acta.Met. 6 195.

43. Fegredo D.M. Greenough.G.B 1958/9 Jnl Inst. Met. 87 1.

44 McEvilyA.J. Machlin.E.S. 1959 Fracture.p.450. J.Wiley & Sons.N.Y.

45. FOrsyth.PJ.E. 1953. Nat. 171. 172, and 1955 Jnl. Inst.Met.83.395

46. Forsyth.PJ.E. StubbingtonC.A.L. 1957 Jnl.Inst.Met.85.339.

47. Hull.D. 1955. Discussion meeting.84.527 of Jnl.Inst.Met.

48. Cottrell.A.H. Hull.D. 1957 Proc .Roy.Soc. 242. 211.

49 Hull D. 1957/8 Jnl.Inst.Met.86.425.

50. Hemple M. 1959. Fracture.p.376 J.Wiley & Sons. N.Y.
1956 Proc. Int. Conf. on fatigue London.p.543. I.Mech.E.1957.

51. Calnan.E.A. Williams.B.E. 1955/6 Jnl.Inst.Met.84.318.

52. Forsyth.PJ.E. 1957.Proc. Roy. Soc. 242.198.

53. 1966 Private communication. Dr.P.H. Frith.

54. Yokobori.T. Nanbu.J. Int Conf.on Fracture Sendai. 1968 p.1529.

55. Martin D.E. 1965. Jnl.Basic Engng. Dec. p.850.

56. Grosskreutz.J.C. Waldron.P. 1963.Acta.Met. 11.717.

57, Clareborough L.M; Hargreaves .M.E;Head.AK. West.C.W. 1957 Proc Roy. Soc. 242.160.

58. Kennedy.A.J. 1962.Creep and Fatigue of Metals. Oliver & Boyd.

59. Mattson.R.L. Roberts.J.G. 1958. Int. Stresses & Fatigue of Metals p.337.

60. Segal R.L. PartridgeP.G.Hirsch.P.B. 1961 Phil.Mag. 6.1493.

61. Segal.R.L. Electron Microscopy and Strength of metals.Wiley.

62. McGrath.J.T. Waldron.G.W. 1964. Phil.Mag. 9. 249.

63. Laufer E.E. Roberts.W.N. 1964. Phil.Mag.10.883.

64. Lukas.P. Klesnil.M. Krejci.J. Rys.P. 1966. Phys.Stat.Sol. 15.71.

65. " " " 1968. ibid. 27.545.

66. " " 1965 Jnl.Iron and Steel Inst.Oct. 1043.

67. " " 1968 Phil. Mag. 17. 1295.

68. Holden.J. 1961. Phil.Mag.6.547.

69. Mitchell A.B. private communication. See also references 205,222.

70. Feltner.C. Laird.C. 1965. Oct. A.I.M.M.E. meeting Detroit.

71. " " 1967. Acta.Met. 15.196.

72. Henry.N.F.M. Lipson.H. Wooster.W.A. Interpretation of Xray Photographs.

73. Honeycombe.R.W.K. 1951/2 Jnl.Inst.Met.80. p.39 and 49.

74. Fourie J.T. 1968. Scripta. Met. 2.63.
" 1967. Can. Jnl. Phys. 45. 777.
" Murphy. H. 1962. Phil. Mag. 7. 1617.

75. Wood.W.A. 1955.Phil.Mag. 46. 1028.

76. Taira S. Honda.K. 1961 Bul. J.S.M.E. 4.14. 230.

77. " " 1963 ibid. 6.21.15. and 1965. ibid.8.557.

78. Arnell. R.D. Teer D.G. Private communication.

79. Avery.D.H. Backofen.WA. 1962. Fracture of Solids.p.339. Interscience.

80. Beacham. 1963. TASM. 56.318. And BeachamC.D. 1962. NRL Rep. 5871.

81. Haigh B.P. Jones .B. 1930. Jnl.Inst.Met. 43.271.

82. Wadsworth.N.J. Hutchins.J. 1958.Phil.Mag. 3.1154.

83. " 1961. Phil.Mag. 6 397.

84. Frost.N.E. 1964. Ap.Mat.Res. July.p.131.

85. Laird.C. Smith.G.C. 1963. Phil.Mag.8.1945.

86 Shanley 1962. Jnl Aero Space Sc. Sept.p.1135.

87. Snowdon.K.U. 1961. Nature.189. 53.

88 " 1964. Acta. Met.12.295

89. Wright.M.A. Hordon.M.J. 1968. T.A.I.M.M.E. 242. 713.

90 Hordon.M.J. 1966 Acta.Met. 14.1173.

91. White.D.J. Private communication.

92. Forsyth.P.J.E. 1952.R.A.E. Rep. No.70.

93. Harris. 1961. Int. Series.of monographs in Aeronautics and Astronautics 6 p.104. Pergamon. Press.

94. Gittins A. 1967. Jnl.Mat.Sc. 1.214.

95. Dolden.R. 1963. Jnl.Nuc.Mat. 8.169.

96. Rarety.L.E. Suhr.R.W. 1966.Jnl.Inst.Met.94.292.

97. Bennet.J.A. 1946. Res. NBS.37. 123.

98. Jackobori.A.1958. ASTM.Bul.2.66.

99. Young J.M. Greenough.A.P. 1960/1. Jnl.Inst. Met. 89. 241.

100.Wadsworth.N.J. R.A.E. Int.Rep.No. Met 251.

lol.Freudenthal.A.M. Weiner.J. 1956 Jnl. Ap. Phys. 27. 44.

102.Eshelby.J.D. Pratt.P.L. 1956. Acta.Met. 4. 560.

103.McCammon R.D. Rosehberg.H.M. 1957. Proc.Roy. Soc. 242.203.

104.Dieter.G.E. 1961. Mech. Metallurgy.p.333. McGraw-Hill.

105. Dr.H.D.Williams. Private communication

106.Cottrell.A.H. 1964. Mech.Prop.Of Matter. Wiley. N.Y.

107.Hull.D. Rimmer.D.E. 1959. Phil. Mag. 4. 673.

108.Nabarro.F.R.N. 1948. Proc.Bristol Conf. 75.

109.Herring.C.1950. Jnl. Appl.Phys. 21.437.

110. Ronay.M. Reimann. W.H.Wood.W.A. 1965. T.A.I.M.M.E. 233.298.

111 a.Gittins.A 1968. Mat.Sc,Jnl. 2.51.
b. Williams H.D. Corti. C. 1968 ibid.2.28.
c. " 1968. Acta. Met. 16. 771.

112. May.M.J. Honeycombe.R.W..K. 1963/4 Jnl.Inst.Met.92. 41

113. Skelton.R.P. 1966. Phil.Mag. 14.563.

114. Rosenberg.H.D.1958. Disc. Jnl.Inst.Met. Vacancies and Point Defects.

115. Sietz.F. Advances In Physics.1952.1.43.

116 Davidge.R.W.Silverstone.C.E. Pratt.P.L. 1959. Phil.Mag.4.985.

117. Feltham.P.1961.Phil.Mag.6.1479.

118. Hull.D.1958. Phil.Mag.3.513.

119. Broom.T. Ham.R.K.1957.Proc.Roy.Soc. 242.166.

120. Kimura.A. Maddin.R. Kuhlman-Wilsdorf.D.1959.Acta.Met.7.154.

121. Galligan.J. Washburn.J. 1963.Phil.Mag.8.1455.

122. Birbaum.H.K.1963. Jnl.Appd.Phys.34.2175.

123. Das.G. Washburn.J. 1965.Phil.Mag.10.955.

124. Maddin.R. Cottrell.A.H. 1955. Phil.Mag.46.735.

125. Tanner L.E. Maddin.R. 1959. Acta.Met. 7.76.

126. Buffington.F.S. Cohen.M. 1952.T.A.I.M.M.E.194.859

127. Lee.C.H. Maddin.R. 1959.T.A.I.M.M.E. 215.397.

128. " " 1961. Jnl.Appld. Phys. 32. 1846.

129. Forestieri.A.F. Girafalco.L.A. 1959. Phys.Chem.Sol.10. 99.

130. Jones.W.J.D. Dover.W.D. 1966. Nature. 209. 704.

131. Freudenthal.A.M. Ronay.M. 1966.Proc.Roy.Soc.292.14.

132. Pearson.S. Board.A.J. Wheeler.C. RAE.Rep.No. Met.94.

133. For Review. Ham.R.K. 1966. Can. Met. Quart. 5.161.

134. Hirsch.P.B. 1959. Jnl.Inst.Met. 87.403.

135. Maleka.A.H. Evershed.G. 1959-60.Jnl.Inst.Met. 88.411.

136. Wilson.R.N. Private communication.

137. Almen J.O. Black.P.H. 1963. Residual Stresses in the Fatigue of Metals. McGraw-Hill. p.22.

138 Wood.W.A. Segal.RL. 1957. Proc Roy Soc. 242. 180.

139. Kettunen P.O. 1967.Phil.Mag.15.253. and 1967.Acta.Met.15.1275.

140. Backofen.W.A. 1962. Fracture of Solids. Interscience. Ed. Drucker D.C. and Gilman.J.J. p.435.

141. Ono.K. Meshii.L. 1965. Ap. Phys. Let.7. 191.
" " 1966. ASM. Mat.Sc. Forum. 59. 573.

142. Kemsley D.S. 1958. Jnl.Inst.Met.87.10.

143. Raymond M.H. Coffin.L.R. 1968. Jnl. Basic Engng. 85.550.

144. Coffin.L.R. 1967. Trans. ASM.60.160.

145. Kemsley.D.S. Paterson.M.S. 1960. Acta.Met.8.453.

146. Kramer.I.R. Demer.L.J. 1961.T.A.I.M.M.E. 221.

147. "" "" 1961. Prog.Mat.Sc. 9 no.3.133

148. "" Feng.C. 1965 T.A.I.M.M.E.233. 1467.

149. "" Demer.L.J.1963 ibid. 227. 529.

150. "" "" 1963. ibid. 227 1003.

151. Forsyth .P.J.E. 1962. Proc.Crack.Symposium. Cranfield.

152. Laird.C. Smith.G.C. 1962. Phil.Mag.7. 847.

153. Wood,W.A. Cousland,McK.S. Sargent. K.R. 1963. Acta. Met.11.643.

154. Dictionary of Metallurgy. 1958. Merriman.A.D. McDonald & Co.

155. Smithells (1967) Metals Reference Book. Butterworths.

156. Grosskreutz.J.C. Reimann,W.H. Wood.W.A. 1966. Acta.Met.14. 1549.

157.a. Laufer.E.E. Roberts.W.N. 1966. Phil.Mag. 12.65.
b. Teer.D.G. Wesson.B.J. Private communication.

158. Wischnitzer.S. Introd. to Electron Microscopy. 1962. Pergamon.

159.a. Grivet.P. Electron Optics. 1965. Pergamon.
b. Little.K. 1962. Jnl.Photographic science. 10. 92.

160. Kay.D.H. 1965.Techniques for Electron Microscopy. Blackwell.

161. Henry. G. Plateau.J. Proc.4 Int.Conf. on Electron Microscopy. Berlin 1958. Springer-Verlag. 1960.

162. Porter.J.Levy.L.C. 1960. Jnl.Inst.Met. 89. 86.

163. Benham .P.P. Ford. H. 1961. Jnl.Mech.Eng.Sc. 3. 149.

164. Cottrell.A.H. 1961. Structural processes in Creep. Iron and Steel Inst.

165. Resnick.R. SEIGLE.L.1957.T.AIMME. 207. 87.
"" " 1959 ibid 209. 87.

166. Boettner.R.C. Robertson.W. 1961.T.AIMME. 221.613.

167. Cocks K.U. Taplin.D.M.R. 1967.Metallurgica. 75. 229.

168. Jacquet.P.A. 1957. ONERA. Tech.Note. No.40. and 1956. Met.Rev. 1. 157.

169. Greenwood.J.N. Miller.D.R. Suiter. J.W. 1954. Acta.Met. 2. 250.

170. Rachinger.W.A. 1952. Jnl.Inst.Met.81 . 33.

171. Davies.P.W. Wilshire.B.1965. Phil.Mag. 11. 189.
" Dutton. 1966. Acta. Met. 14. 1138.

172. Bowring. Davies.P.W. Wilshire.B. 1968. Mat.SC. Jnl. 2. 168.

173. Ratcliffe.R.T. Greenwood. G.W. 1965. Phil.Mag. 12.59.

174. Ishida.Y. Mullendore.A.W. Grant.N.J. 1965. T.AIMME. 233.204.

175. Reviews. a. Gifkins. 1959. Fracture. London. Chapman & Hall p.579.
b. Garafalco. F. 1965. Fundamentals of Creep & Creep rupture im Metals. MacMillan.
c. Grant.N.J. Mullendore.A.W. 1965. Deformation & Fracture at Elevated Temperatures. McGraw-Hill.
d. Dorn.J.E. Mechanical Behaviour of Materials at Elevated Temperatures. McGraw-Hill.
e. Davies.P.W. Dennison. J.P. 1958-9. Jnl.Inst.Met.87. 119.

176. Review of Grain boundaries.Gifkins.R.C1967.Mater.Sc.Engng.2.181.

177. McLean.D. Grain boundaries.in Metals 1957. Oxford.

177b "" 1963. Jnl.Aust. Inst.Met. 8. 45.

178. Wheatley.J.M. Smith.G.C. 1963. Powder Met. 12.141.

179. Penfold.A.B. Forrest. P.G. 1961. Engineering. 20th Oct. 522.

180. Snowdon. K.U. 1966. Phil.Mag.11. 1019.

181. Ritter.D.L. Grant.N.J. 1967. Thermal And High Strain Fatigue.p.80. London. Inst.Met.

182. McArthur.H. Unpublished work using plastic-carbon replicas.

183. Van Vlack. L.H. 1964. Elements in Materials Sci. .Addison-Wesley.

184. Clarebrough.L.M. Hargreaves M.E. 1959. Prog.in Met. Phys. Chalmers 8.1. Schmid.E Boas.W.1968. Plasticity of Crystals. Chapman & Hall.

185. Bragg.W.L. Nye. J.F. Proc.Roy. Soc. 1947. 190.474.

186. Mott.N.F. 1948. Proc.Phys.Soc. 60. 391.

187. Weinberg.F. Progress in. Met.Phys. 8.105.

188. Read.W.T. Dislocations in Crystals.1953. McGraw-Hill.

189. Brandon.D.G. et.al. 1964. Acta.Met.12.813.

190. Goux.C 1961. Mem.Scientifiques.Rev.Met.LVIII.662.

191a. Ralph.B. Brandon.D.G. 1963.Phil .Mag.8.919
b. Morgon.R. Ralph.B. 1967.Acta.Met.15.341.

192. Ryan.N.F. Suiter.J. 1967 Phil.Mag.12. 727.

193. Review by S.Ranganathan in Hren.J.J. and Ranganathan.S, Field-ion microscopy.1968, Plenum.

194. Friedel.J Internal Stresses in Metals.p.221.

Sully.A.H. 1956. Progress Met.Phys. 6p.135.
Bollman.W. 1964. Disc. of the Faraday Soc. p.26.

195. Wilms.G.R. Wood.W.A. 1948-9. Jnl. Inst.Met. 75. 693.

196. Stevens. R.N. Met.Rev. 1966. 11. 129.

197. Broom.T. 1968-9. Mat.Sc.& Engng.3.138.

198. CharnsleyP. Thompson.N. 1963. Phil.Mag. 8. 77.
Buckley.S. Entwistle.K. 1956. Acta. Met. 4. 352.

199. Williams.H.D. Corti.C. 1968.Jnl.Mat.SC. 2. 28.

200. Taylor.G.I. 1938. Jnl.Inst.Met.62.307.

201. Cottrell.A.H. 1949. Prog.in met.Phys. p.77. Ed. B Chalmers.
"" 1953. ibid. 205.

202. King.A.E. Teer.D.G. English Electric Rep.W/M(5b).p1462.
1967 PM 15 425
203. Wadsworth.N.J. 1958. Advances in Physics. 7. 73. 1967. Phil.Mag.15. 425.

204. see.ref. 62, 63, 64,
205. Mitchell.A.B. Teer.D.G. English Electric Rep. W/M5b p1461.
206. Grosskreutz.J.C. Waldron.P. 1963.Acta.Met.11.717.
"" Hancock. 1969 ibid. 15. 77.

207. Chin.G.Y. Backofen.W.A. 1961/2.Jnl.Inst.Met. 90. 13.

208. Kemsley.D.S. 1957.Phil.Mag. 2.131.

209. Wei.R.P. Baker.R.P. 1965.Phil.Mag. 12.1005.
and ref 159 a.

210. Smith.C.S. 1964.Met.Rev.9.1.

211. Forty.A.J. 1964.Disc.Faraday.Soc. 56.

212. See refs: 166.173, 175b,176,177b,194,

213. Dorn.J.E. 1954. Jnl.Mech.& Phys.of Solids.3.85.

214. See references,107, 173,

215. " " 171a,171b,216a,216b,

216. a.Taplin.D.M.R. Barker.L.J. 1966. Acta.Met.14.1527
b " Wingrove. 1967. ibid. 15.1231.

217. Scaife.EC. James.P.L. 1968. Mat.Sc.Jnl.2.217.

218. Quoted in 217. Bleakney.H.H. 1952. Canad. J.Technol.30.340.
Price.C.E. 1966.Acta.Met.14.1787.

219. See 94, 111a

220a. SkeltonR.P. 1966. Phil. Mag. 14. 563.
b " 1967. Mat.Sc.Jnl. 1. 140.

221. Gittins.A. 1968. Mat.Sc. Jnl. 2. 51.

222. Mitchel.A.B. Teer.D.G. To be published Phil.Mag.

223. Coffin.L.F. 1962.Applied.Mat.Res. October.p.129.

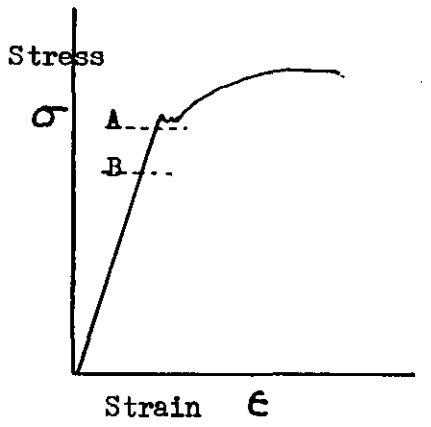

a

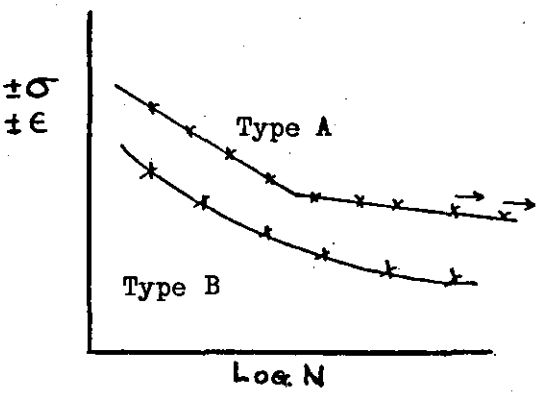

b

DISPLACEMENT OF A SCRATCH ON THE SURFACE OF

FATIGUE

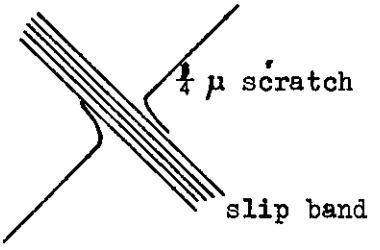

gives zero overall displacement

c

STATIC TENSILE TEST.

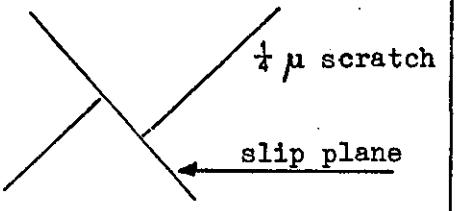

gives an overall displacement.

d

stress to
produce the
next half cycle.

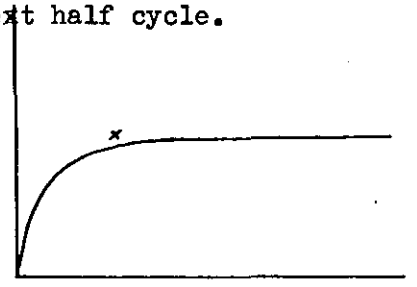

strain summed irrespective of
sign

e

Figure. 1

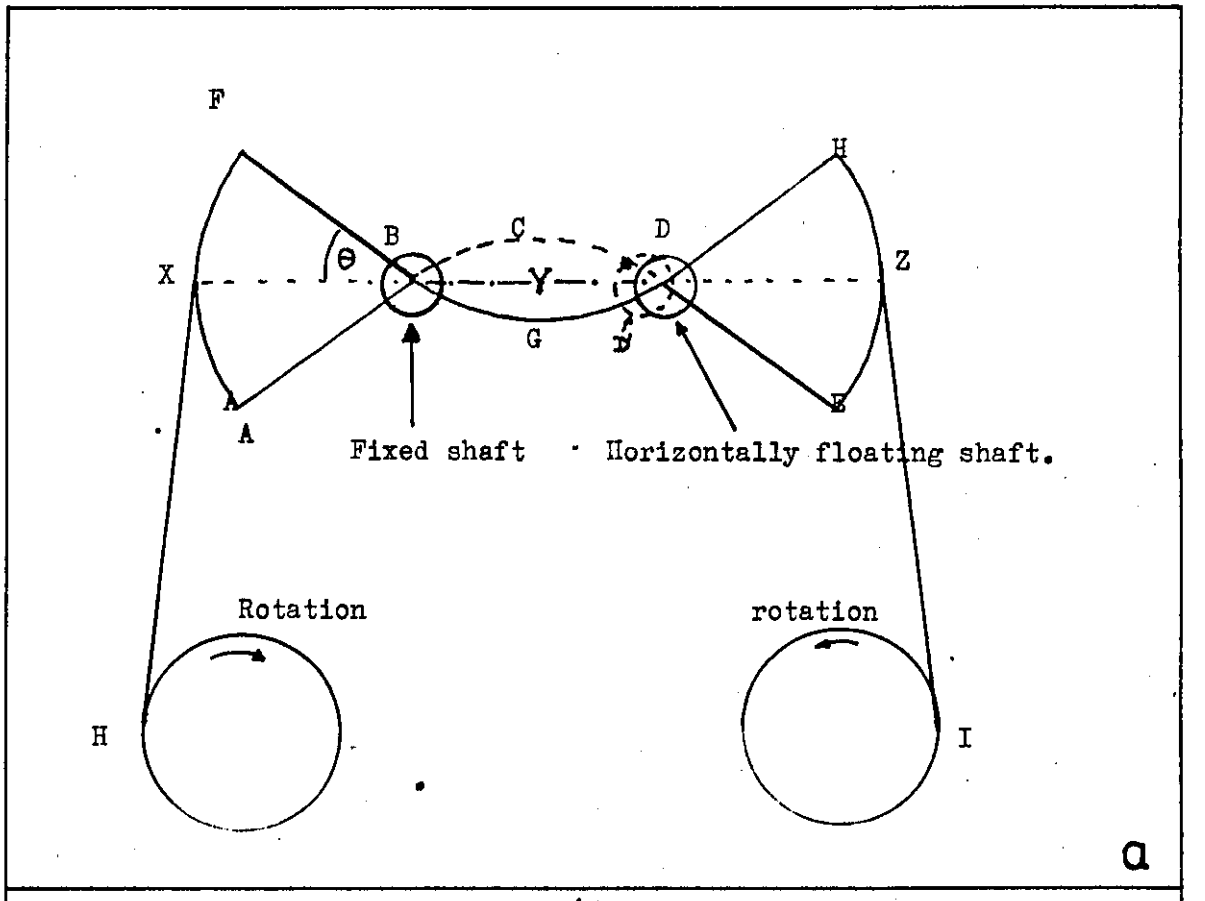

MECHANISM OF HIGH STRAIN BENDING FATIGUE MACHINE.

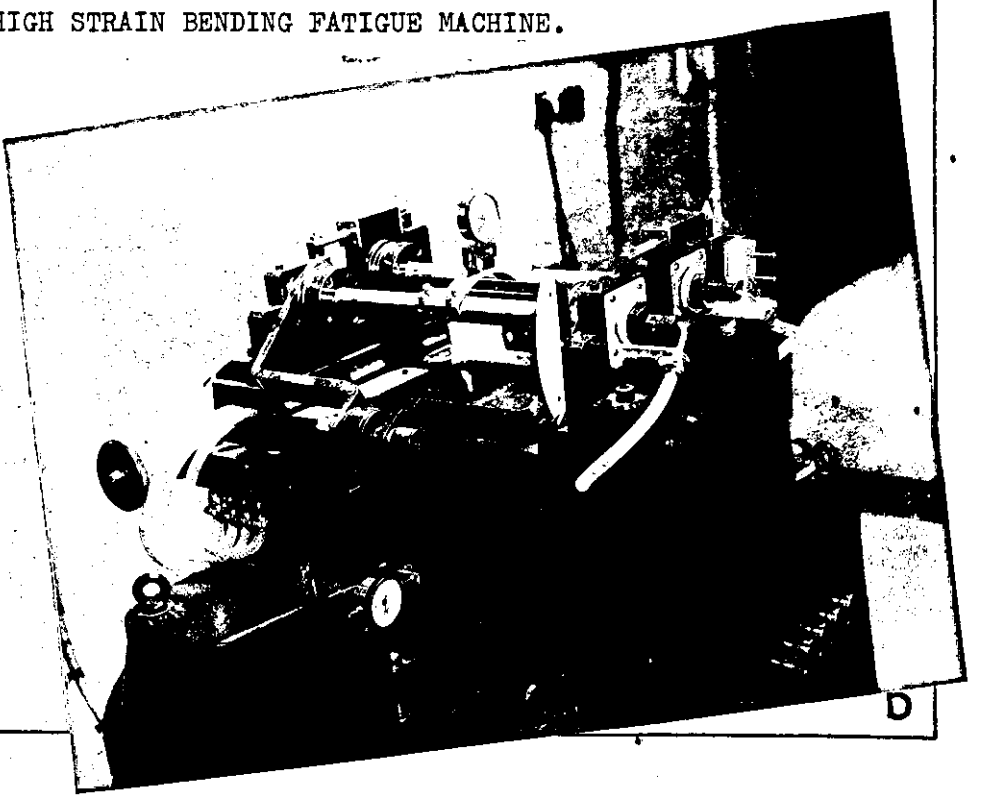

Figure. 2

FIGURE. 2
Page. 59

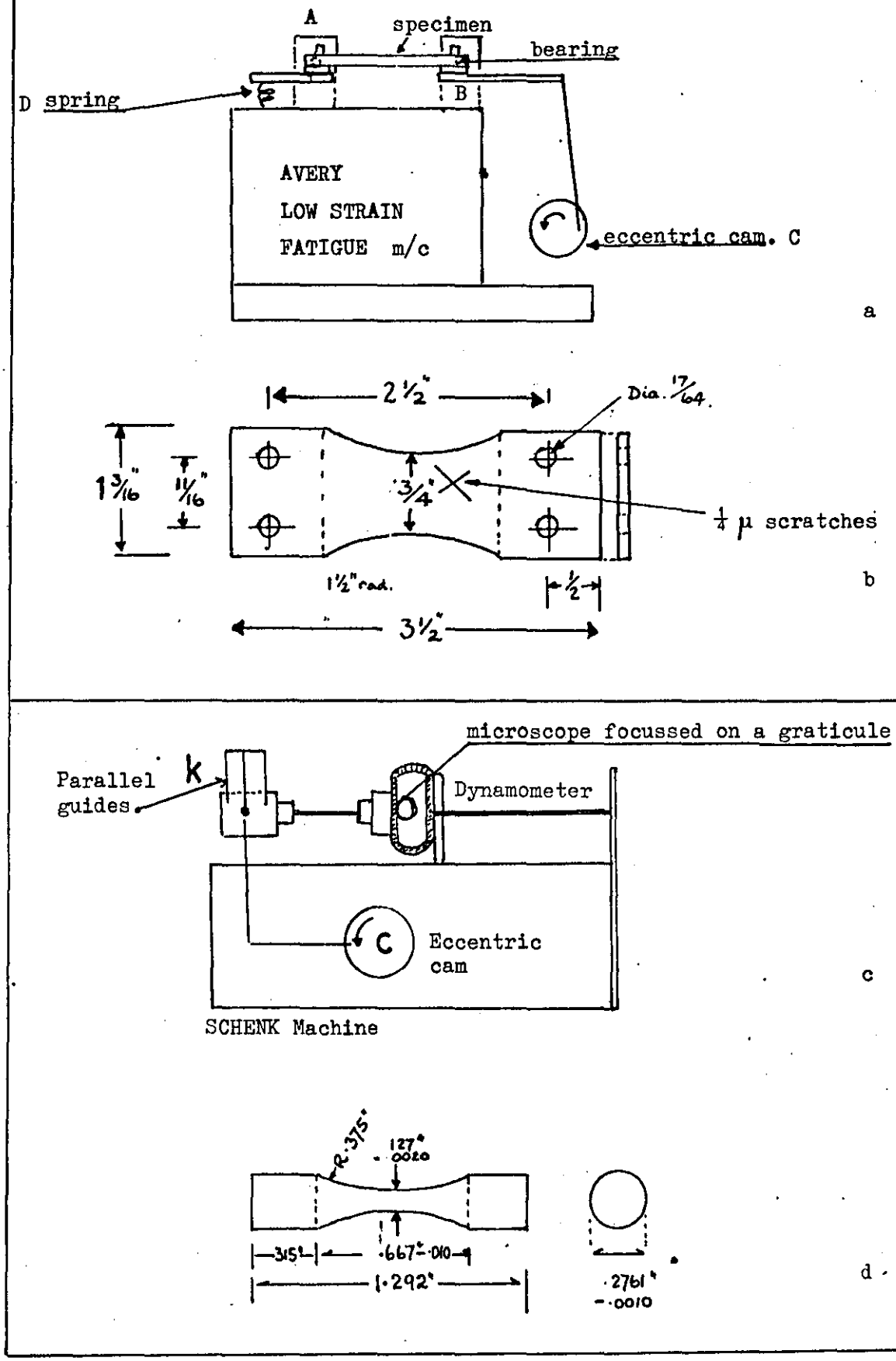

LOW STRAIN FATIGUE MACHINES USED IN THIS THESIS.

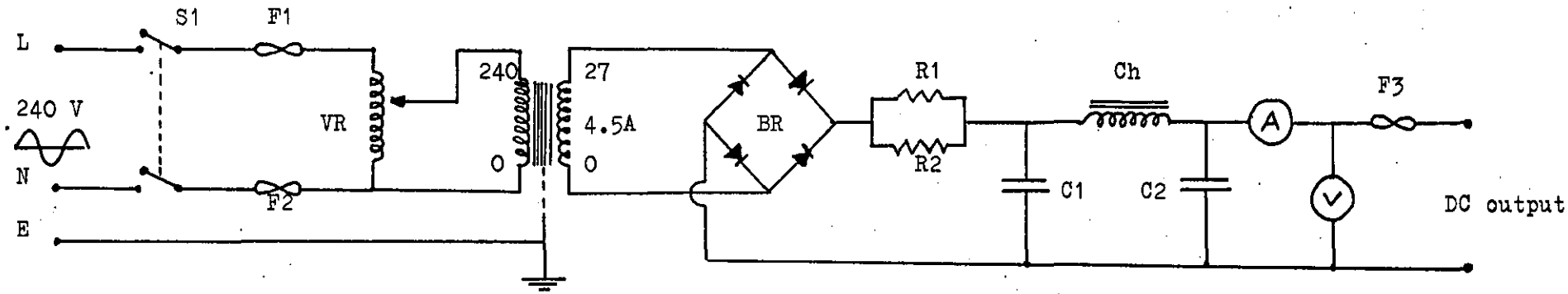

S 1 Toggle switch, double pole, on/off, 250V 2A.
F 1 & F2 2 amp fuses.
VR. Variac, 2.5 amp
TR. Universal LT transformer. Secondaries connected to give 27V.at 4.5A 90 watt.
BR. Ferramti type bridge full wave rectifier.
R1 &R2. Wire wound resistors 1 Ω. 5 watt.
C1 &C2. Capacitor 8,000 μF 60V dc max working.

CH Choke. Formed by connecting secondaries of universal LT transformer for 40 V at 3 amp. Primary not connected.
A Ammeter, moving coil, 0-5 amp.
V Voltmeter, moving coil, 0-30 volt.
F3 Output fuse 5 amps.

CIRCUIT DIAGRAM FOR THE BENCH ELECTROPOLISHING UNIT.

FIGURE 4
Page 61

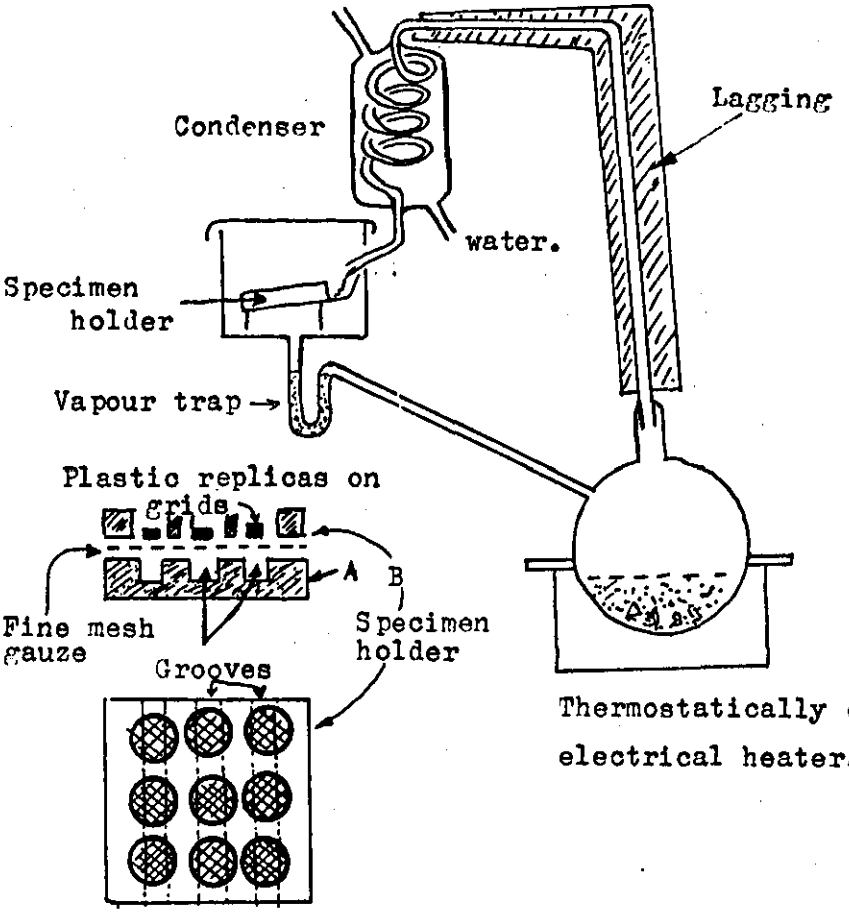

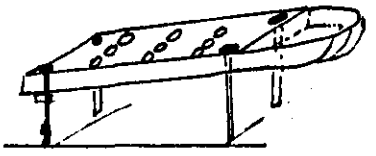

Specimen tray is tilted slightly to allow the distillate to flow through grooves and beneath the grids.

Apparatus for the redistillation of solvents for thick plastic films.

The specimens rest on a fine gauze which is clamped between a grooved base A and a specimen holder B which is a piece of brass with holes slightly larger than the diameter of a grid. This prevents the grids from floating away on the surface of the distillate.

FIGURE 5
Page 62

SURFACE REPLICAS

Surface replicas from fatigued specimen

Stage 1

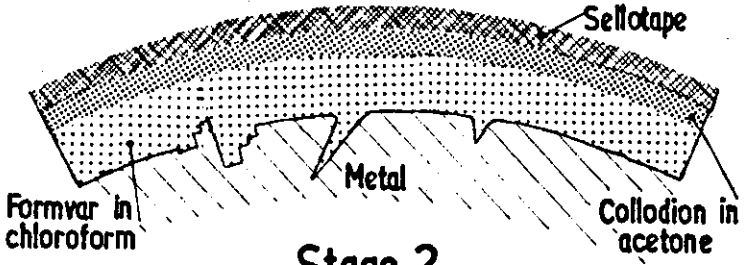

Plastic replica made of tension side of fatigue specimen. The very rough surface necessitates use of a strong composite replica.

Stage 2

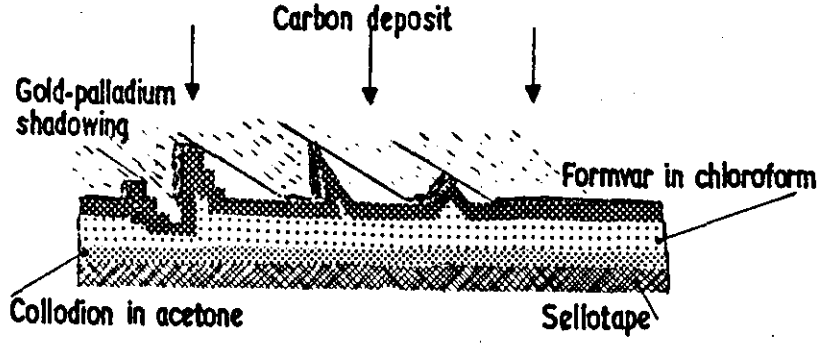

Negative plastic replica stripped from the surface and placed in vacuum chamber.
Carbon layer evaporated normal to the surface followed by Gold-Palladium shadowing at an oblique angle.

Stage 3

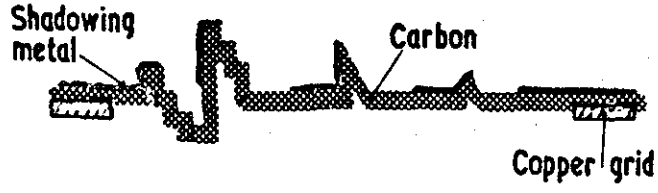

Support grid attached to the carbon layer and all plastic removed in solvents.

FIG 6

FIGURE 6
Page 63

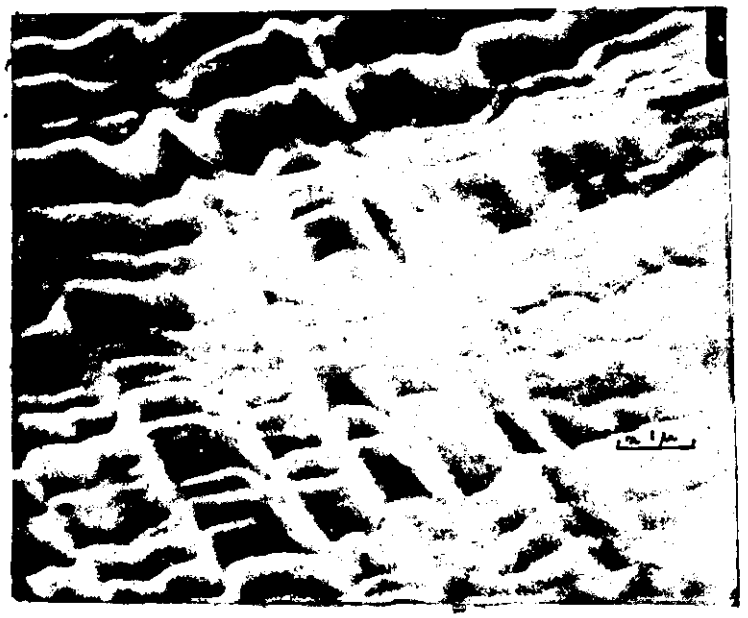

Scanning Electron Micrograph.

High strain fatigue dwell tests. Expected life 1,200 cycles. Test stopped with the same surface in tensile at ¼ cycle and then every 10 cycles for ten minutes. Test stopped at 250 cycles. See also figure 33a. for direct carbon replicas. Micrograph shows the rough surface topography formed with intersecting slip systems.

FIGURE 7
Page 64

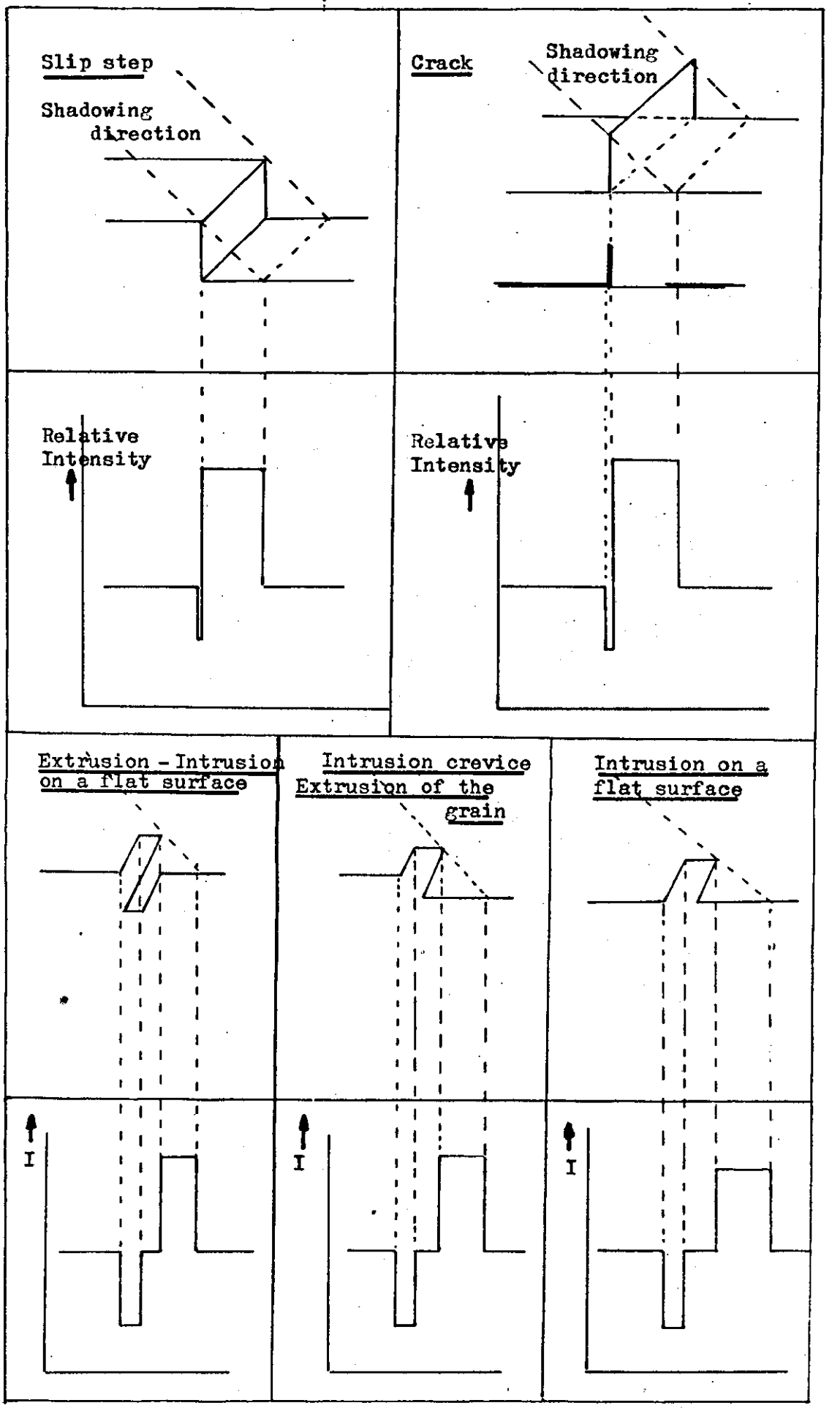

SHADOWING ON NEGATIVE CARBON REPLICAS

FIGURE 8
Page 65

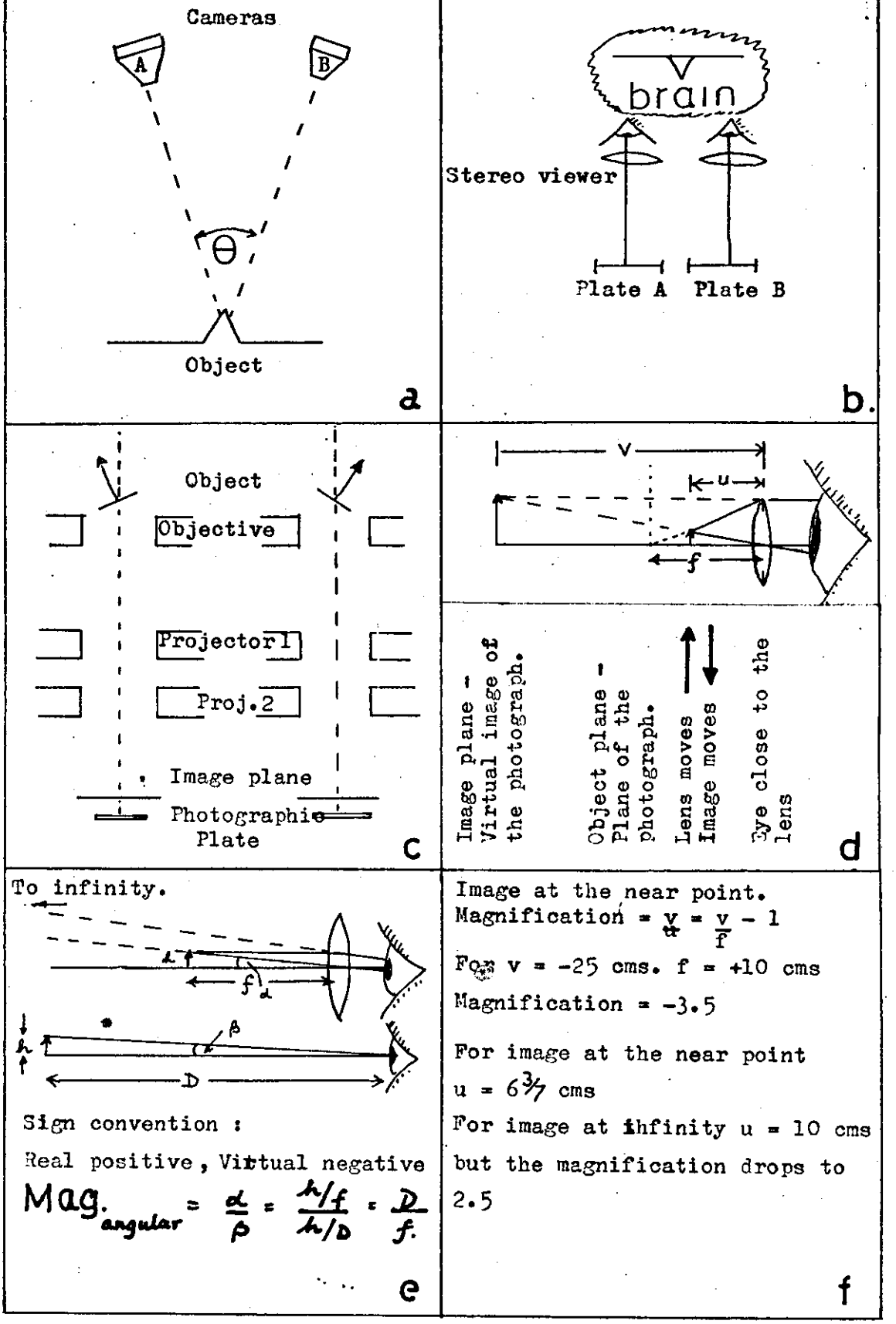

STEREO ELECTRON MICROSCOPY.

FIGURE 9
Page 66

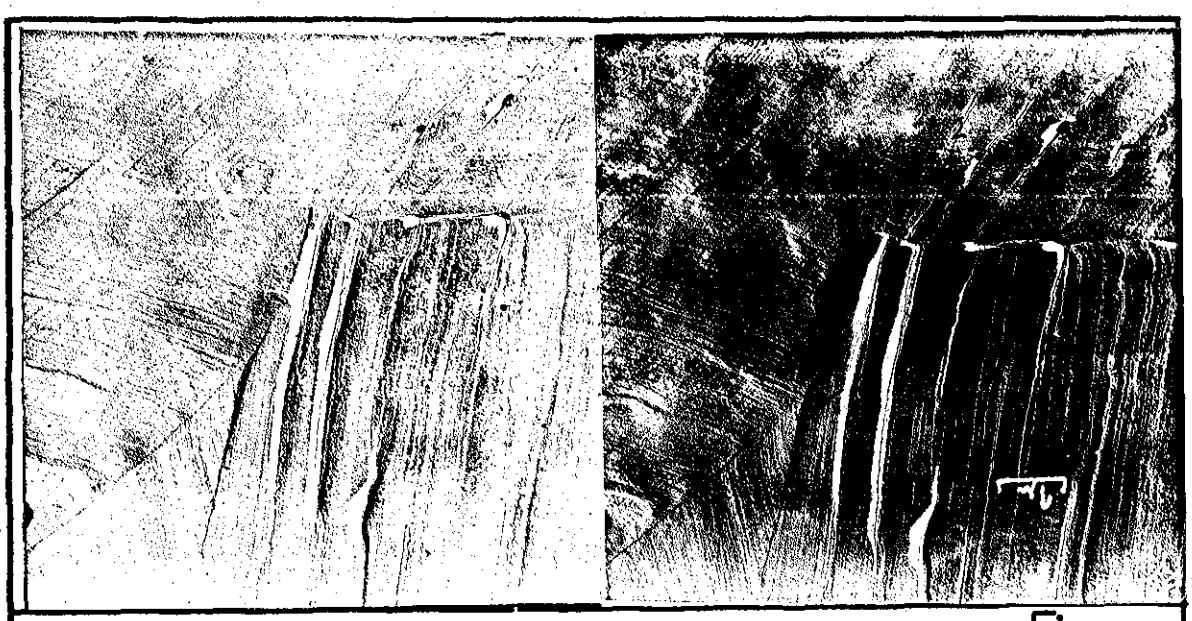

a

Fig

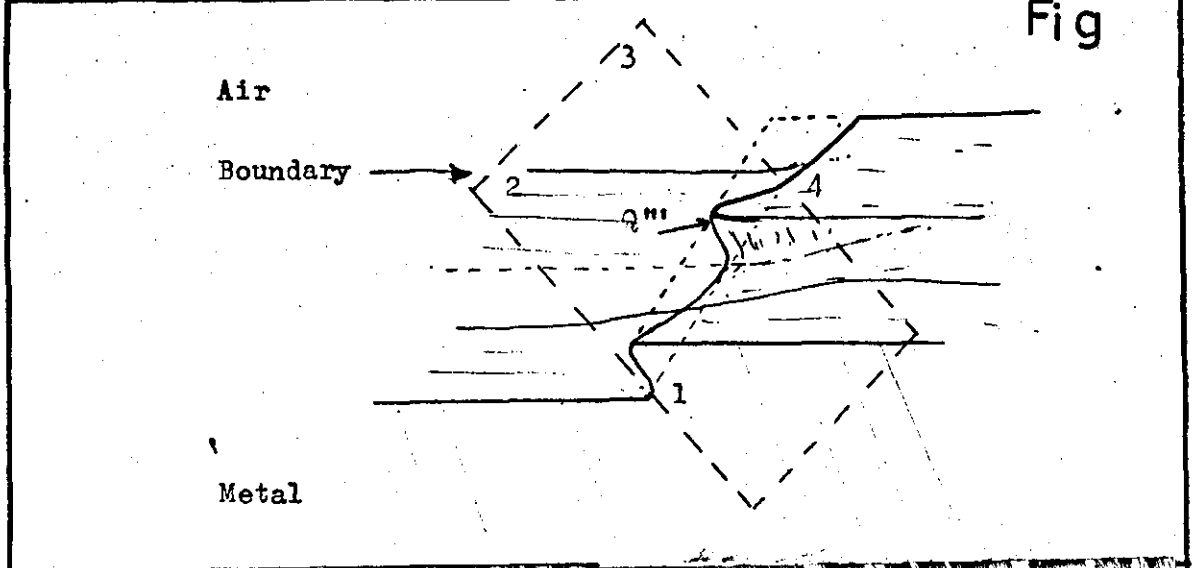

b

c

Stereo Electron Micrographs Prepared From Negative Carbon Films. Specimen history. High Strain Fatigue. Expected number of cycles to failure 1200. Replica taken at 250 cycles

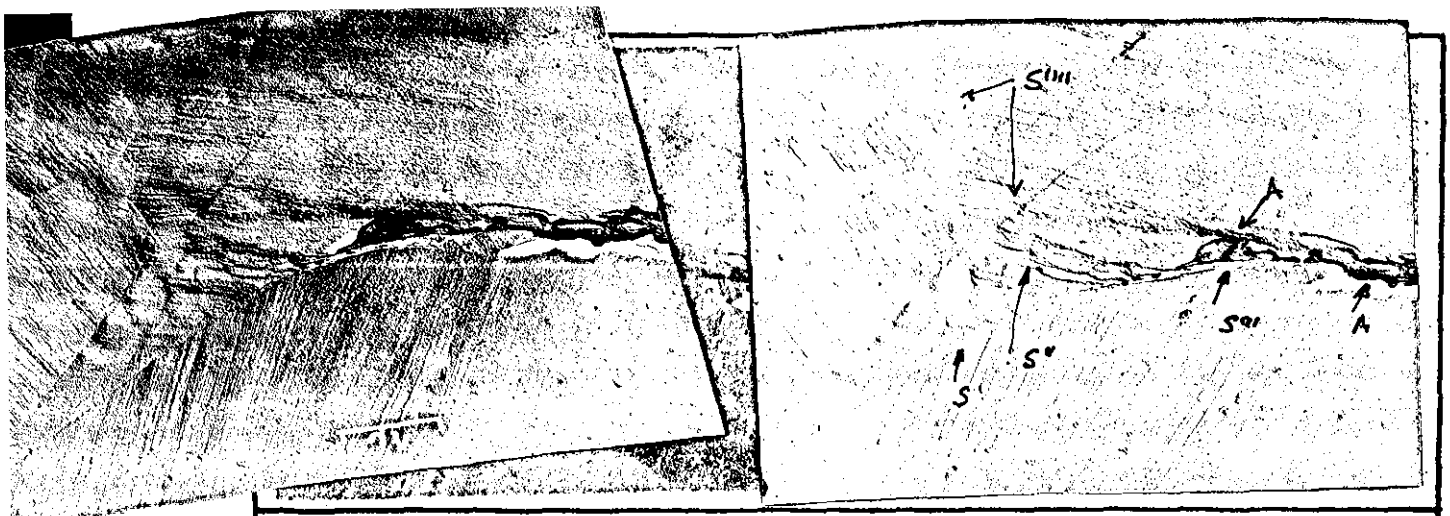

a

Grain boundary cracking in high strain fatigue. Expected life 1200 cycles. Negative carbon replica at 250 cycles.

b

c

Stereo electron micrographs from a two stage plastic carbon replica taken from a low strain fatigue specimen at life 10^6 cycles. Both micrographs show intergranular and transgranular cracking.

FIGURE 11
Page: 68

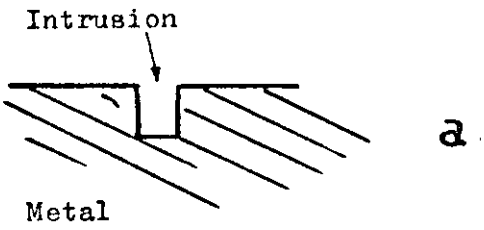

a

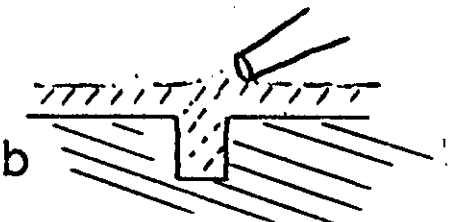

b

Glass dropper delivering the plastic replicating medium.

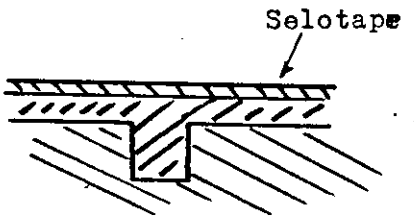

c

Plastic replica ready to strip.

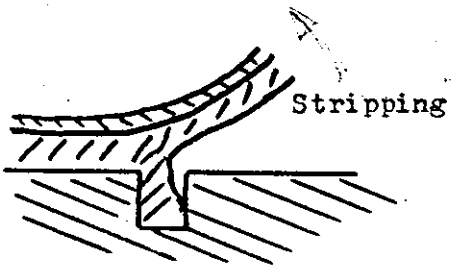

d

The plastic replica shrinks away from the sides of the intrusion to release itself.

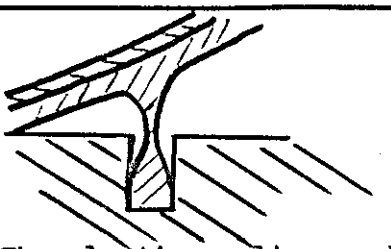

e

The plastic replica necks down and may fracture leaving some plastic behind.

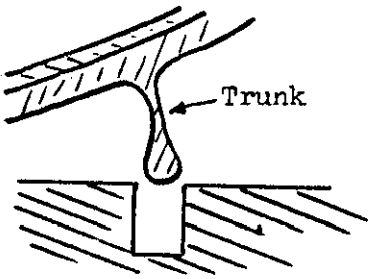

f

The last portion of the plastic replica to free from the intrusion is fatter than the trunk

Residual elastic strain gives :

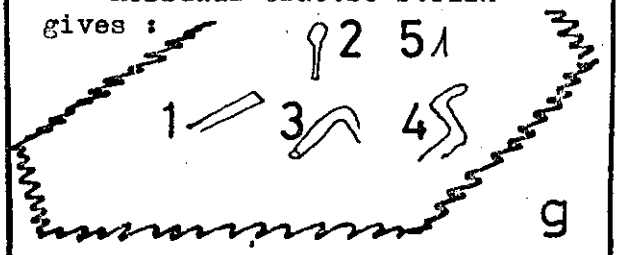

g

ARTEFACTS.

1. Plastic lies parallel to the surface. A'
2. Tip fatter than the trunk. B
3. Folding to give an archway.
4. Plastic film forms a cork screw.
5. Tapered spike due to fracture.

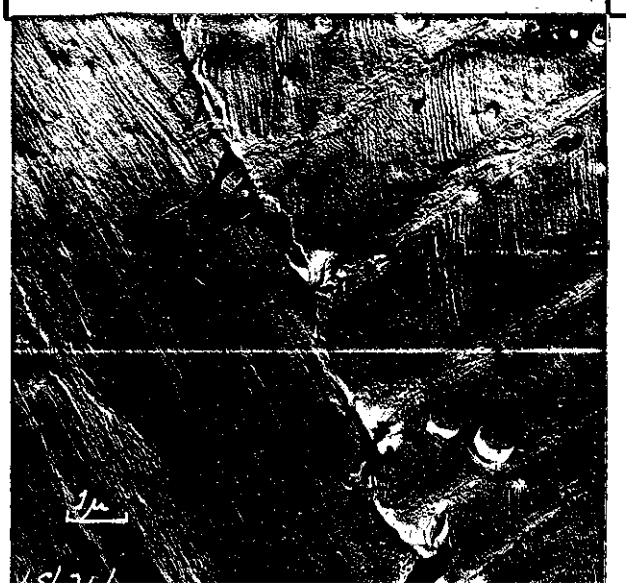

h

ARTEFACTS FROM PLASTIC PRIMARY REPLICAS

FIGURE 12
Page 69

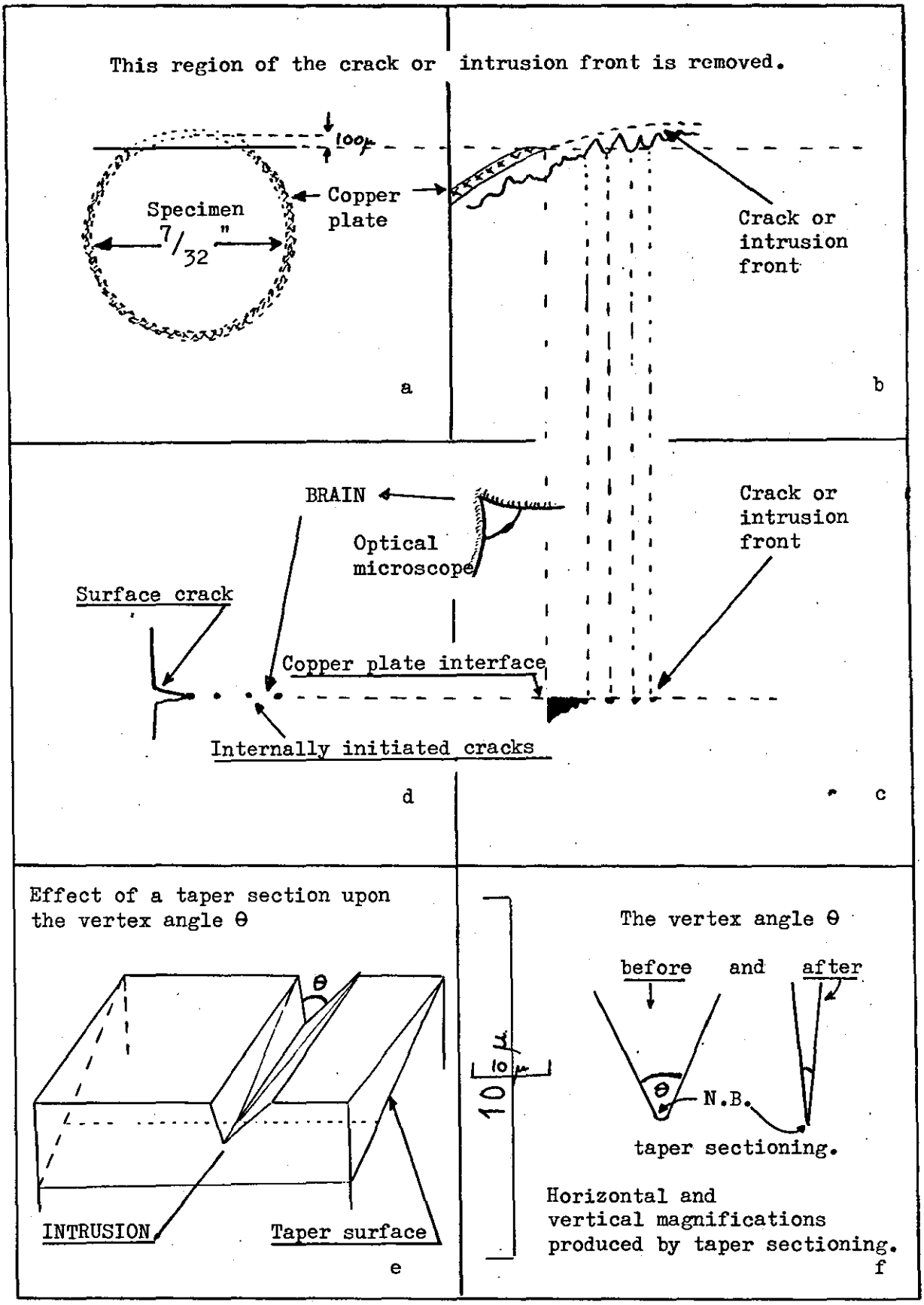

Interpretation of the results of Wood's work on taper sections

FIGURE 13
Page 70

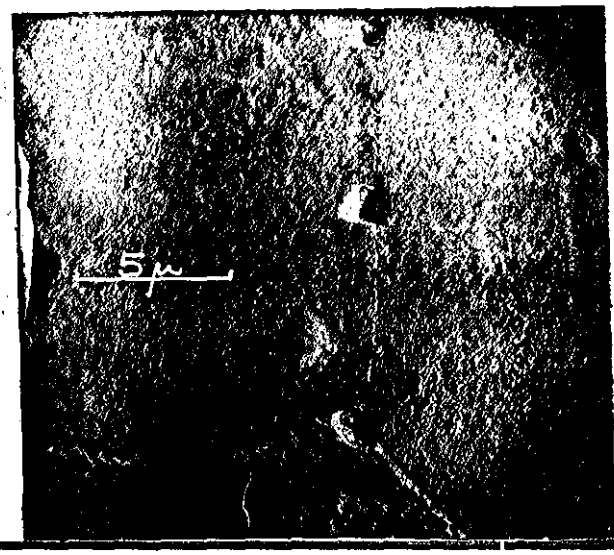

Effect of etchants upon the internal structure formed by repeated quenches. Specimen has been quenched into water from 1,000°C ten times and then annealed at 300 C for 10 hours. Plastic carbon replica.
Metallographic preparation. ɣ Alumina in a slurry with a few drops of ammonia and ammonium persulphate.
Final etchant Alcoholic Ferric chloride.

FIGURE 14

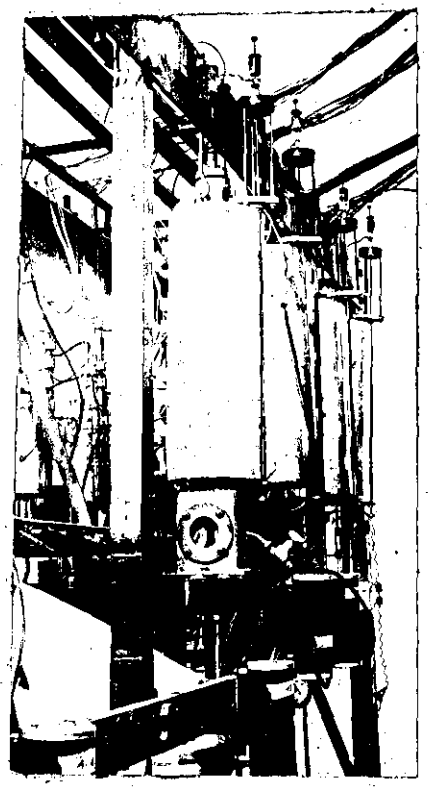

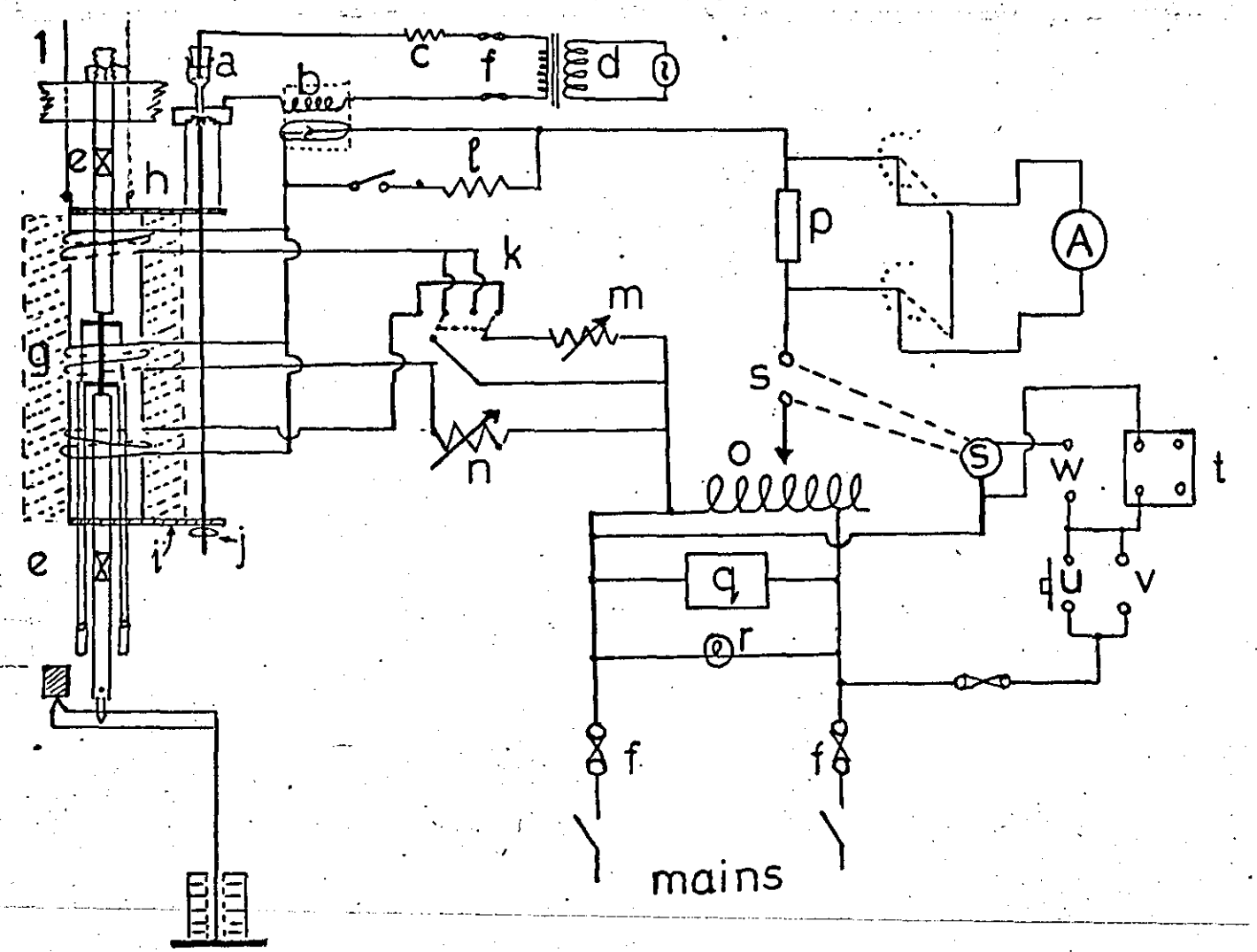

a. CREEP FRAME

b. CIRCUIT DIAGRAM.

Fig. 15.

Fig 15

72

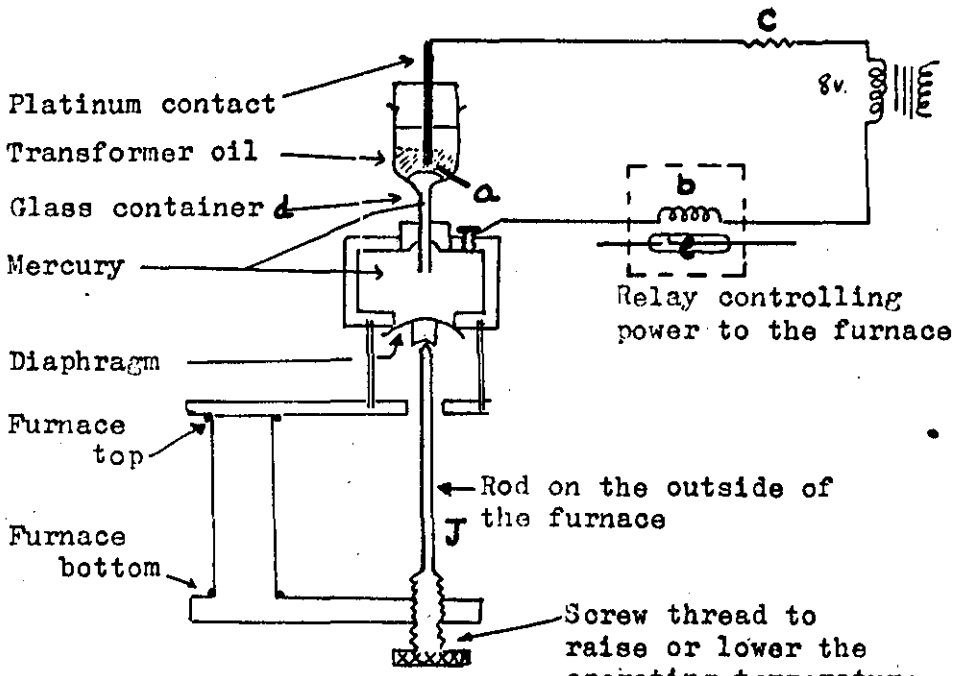

TEMPERATURE CONTROL

FIGURE 16

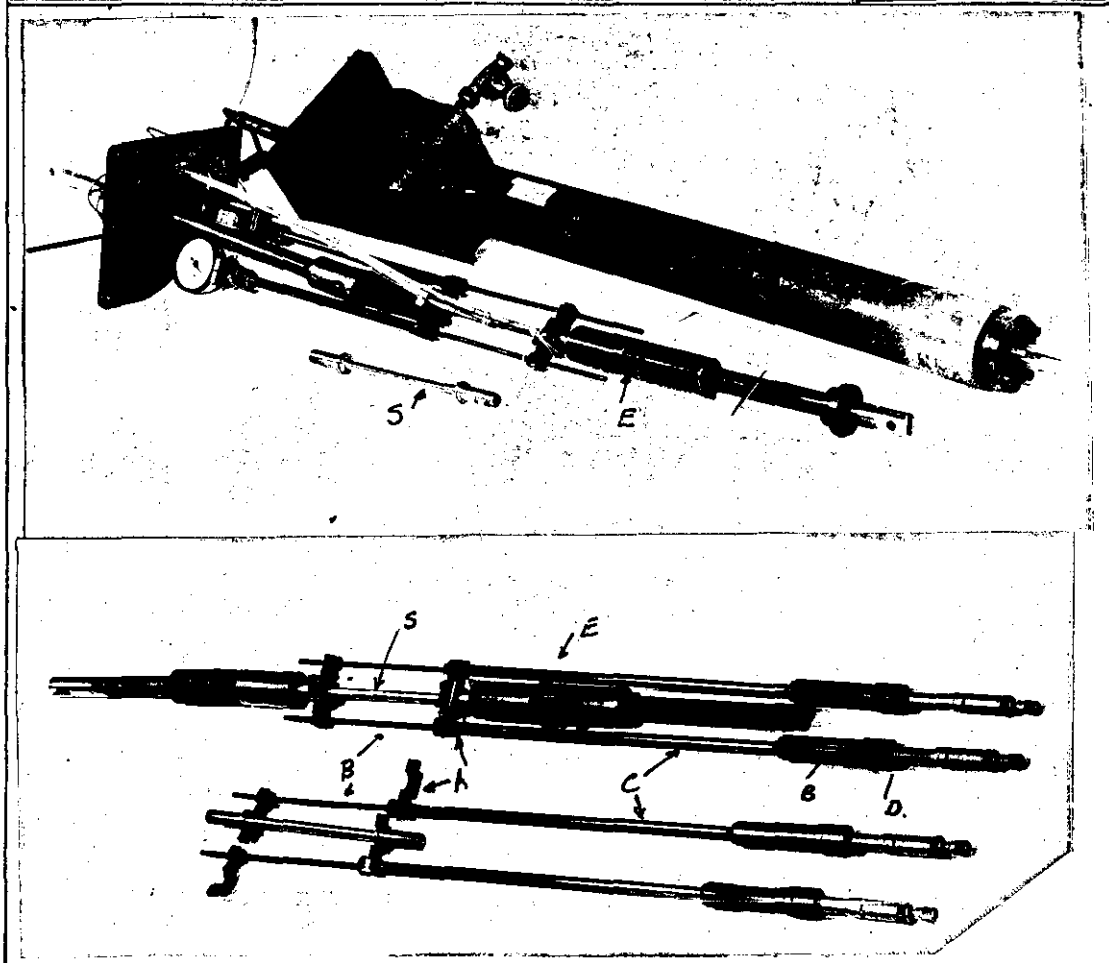

EXTENSOMETERS

FIGURE 17

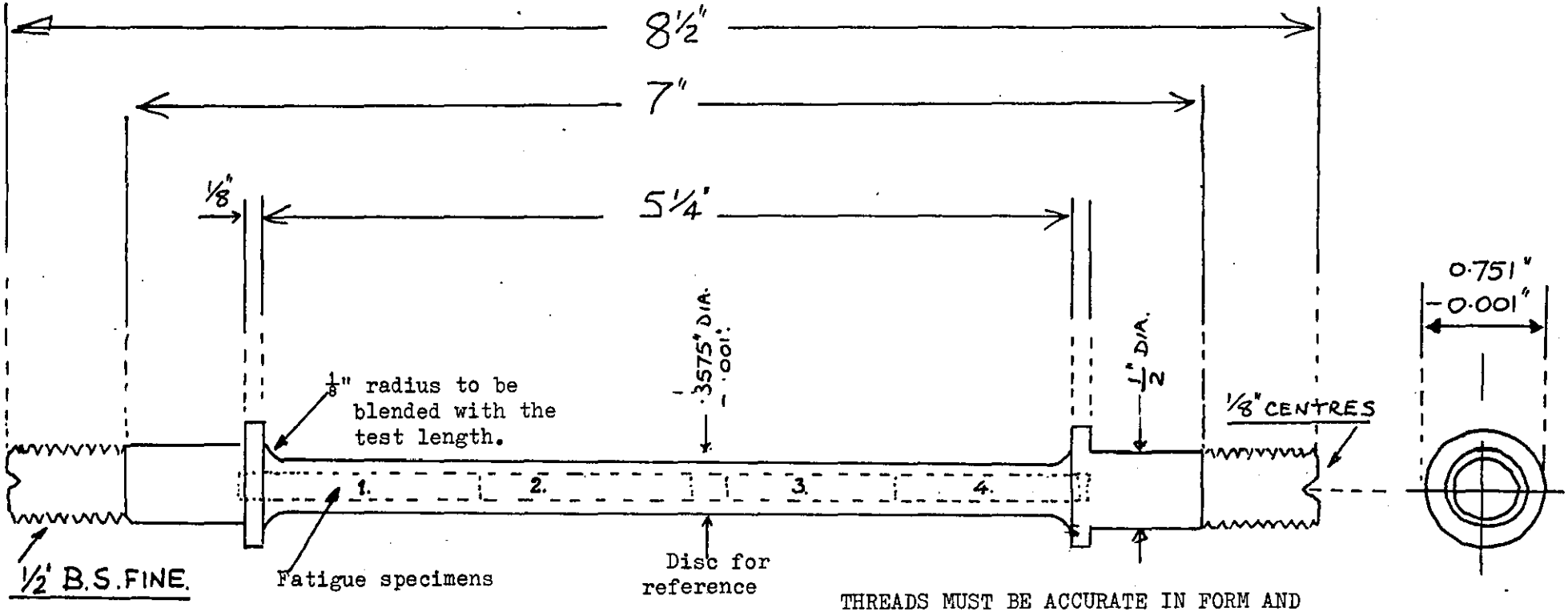

CREEP SPECIMEN.

FIGURE 18

Metallography of α Brass.

α Brass showed negligible ductility at 200°C due to the second phase present at the grain boundary x 550.
PREPARATION. Polished in a slurry of γAl_2O_3 and 10 % ammonium persulphate and ammonia.

FIGURE 19
Page 75

Specimen	Stress	Temp.	Total time hours.	Initial extension per cent. e_L	Total creep per cent.	e_o	Creep rate $\times 10^{-6}$ in/in/hr.
5	8,500	249	2856	2.06	2.104	0.0064	7.2
4	5,190	249	1617	0.70	0.686	0.0042	1.8
8	10,130	204	2520	3.32	2.07	0.016	3.8
2	6,580	204	1576	2.83	0.72	0.0055	2.0
7	11,820	149	2688	4.24	1.00	0.48	3.3
1	10,120	149	1236	2.20	1.78	0.0035	3.2

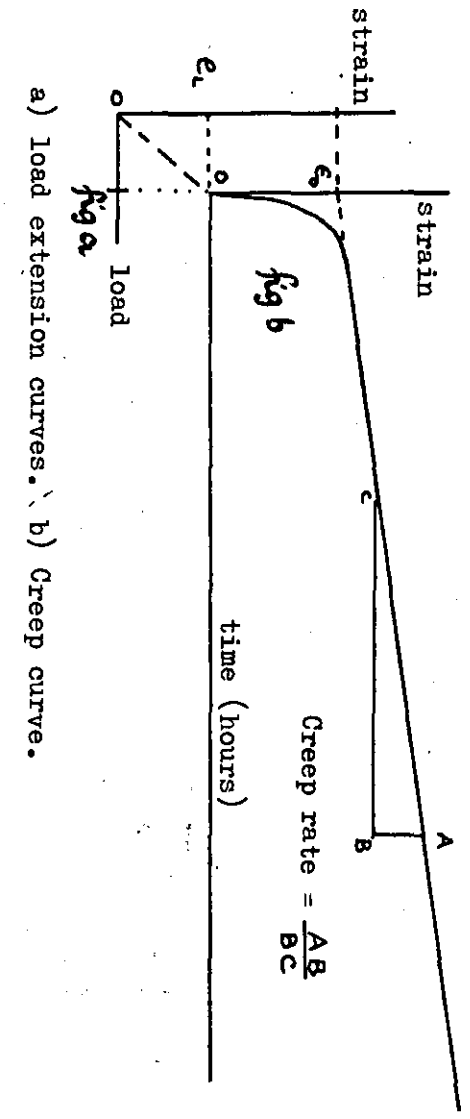

a) load extension curves. b) Creep curve.

Creep test. Summary of tests at low temperatures, high stresses to produce intergranular cavities.

FIGURE 20

a. As received copper prior to creep testing.

b. After creep testing at 249 C , Specimen 5.

c. After creep testing at 204 C , Specimen 8.

d. After creep testing at 149 C , Specimen 2.

e. Specimen 2/2 fatigued cycled for 75 % life. Micrograph shows internal crack growth from the internal intergranular cavities near the surface.

f. As fig e. Crack growth 400 μ below the surface.

METALLOGRAPHIC PREPARATION. Fig a-d. Al_2O_3 slurry with ammonia and ammonium persulphate.

Fig e-f. Polished on brasso with intermediate light etches in alcoholic ferric chloride.

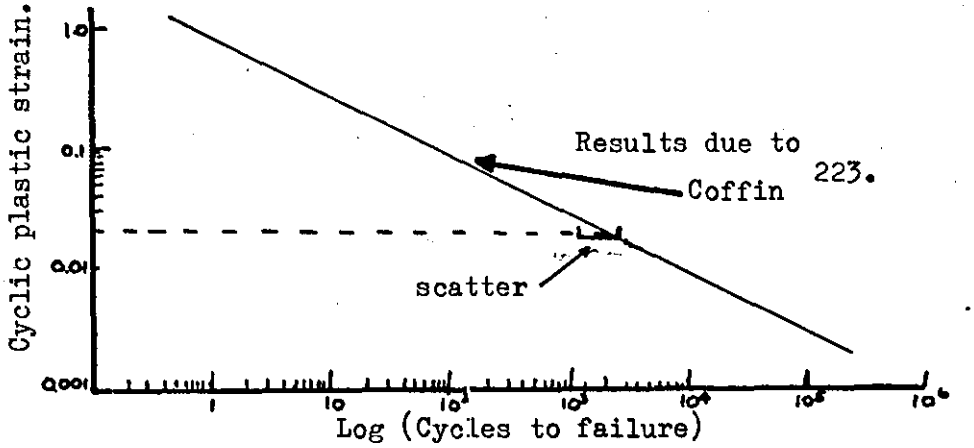

a

Cyclic plastic strain v Log (Cycles to failure) for the high strain fatigue programme.

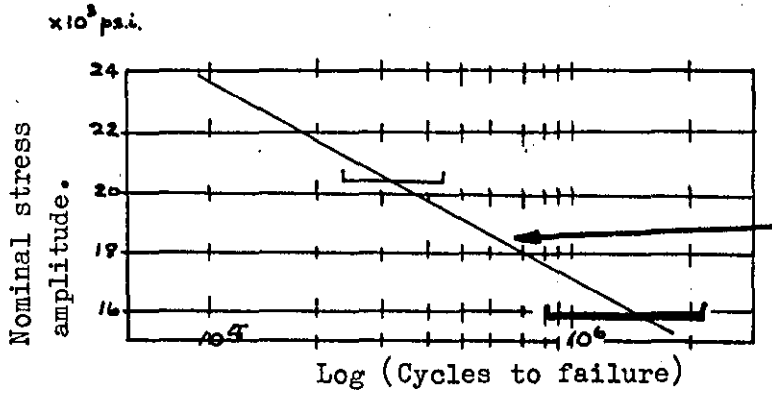

b.

Nominal stress amplitude v Log (cycles to failure) for the low strain fatigue programme where specimens were tested in an Avery bending Fatigue machine. (Not applicable to push-pull)

Figure. 22.

a. Shows slip activity at the grain boundary which has slipped at U.

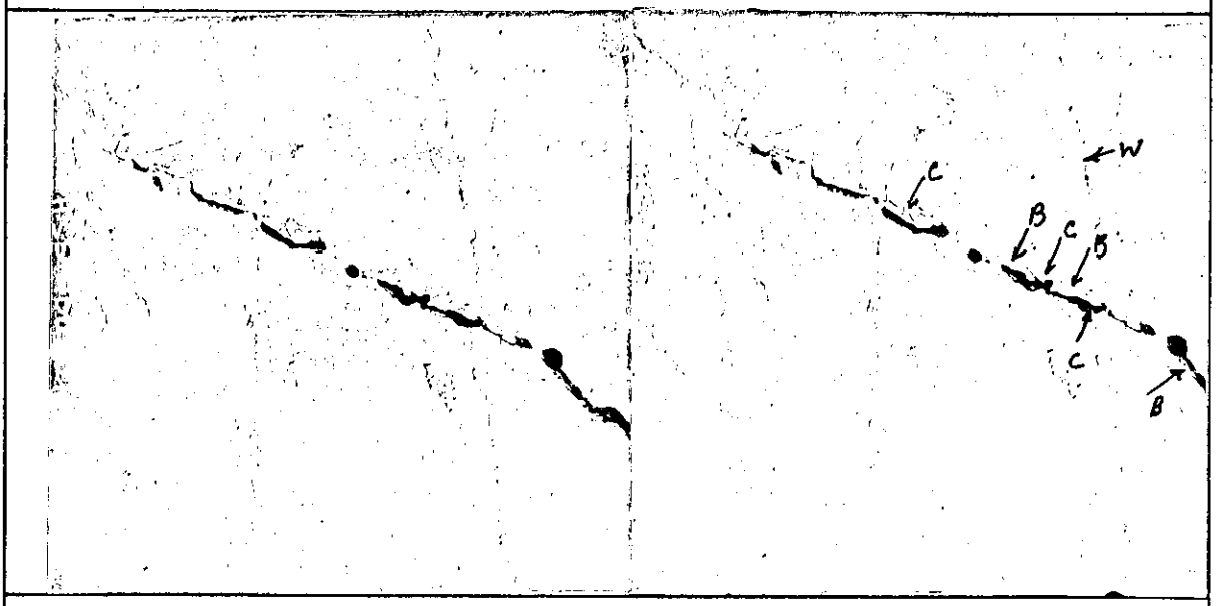

b. Slip at the grain boundary may arise from grain boundary extrusion C and intrusion B, taking place within the grain boundary.

HIGH STRAIN FATIGUE. Expected life = 1,200 cycles, Direct carbon replica at 100 cycles.

Figure. 23.

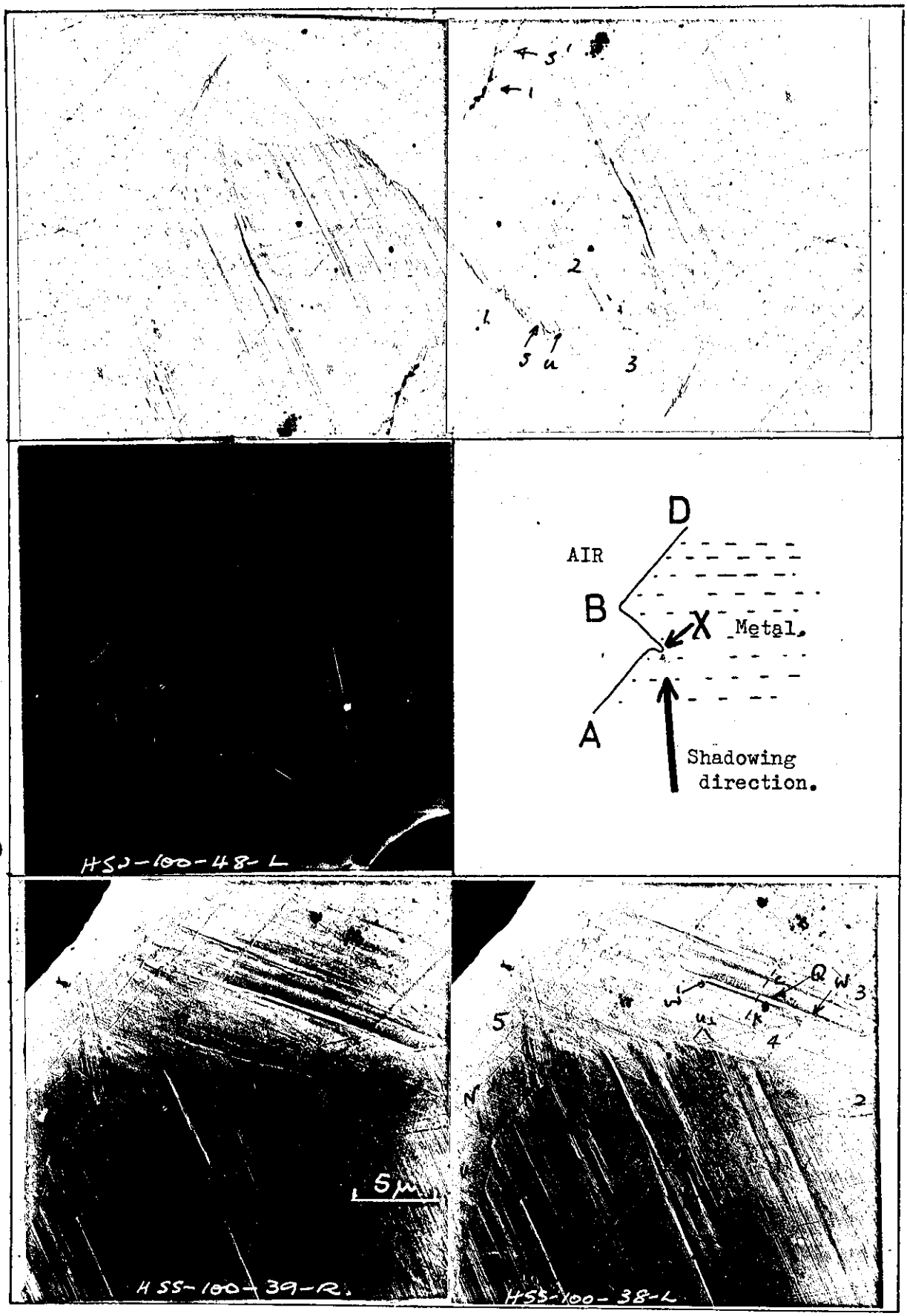

HIGH STRAIN FATIGUE. Expected life 1,200 cycles. Direct carbon replica at 100 cycles. Micrographs show early stages of surface deformation. LEGEND. N. Microcracks at the intersection of the slip plane with the grain boundary. G Slip band intrusion. H Slip band extrusion. s Grain boundary movement or migration.

Figure. 24

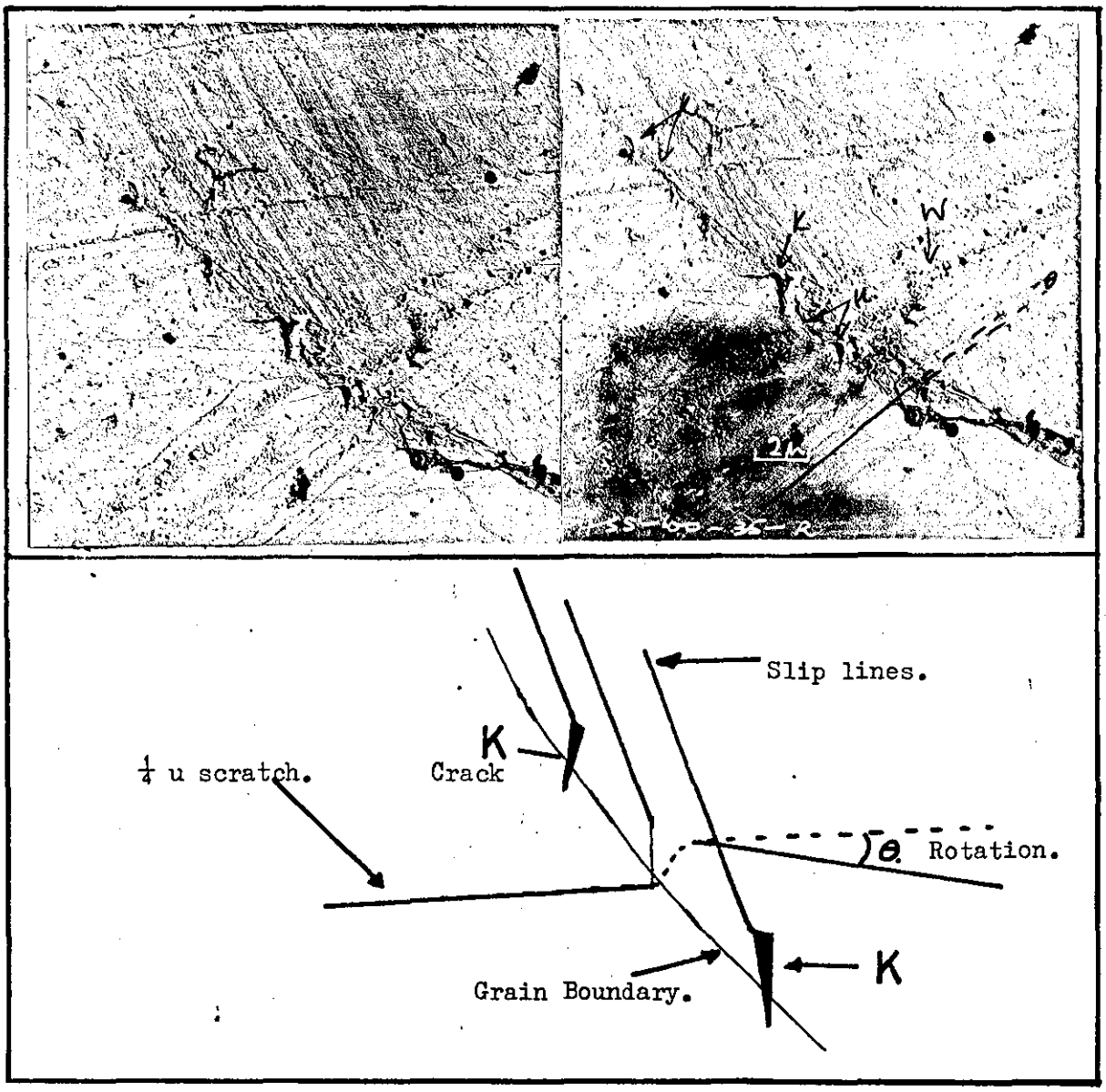

HIGH STRAIN FATIGUE. Expected life 1,200 cycles. Direct carbon replica at 100 cycles. Micrographs show that the formation of a serrated grain boundary is accompanied by the relative movement of the adjacent grain, and the formation of microcracks K.

Figure. 25

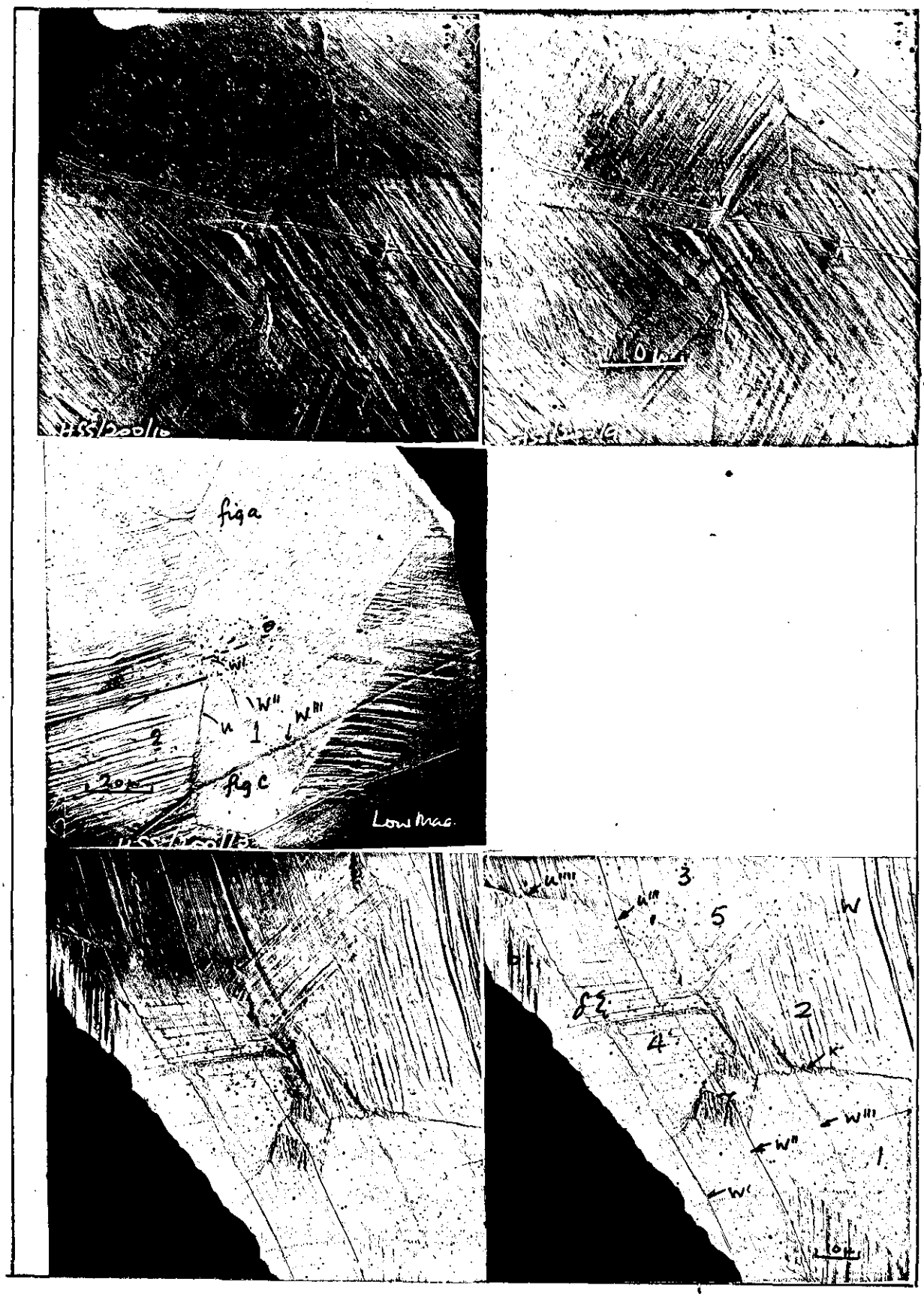

High Strain Fatigue. Expected life 1,200 cycles. Direct carbon replica at 200 cycles. The micrographs show the general phenomena of grain boundary delineation, grain boundary rotation and regions in the grain boundary which slip. These processes preceed crack nucleation in the boundary at these strains.

Figure. 26

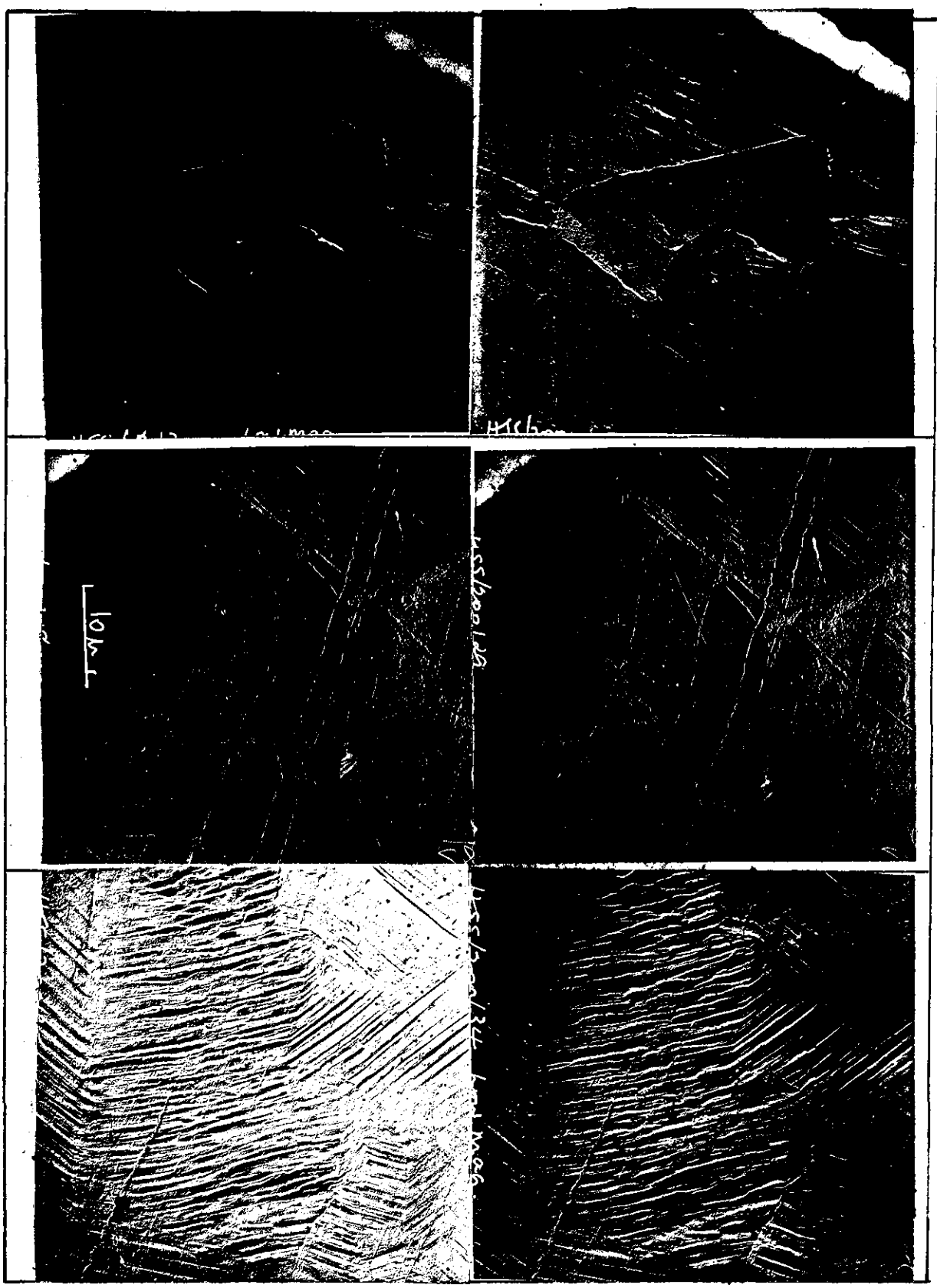

HIGH STRAIN FATIGUE. Expected life 1,200 cycles. Direct carbon replica at 200 cycles. Deformation in high strain fatigue proceeds by surface "folding" or by intrusion formation (fig a at X.)(fig b at G.) and fig c at H. In some cases these phenomena give rise to grain boundary slip U with the formation of microcracks O, grain boundary intrusions B and microcracks at triple points U!

Figure. 27.

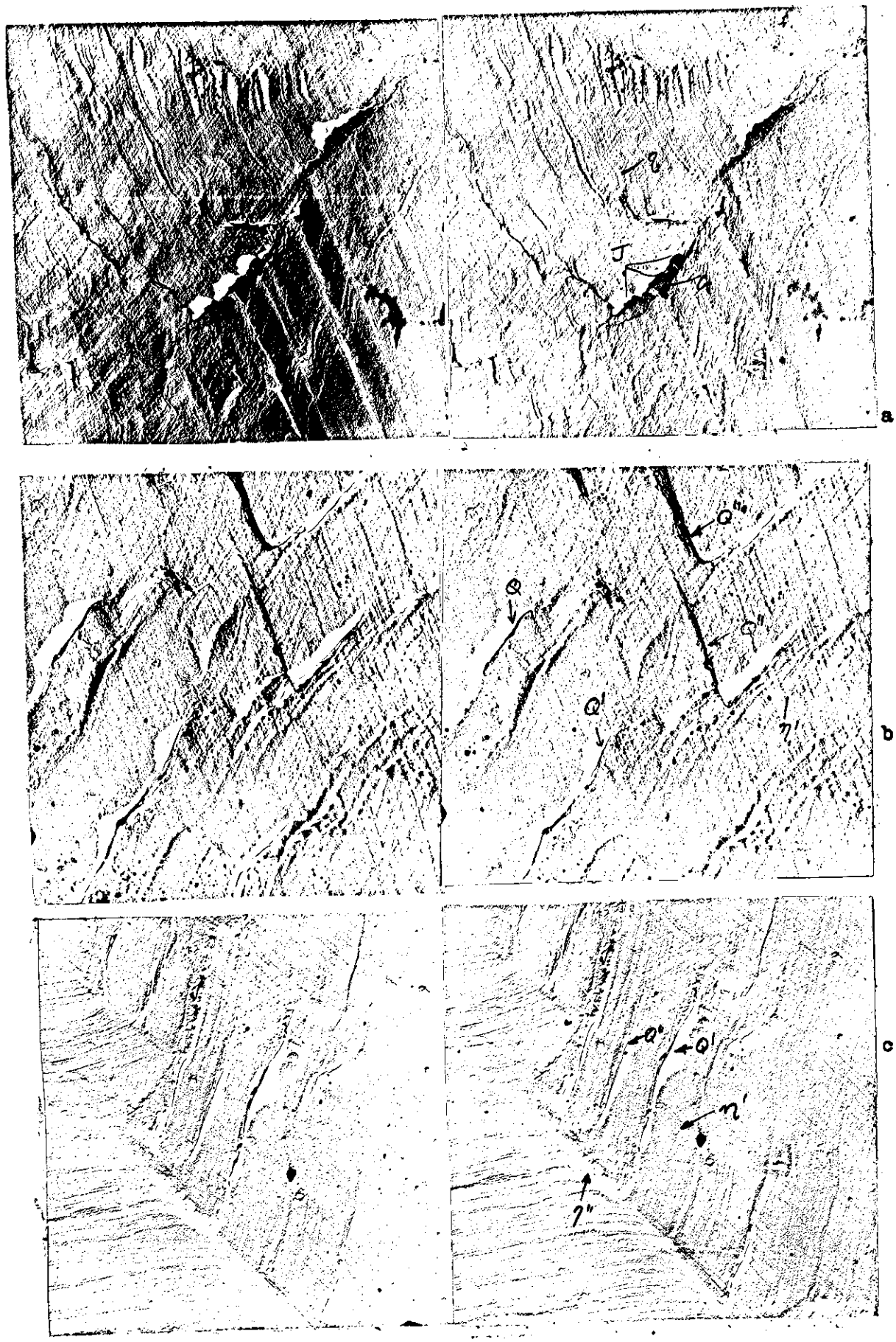

HIGH STRAIN FATIGUE. Expected life 1200 cycles. Direct carbon replicas at 250 cycles. (a) Shows a grain boundary intrusion G from which microcracks J have nucleated. The upper grain is undulating and shows lattice bending η. (b). Transgranular phenomena Q are steep slip steps. (c). "Lattice bending" at the intersection of slip planes with a slipped grain boundary.

Figure. 28

84

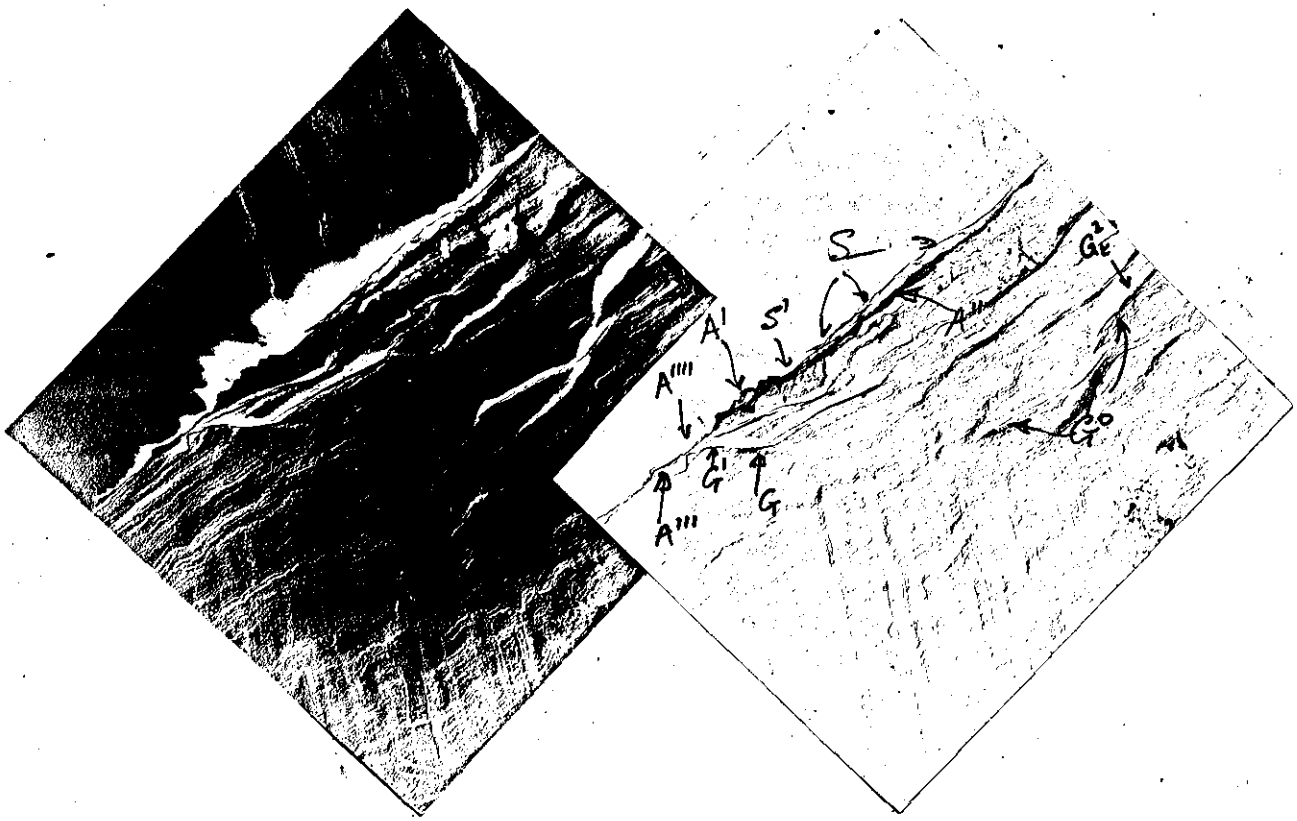

a

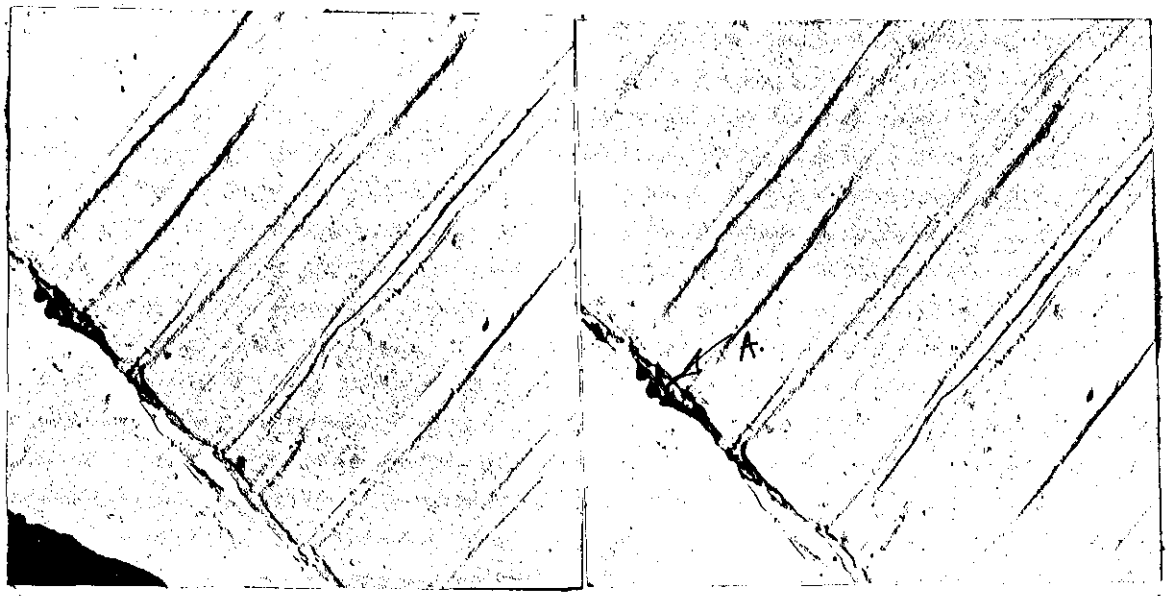

b

HIGH STRAIN FATIGUE. Expected life 1200 cycles. Direct carbon replica at 250 cycles. a and b . Showing intergranular cracks between grains which have slipped. (a). Intrusions G, G° and G' Grain boundary migration S and S'. (b). Slip within the grain and at a boundary which separates two grains which have undergone different amounts of plastic deformation.

Figure 29

85

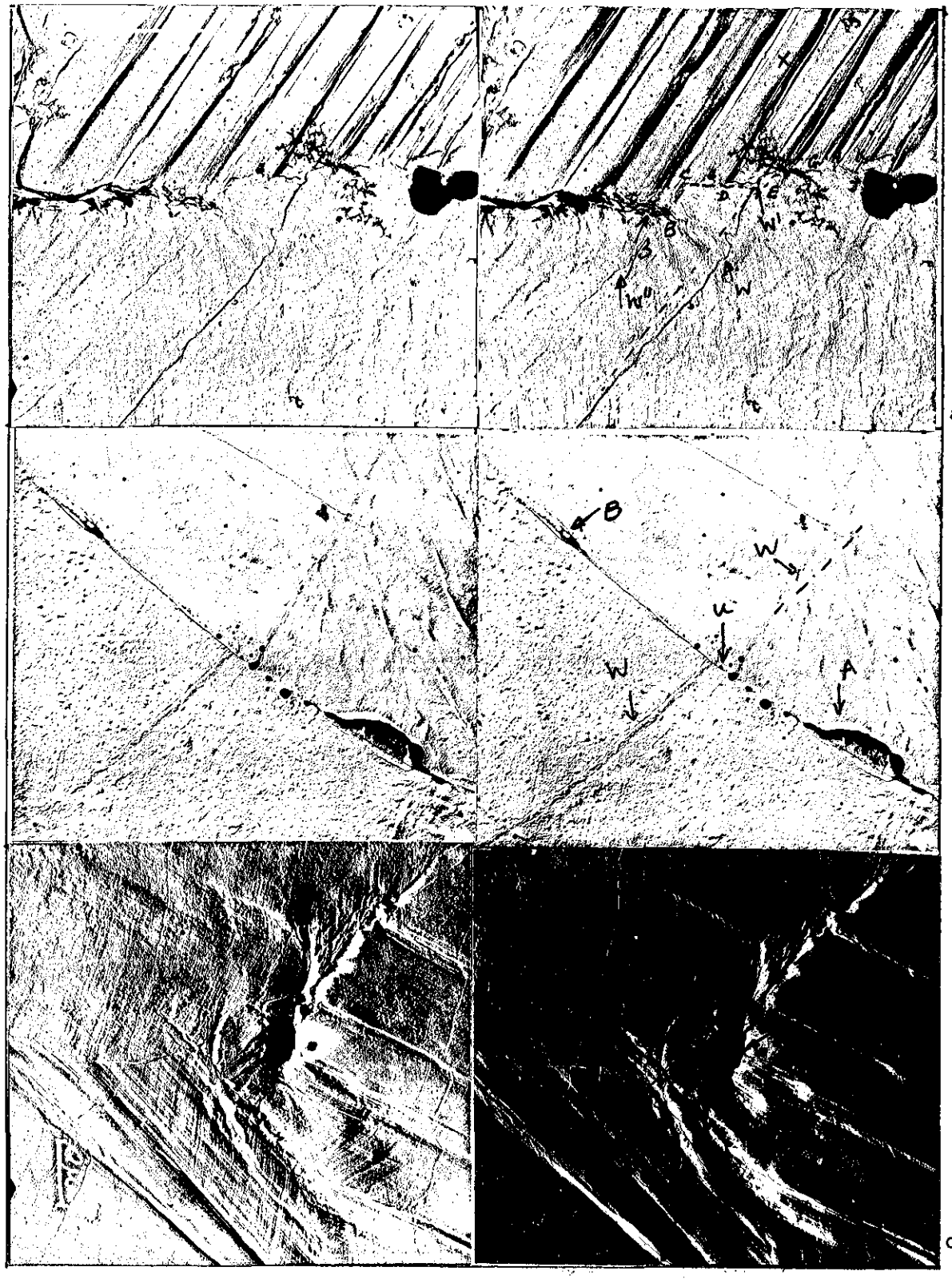

HIGH STRAIN FATIGUE. Expected life 1200 cycles. Direct carbon replica at 300 cycles. a/ Formation of grain boundary slip steps at the ends of slip bands which may give rise to grain boundary microcracking Fig b formation of a intrusion B in a grain boundary which is also host for a crack A. Fig c. shows a triple point crack A' formed from grain boundary slip as a result of unidirectional deformation as shown by the displacement of the scratches W and W'.

Figure. 30

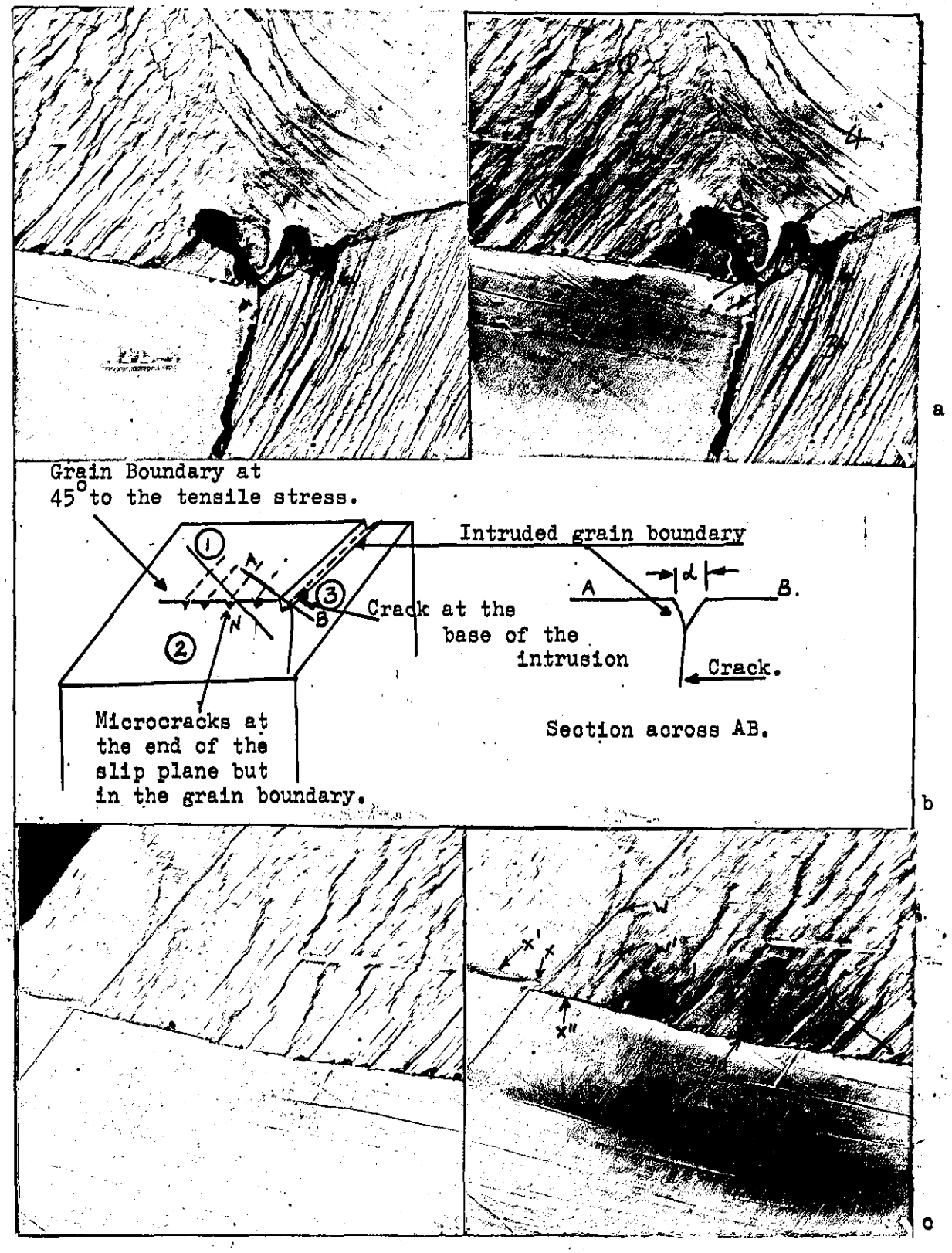

HIGH STRAIN FATIGUE. Expected life 1200 cycles. Direct carbon replica at 300 cycles. Formation of grain boundary microcracks N at a sliding grain boundary

Figure. 31.

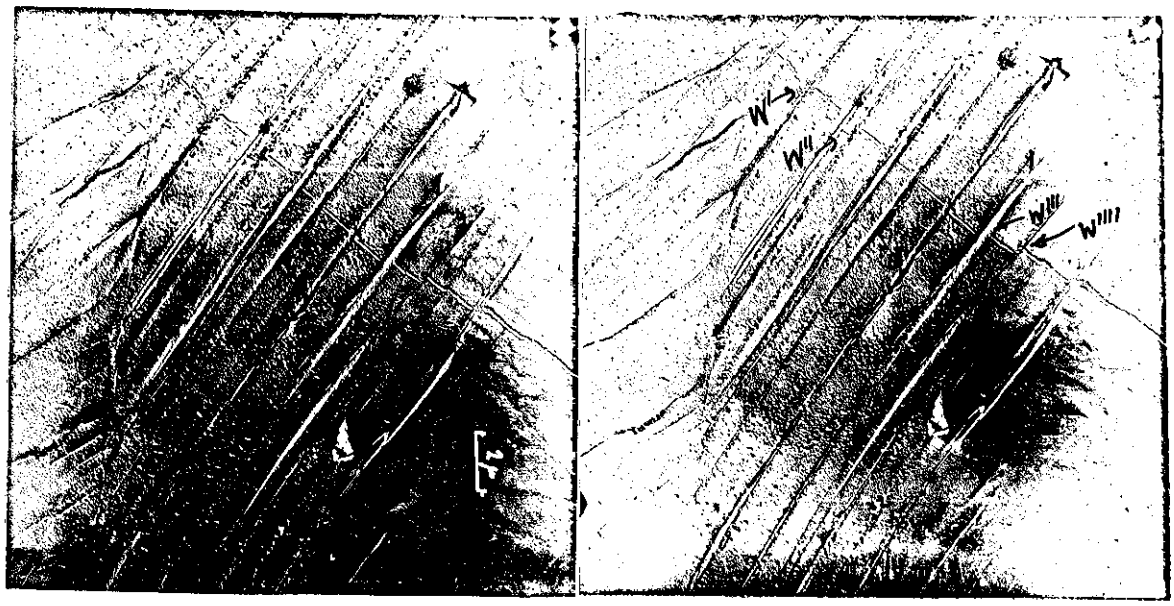

(a) Stereo electron micrographs showing the unidirectional displacement of $\frac{1}{4}\mu$ scratches W

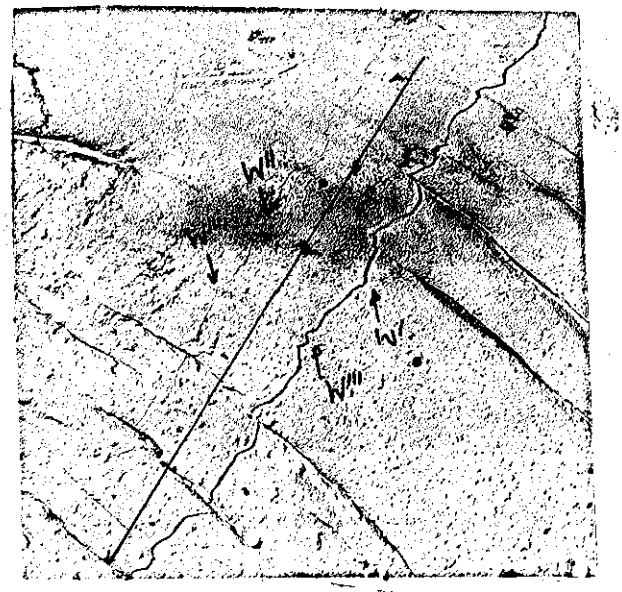

(b) Shows the displacement of two parallel scratches. The displacement of the scratches are different over a distance of 2μ e.g. at W' and W"

DISPLACEMENT OF $\frac{1}{4}\mu$ SCRATCHES DURING HIGH STRAIN FATIGUE.

Figure. 32.

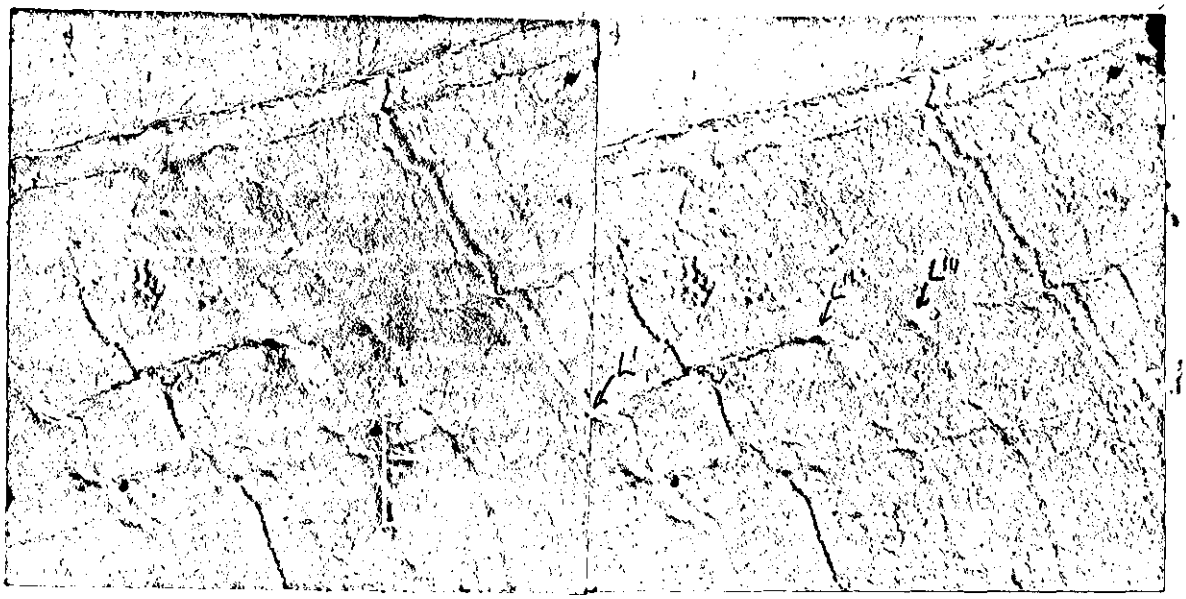

HIGH STRAIN FATIGUE DWELL TESTS. Expected life 1200 cycles. Test stopped with the same surface in tensile at $\frac{1}{4}$ cycle and then every 10 cycles for 10 minutes. Shows crack nucleation at the intersection of slip systems.

Figure. 33 a.

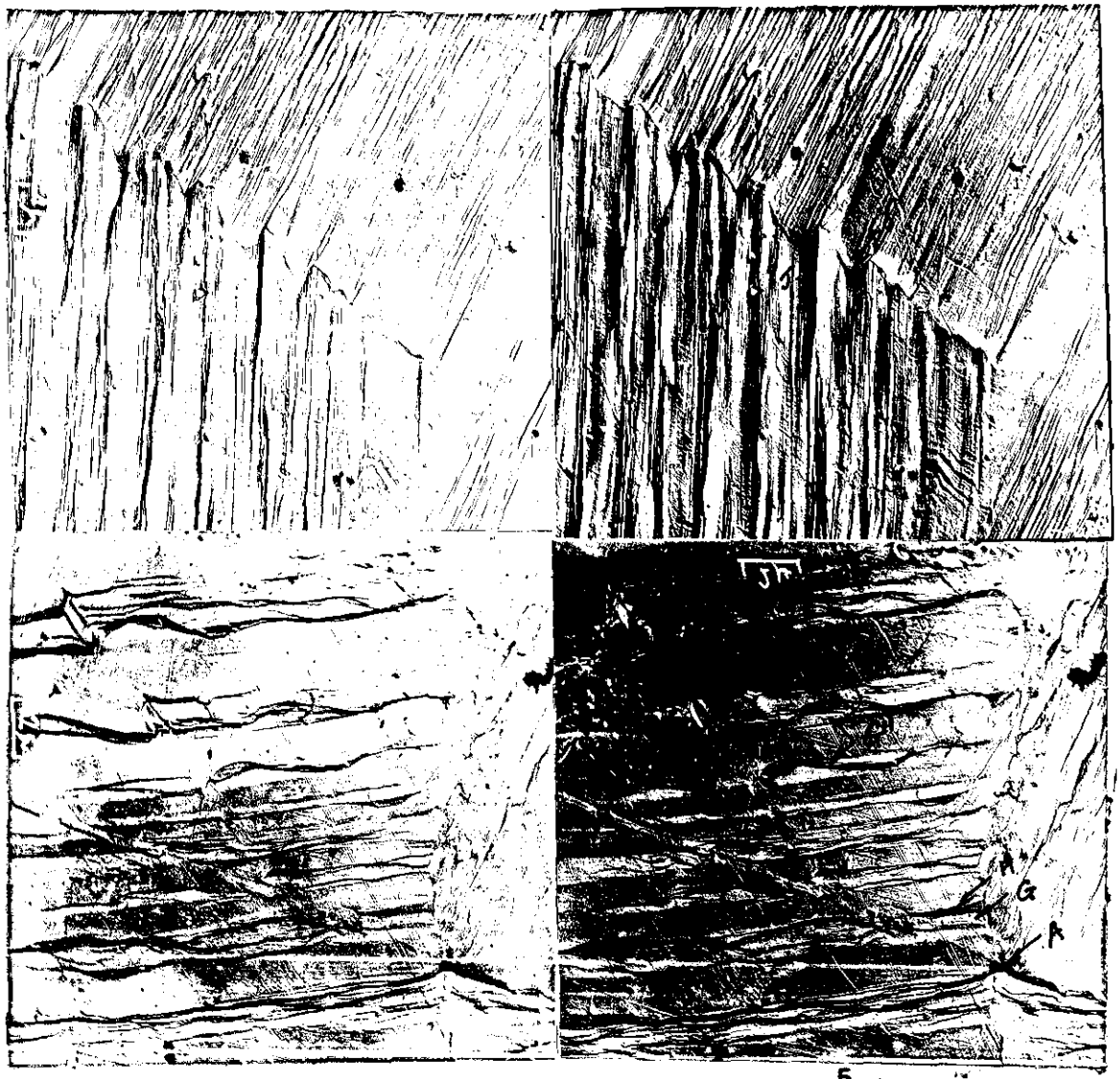

COMPRESSION FATIGUE. Direct carbon replicas at life 10^5 cycles.

(b) Damage at the grain boundary includes slip giving an atomically smooth surface ^{b}, lattice bending due to grain boundary deformation.

(c) Intrusion triple point A and microcracks at the twin boundary V" V""

Figure 33

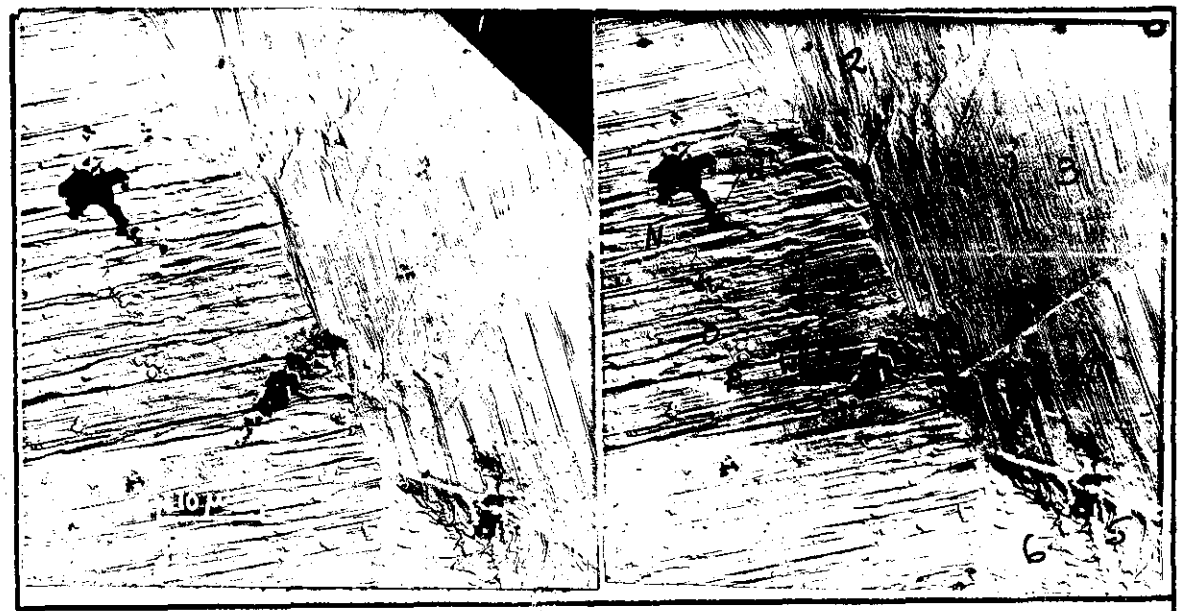

a.

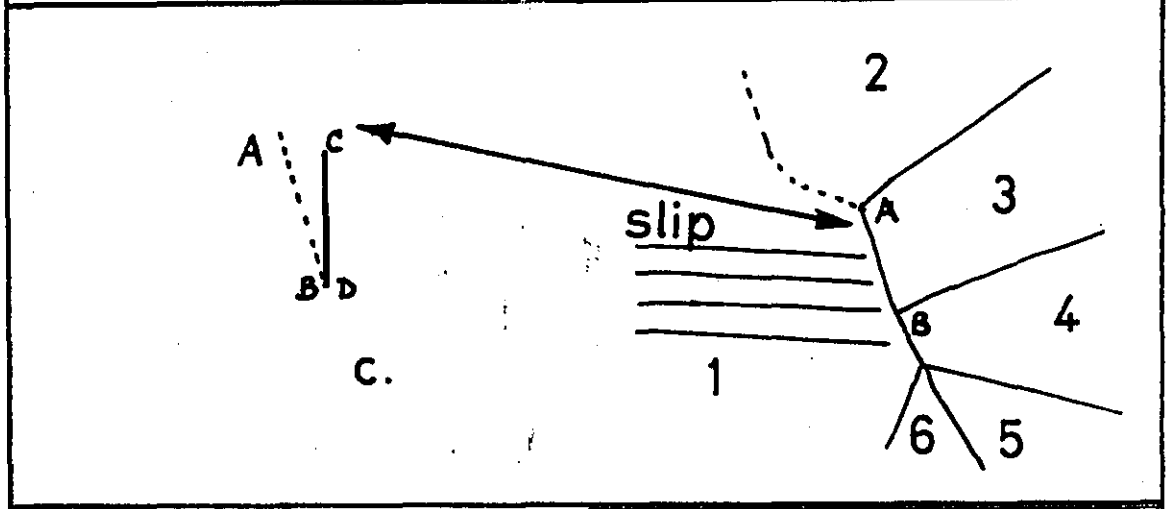

c.

b.

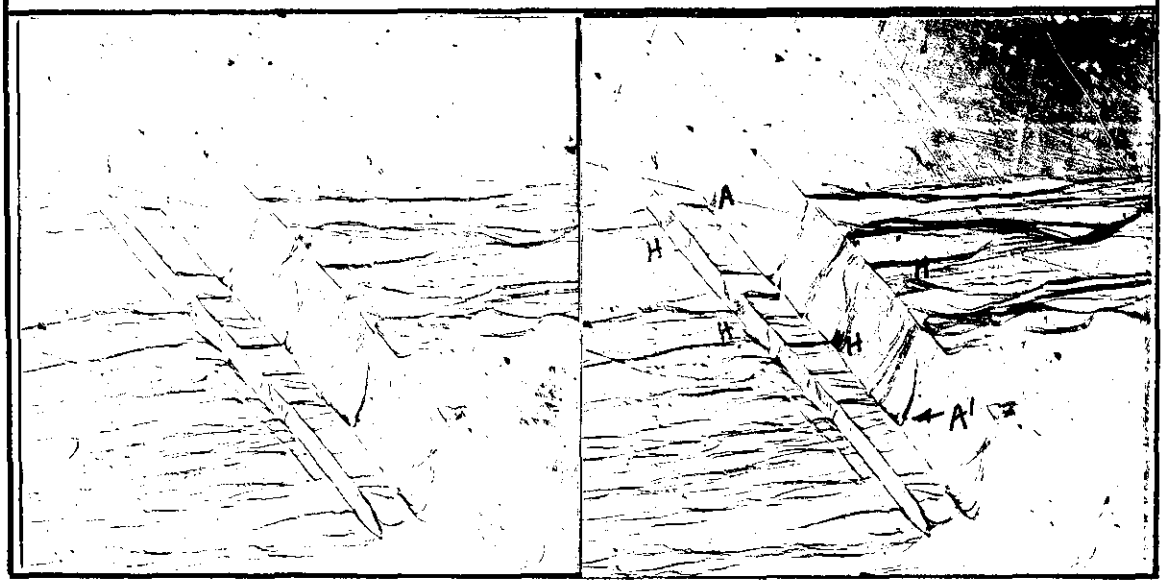

d.

COMPRESSION FATIGUE. Direct carbon replicas at life 10^5 cycles.

(a) Showing slip in the grain boundary after migration. S

(b) Outline of the grain boundaries in (a) before fatigue testing and

(c) the outline of the boundary AB fig (b) at replication, showing the migration and rotation.

(d) Surface topography at a twin boundary showing large extrusions H and grain boundary microcracks A.

90

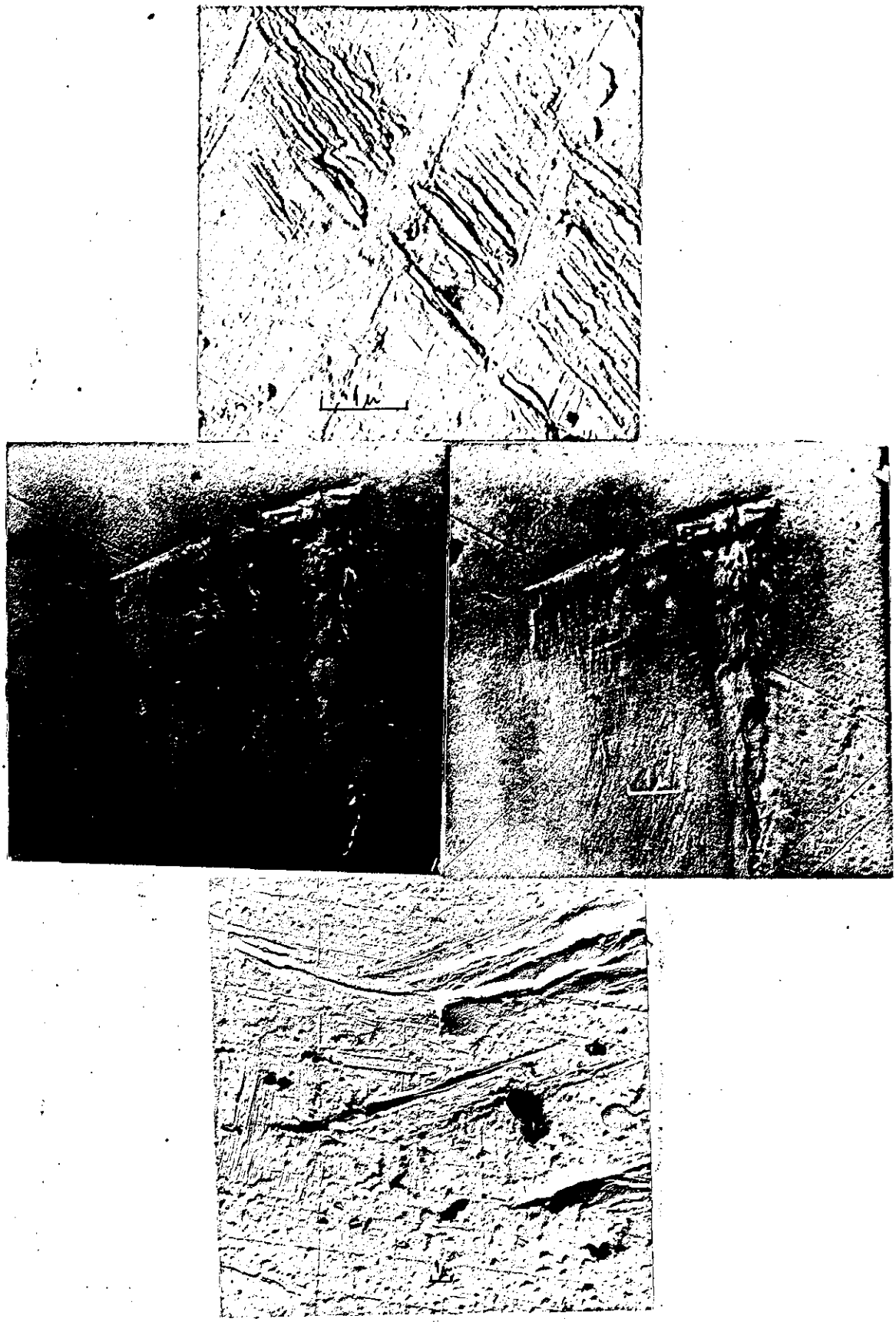

LOW STRAIN FATIGUE.

(a) Surface slip arrested at the $\frac{1}{4}$ μ scratches.

(b) Slip band arrested at the grain boundary, with grain boundary damage and nucleation of a microcrack at the base of the intrusion R.

(c) Displacement of scratches in low strain fatigue. This should be viewed along the plane of the micrograph.

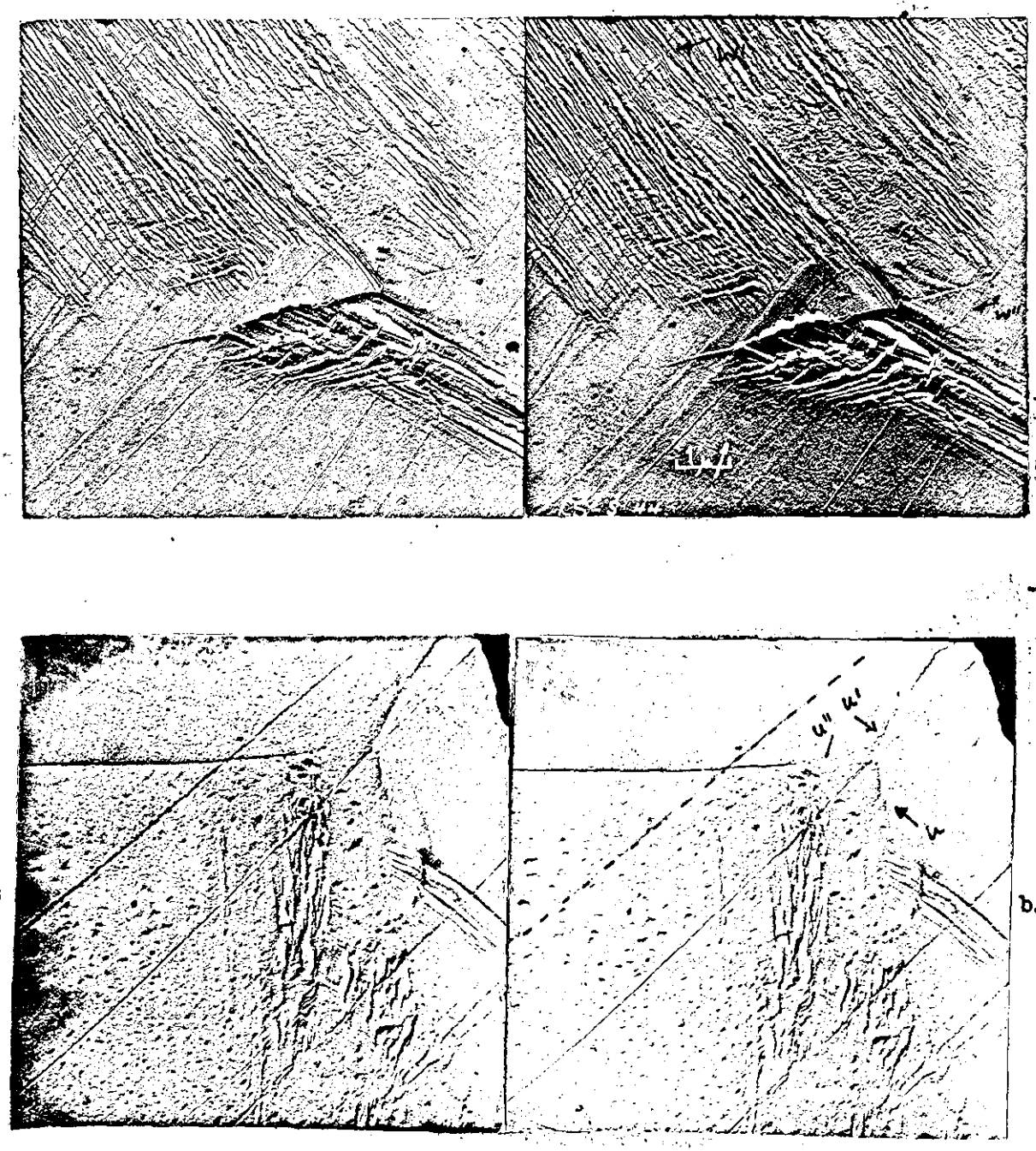

LOW STRAIN FATIGUE. Life 10^7 cycles. Replicas at 9.8×10^6 cycles.
(a) An intruding grain boundary showing the nucleation of several microcracks A
(b) Grain boundary deformation near a triple point. Grain boundary slip can be detected at U , U' and U''

Figure. 36

92.

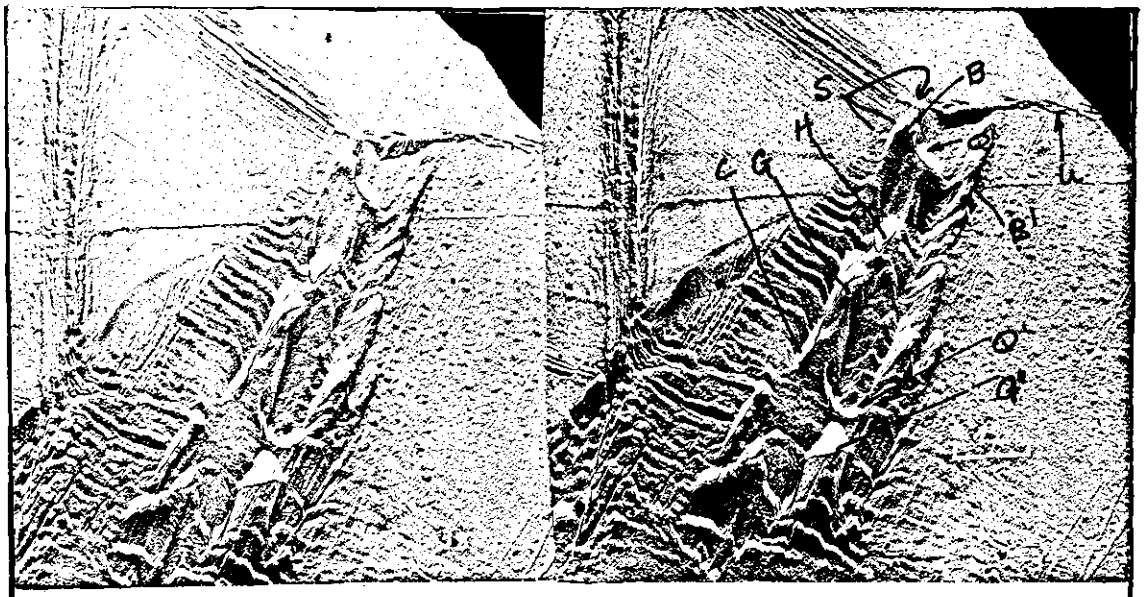

a

Low strain fatigue. Life 10^7 cycles. Replica at 9.8×10^6 cycles. Stereo electron micrographs showing grain boundary slip (u). The lower grain has undergone severe deformation and shows the intrusion (G) / extrusion (H) phenomena.

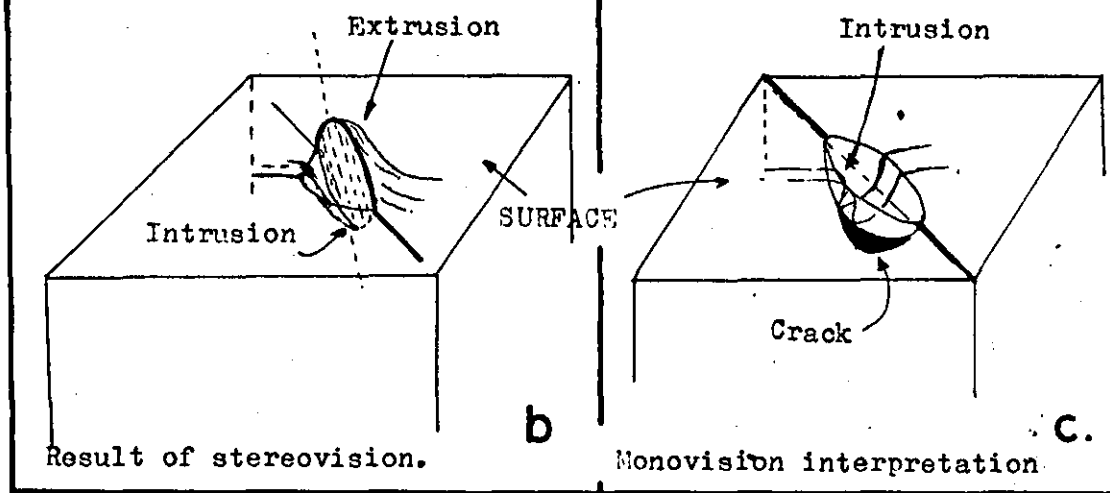

TOPOGRAPHY AT Q"

Figure. 37.

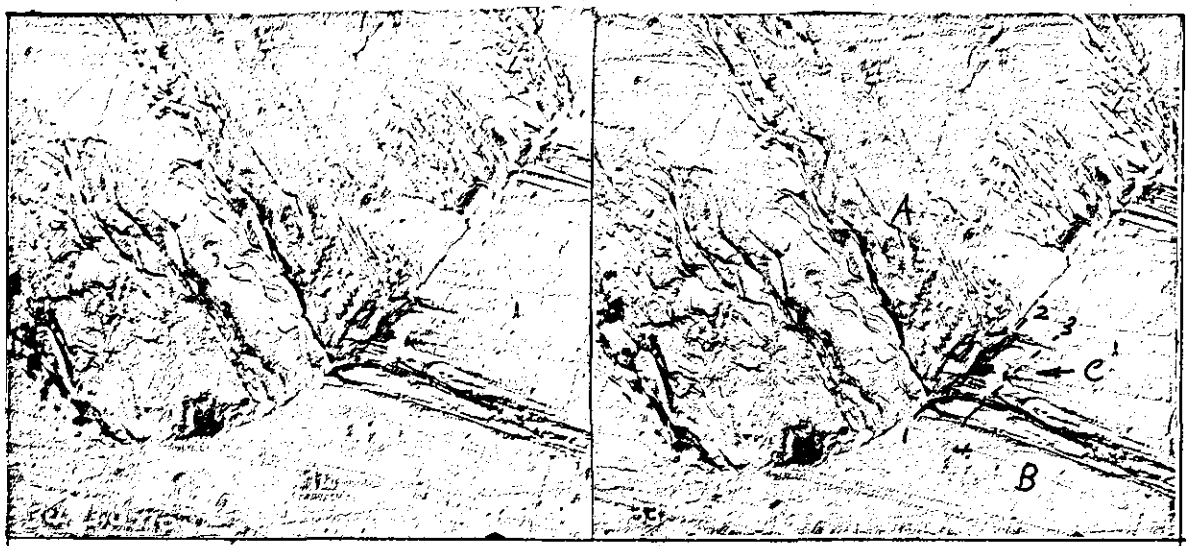

a

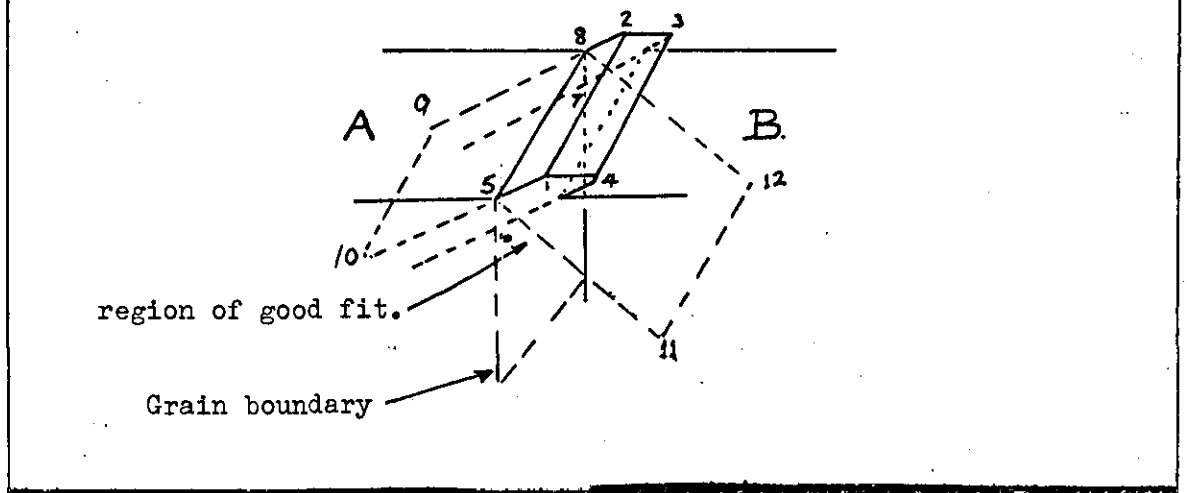

b

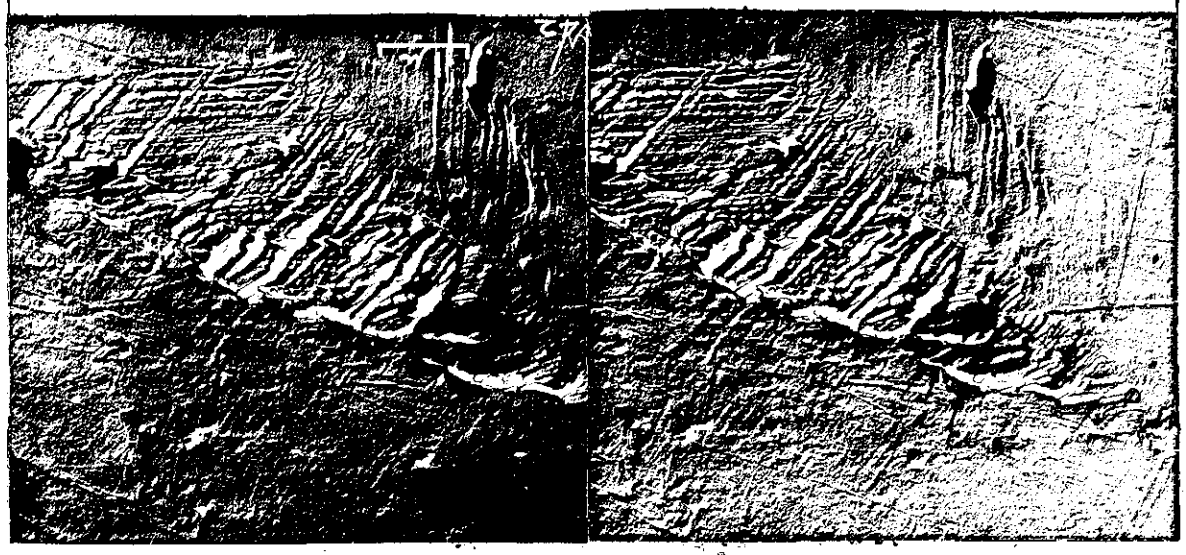

c

LOW STRAIN FATIGUE. Direct carbon replica at 3.4×10^6 cycles. Cyclic deformation resulting in grain boundary extrusion C and C'

Figure. 38.

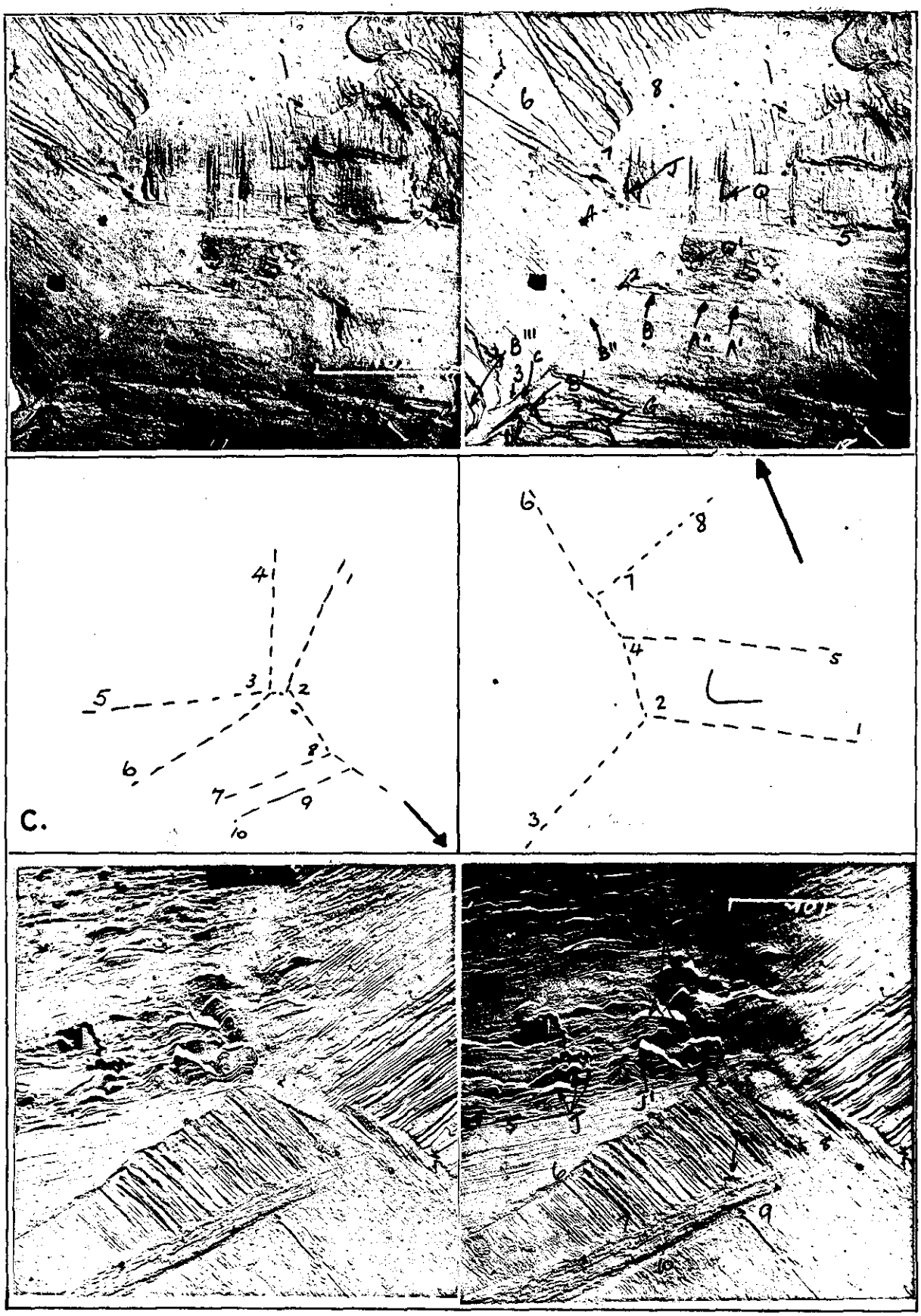

LOW STRAIN FATIGUE.

(a) General view of the surface topography developed during fatigue

(b) Line drawing of the grain boundaries in (a) .

(c) Line drawing of the grain boundaries in (d).

(d) General view of the surface topography developed in fatigue.

LEGEND. A grain boundary crack, B Grain boundary intrusion, C Grain boundary extrusion, J Intrsuion cracks. G Slip plane intrusion.

Figure 39.

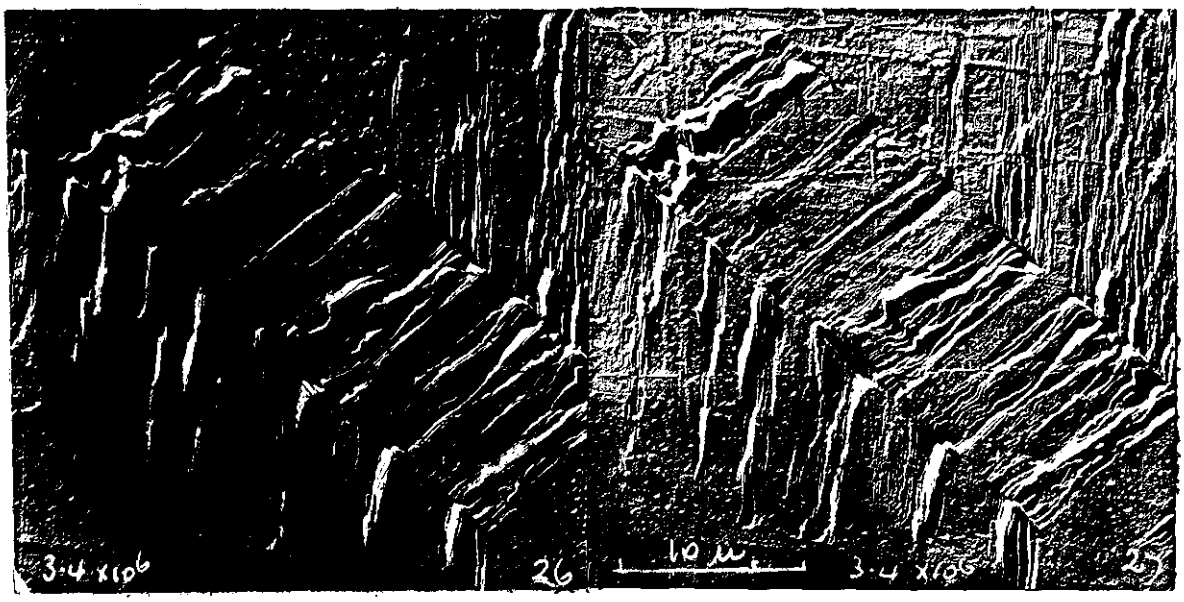

a

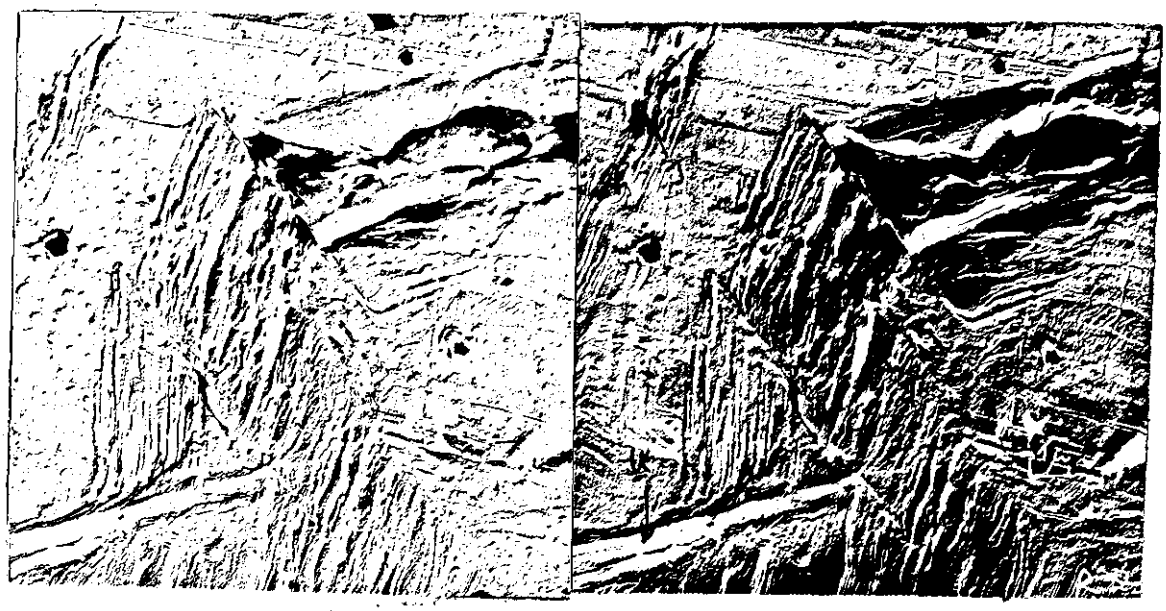

b

LOW STRAIN FATIGUE.

(a) Slip concentrated at twin boundaries leading to boundary slip steps and transgranular microcracking J'

(b) Severe surface roughening due to slip concentration at the grain boundary region.

Figure 40

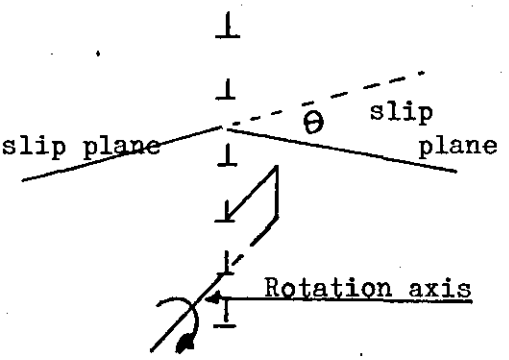

Grain boundary as an arrangement of edge dislocations.

a

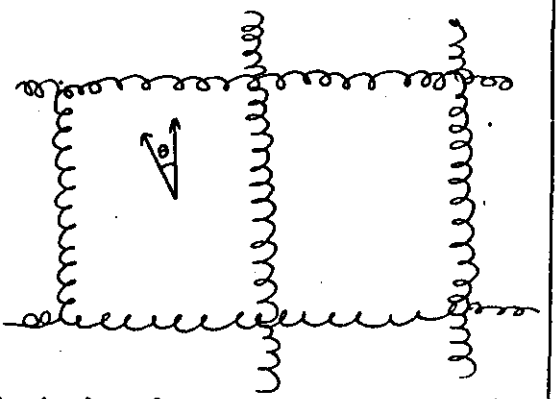

Grain boundary as an arrangement of screw dislocations.

b

Effect of a screw dislocation upon a $\frac{1}{4}$ μ scratch

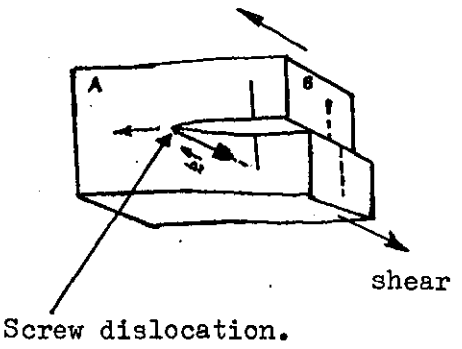

c

Effect of a screw dislocation upon a $\frac{1}{4}$ μ scratch

Face A	Face B
Slip step.	No slip step.

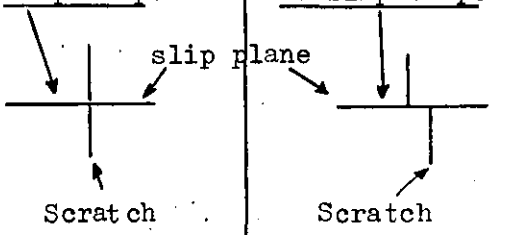

d e

Effect of an edge dislocation upon a $\frac{1}{4}$ μ scratch.

Edge dislocation

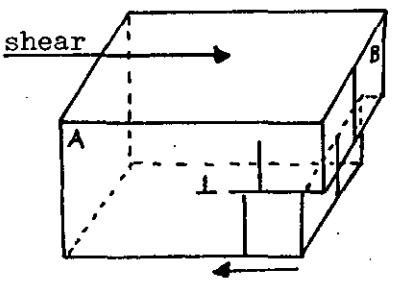

f

Effect of an edge dislocation upon a $\frac{1}{4}$ μ scratch.

Face A	Face B
No slip step.	Slip step.

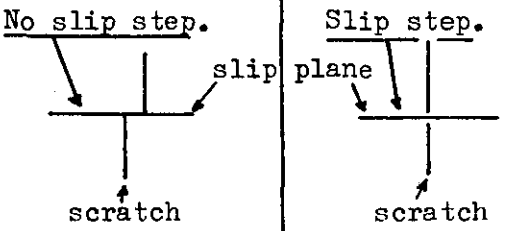

g h

Figure. 41

97

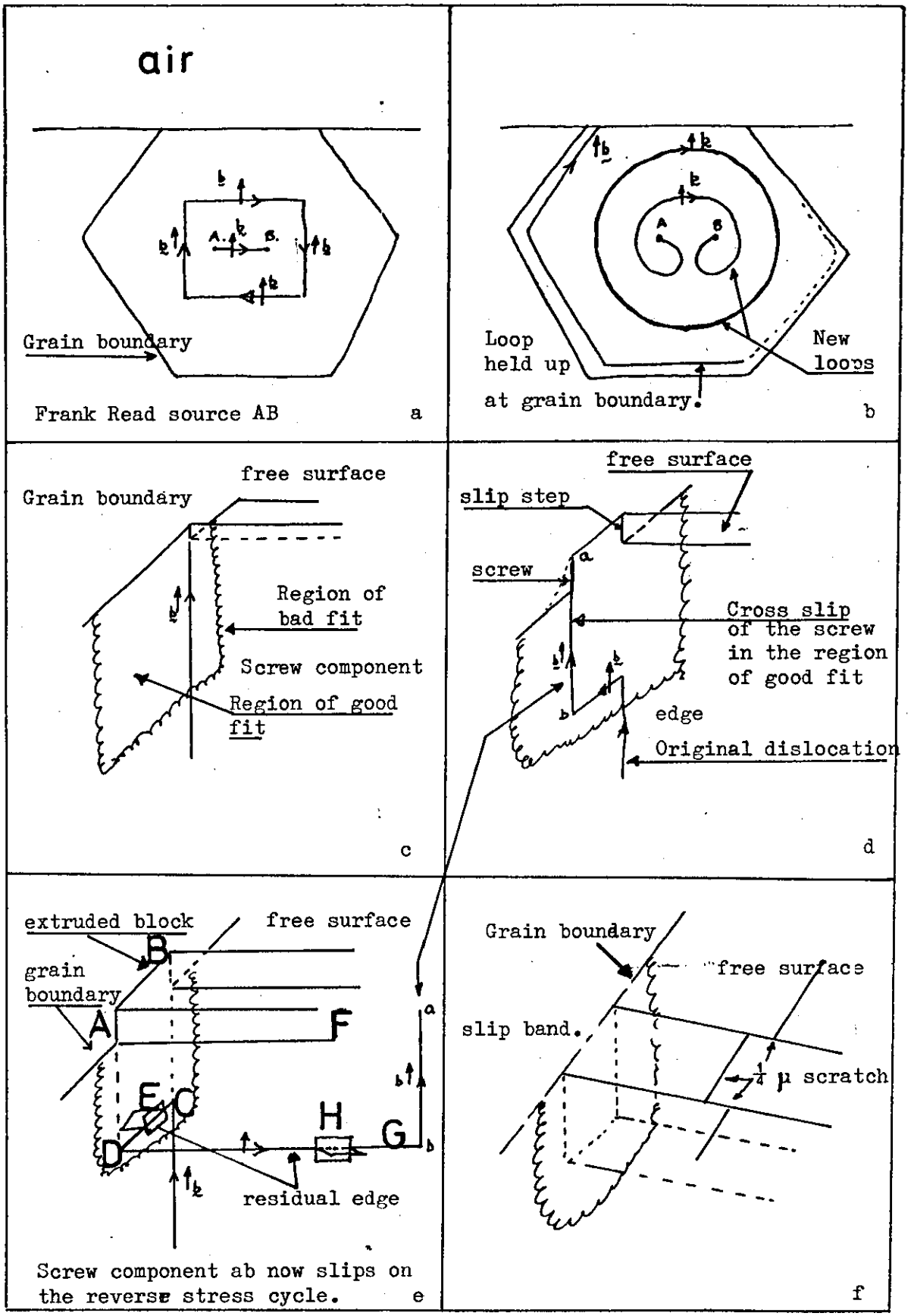
air
Grain boundary
Frank Read source AB
a
Loop
held up
at grain boundary.
New
loops
b
Grain boundary
free surface
Region of
bad fit
Screw component
Region of good
fit
c
free surface
slip step
screw
Cross slip
of the screw
in the region
of good fit
edge
Original dislocation
d
extruded block
free surface
grain
boundary
residual edge
Screw component ab now slips on
the reverse stress cycle.
e
Grain boundary
free surface
slip band.
μ scratch
f

Figure. 42

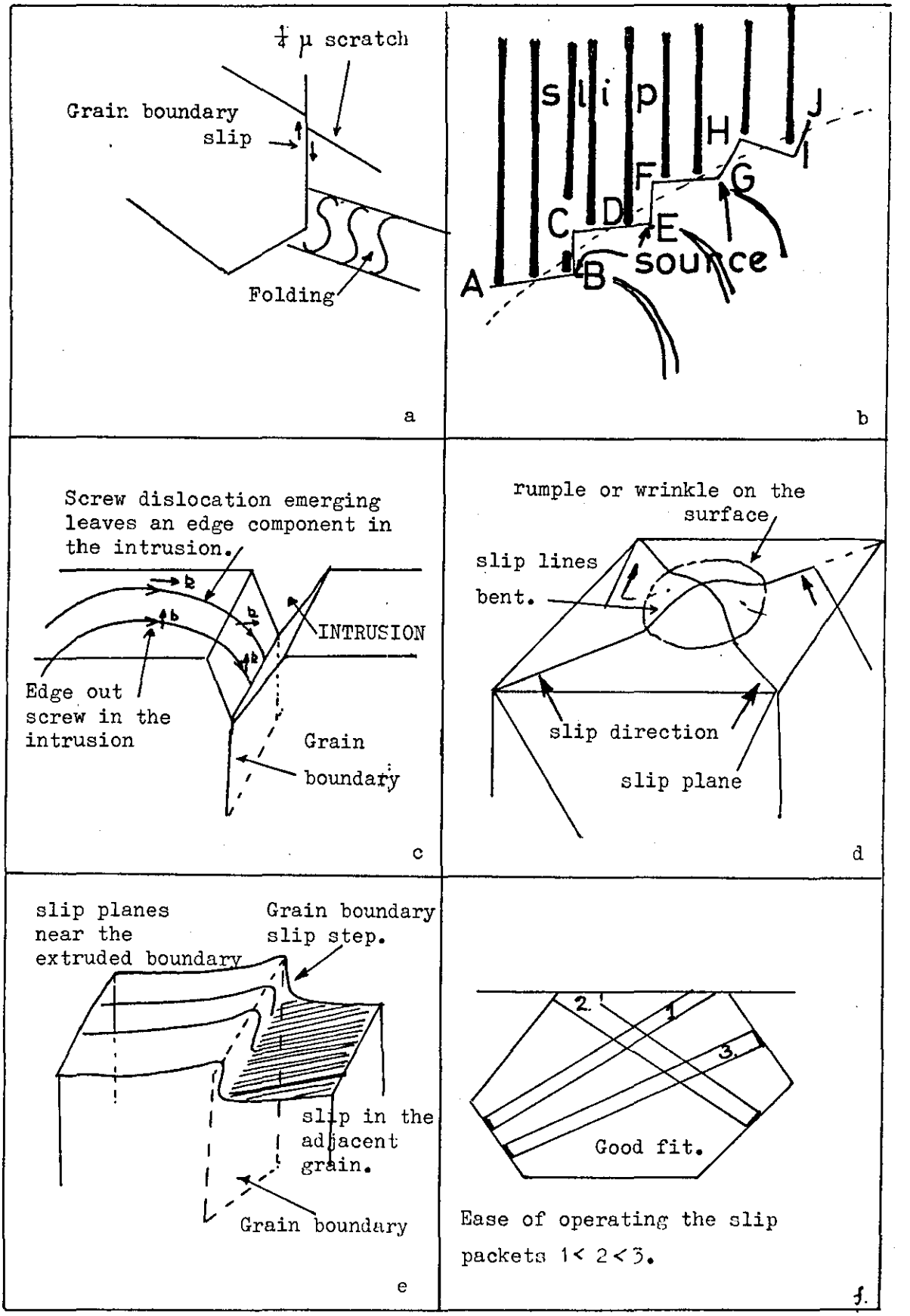
¼ μ scratch
Grain boundary slip
Folding
a
slip
A
B
C
D
E
F
G
H
I
J
source
b
Screw dislocation emerging leaves an edge component in the intrusion.
INTRUSION
Edge out screw in the intrusion
Grain boundary
c
rumple or wrinkle on the surface
slip lines bent.
slip direction
slip plane
d
slip planes near the extruded boundary
Grain boundary slip step.
slip in the adjacent grain.
Grain boundary
e
1
2
3
Good fit.
Ease of operating the slip packets 1< 2< 3.
f.

Figure. 43.

Spec.	Test temp. °C	Creep rate $x10^{-8}$ in/in per hour.	25 % life x 10^5 cycles	Surface removed	25 % life x 10^5 cycles	Surface removed	25% life x 10^5 cycles	Surface removed	25 % life x 10^5 cycles	surface removed	25 % life x 10^5 cycles	Surface removed	25 % life x 10^5 cycles	surface removed	26% life x 10^5 cycles		Total life life x 10^5
1/1																	22.6
1/2	149	3.2															4.9
1/3																	4.16.
2/1			0.314	25 μ	1.01												1.32
2/2	204	2.0	1.756	25 μ	1.638	50 μ	0.671	50 μ	0.23								3.3
2/3			0.68	25 μ	1.95	50 μ	0.144										2.77
2/4																	19.
4/1			4.5	75 μ	5.535	50 μ	3.013										12.8
4/2	249	1.8															13.2
4/3			4.109	75 μ	4.135	50 μ	3.0	50 μ	1.857								13.4
4/4																	22.6
5/1			1.213	50 μ	1.79	37 μ	1.77	25 μ	1.64								6.41
5/2	249	7.2	1.213	50 μ	0.14												1.35
5/3																	30.0
5/4			1.51	75 μ	0.258												1.76
7/1																	6.2
7/2	149	3.3	1.45	42 μ	0.537												2.0
7/3																	6.13
7/4			1.96	42 μ	1.63	55 μ	1.8	60 μ	1.16	70 μ	1.636	40 μ	2.38	75 μ	1.4		12.16
8/1																	4.95
8/2	204	3.8	1.72	32 μ	1.79	87 μ	1.65										5.16
8/3			1.51	45 μ	1.75	100 μ	1.52	25 μ	1.904	75 μ	1.83						8.51
8/4																	

The figures below for the control specimens refer to the number of cycles in each 25 % life ($x10^5$ cycles). At these stages 25 u was removed from the specimen surface prior to fatiguing for another 25 % life.

Annealed control specimens	1.695	1.82	1.8	1.79	1.81	1.8	1.8	1.96	1.24							15.71
	1.48	1.7	1.58	1.8	1.8	1.7	1.7	1.7	1.65	1.8	1.8	1.6	1.7	1.5	1.4	23.41

Average life of 7 specimens continuously cycled at this stress was 6.2 x 10^5 cycles. (lives $x10^5$: 7.2,5.8,6.5,6.3,6.8 6.4, 4.0.

Table 1 Effect of surface removal after 25 % fatigue life on fatigue specimens machined from previously creep tested material.

TABLE 2 Summary of Grain boundary slip and Rotation.

Strain Range	No of cycles to failure	No of cycles at observation.	Rotation (degrees)	Displacement (microns)	Grain boundary cracks.
± 0.98 %	1,600	100	5	just detectable	No
			4	$//^{\ell}$ 0.1 μ	No
			2	0.75 μ	Yes
			0	0.05 μ	yes
			0	$//^{\ell}, \perp^{r}$ J.D	No
			10	0.05 μ	Yes
			o	o.1 μ	Yes
0.98	1,600	200	12	J.D	No
			2	J.D	No
			0	0.1 μ	No
1.16	1,200		5	triple point	No
1.16	1,200	250	0	.5μ	Yes
			8	1. μ	Yes
			2	2.0 μ	Yes
0.98	1,600	400	4		No
			2	0.1μ	No
			0	0.4μ	Yes.
1.0	1,600	500	0	1.0 μ	Yes
			10	0.05μ	No
			2	1.0μ	Yes
			0	0.75μ	No
Compression fatigue.	10^4 cycles	10^4 cycles.	1	J.D.	No
			1	J.D.	No
					No
Low strain fatigue.	10^7	10^7			
		$9.8\ 10^6$	3	J.D.	No
			1	$\perp^{r}$ J.D.	No
			0	0.05u	No
			0	$\perp^{r}$	No

Legend
Slip parallel to the boundary is shown $//^{\ell}$

Slip perpendicular to the surface is shown $\perp^{r}$.